European Commission

Joint Research Centre

Drought in East Africa and Middle East / Central Asia April 2026

GDO Analytical Report

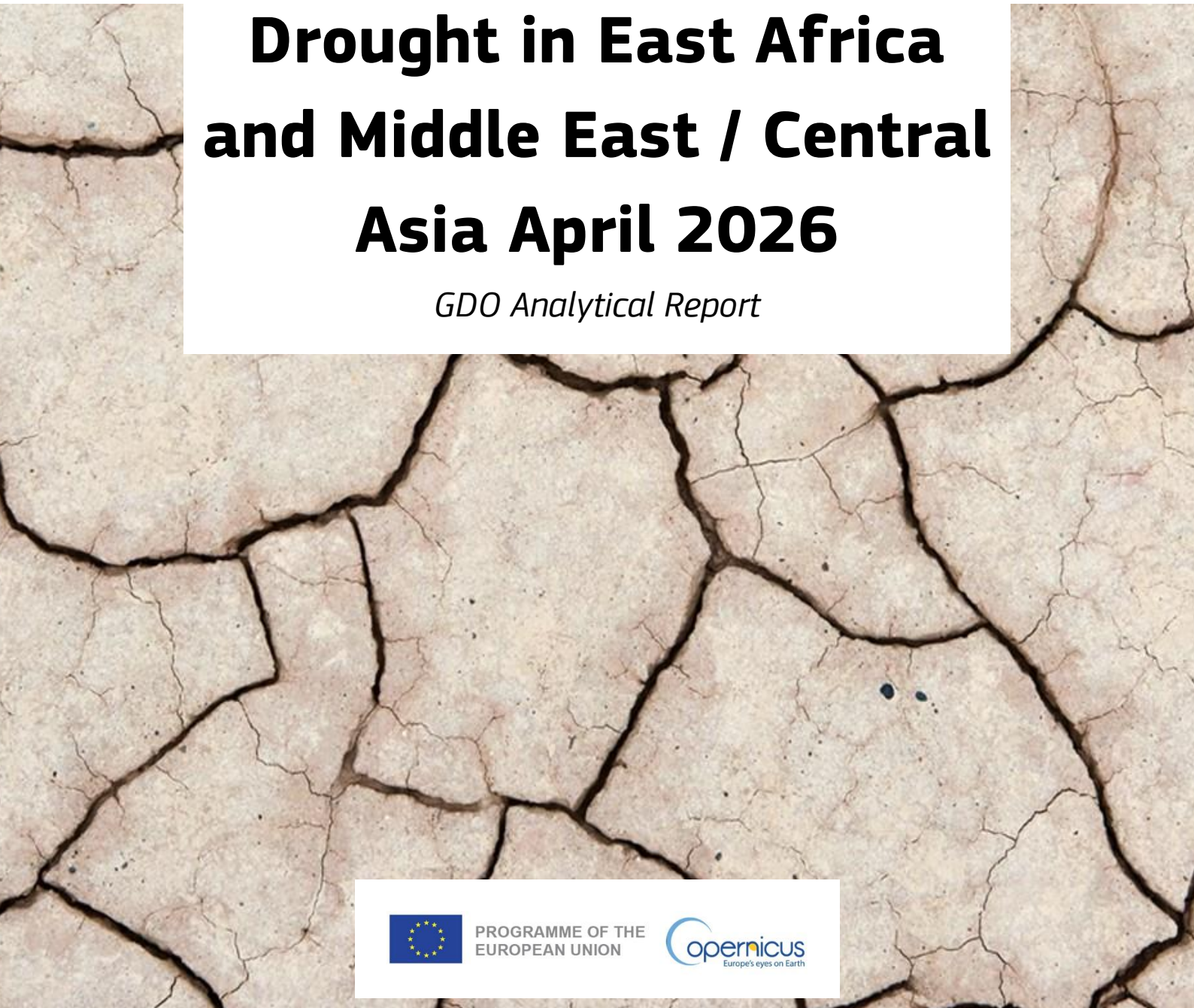

PROGRAMME OF THE EUROPEAN UNION

Copernicus Europe's eyes on Earth

Contact information
Name: Andrea Toreti
Address: Via E. Fermi 2749, I-21027 ISPRA (VA), Italy
Email: Andrea.TORETI@ec.europa.eu

The Joint Research Centre: EU Science Hub
https://joint-research-centre.ec.europa.eu

JRC146777
EUR 40717

PDF ISBN 978-92-68-39795-4 ISSN 1831-9424 doi:10.2760/8763155 KJ-01-26-200-EN-N

Luxembourg: Publications Office of the European Union, 2026

How to cite this report: Toreti, A., Bavera, D., Acosta Navarro, J., Magni, D., Hrast Essenfelder, A. et al., *Drought in East Africa and Middle East/Central Asia April 2026 - GDO Analytical Report,* Publications Office of the European Union, Luxembourg, 2026, https://data.europa.eu/doi/10.2760/8763155, JRC146777.

Contents

Abstract

A sequence of drought events has been affecting East Africa and the Middle East/Central Asia since 2021. Warmer temperatures and heatwaves compounded with precipitation deficits and contributed to shape these climate extremes.

Large-scale climate drivers, such as El Niño Southern Oscillation and the Indian Ocean Dipole, have contributed to reinforce precipitation deficits and enhance atmospheric evaporative demand in the most severe drought episodes observed in East Africa (2021-2022, 2025) and the Middle East/Central Asia region (2021-2022, 2025). Rising temperatures due to anthropogenic climate change, evident in the time series of temperature anomalies, contribute to increase atmospheric water demand and exacerbate soil moisture depletion across both regions.

In East Africa, the drought is gripping Somalia, south-eastern Ethiopia and eastern Kenya, leading to historic low soil moisture levels and severe vegetation stress.

In the Middle East/Central Asia region, persistent dry conditions are observed in northern Iran, Turan Depression, Afghanistan and parts of Central Asia, with runoff and river discharge anomalies remaining negative.

Agricultural impacts of the drought events are here evaluated by using FAOSTAT data from 2016 – 2024. The production of sorghum decreased in Kenya, Ethiopia and especially in Somalia (~40 %) from 2016-2020 to 2021-2024. Maize production remained stable in Somalia and Kenya and even increased in Ethiopia and Tanzania. In Central Asia, wheat production declined only in Turkmenistan, while it remained stable in Afghanistan and even increased in Iran, Uzbekistan, Pakistan. These changes are clearly influenced by irrigation. In some cases, e.g. in Iran, these changes are associated with unsustainable water resource management and overexploitation.

The analysis of hydrological impacts shows prolonged negative runoff anomalies in the Ethiopian Highlands, the Upper Nile basin and the Middle East, reducing water availability for irrigation and domestic use.

The humanitarian situation in East Africa is worsening, with 4.6 million people affected, over 135 000 displaced in Somalia, and acute malnutrition threatening ~2 million children.

Seasonal forecasts from the multi-system ensemble predict only marginally wetter conditions for southern Somalia and south-eastern Kenya, with high uncertainty and limited expected relief before the next rainy season.

Funding shortfalls compound the crisis: by early 2026 only €370 million of the €1.4 billion required for humanitarian response had been secured, jeopardising life-saving assistance.

Acknowledgements

We gratefully acknowledge the support provided by the Copernicus programme and the Directorate-General for Defence Industry and Space (DG DEFIS), and the Directorate-General for European Civil Protection and Humanitarian Aid Operations (DG ECHO). We thank A. De Jager, G. Fioravanti, D. Volpi, L. Acquafresca, A. Ficchì, P. Barbosa for their key contributions to the European and global drought observatories of the Copernicus Emergency Management Service.

Authors

- Toreti A., European Commission, Joint Research Centre, Ispra, Italy
- Bavera D., Arcadia SIT, Milano, Italy
- Acosta Navarro J., European Commission, Joint Research Centre, Ispra, Italy
- Magni D., Arcadia SIT, Milano, Italy
- Hrast Essenfelder A., European Commission, Joint Research Centre, Ispra, Italy
- Santos Nunes S., Seidor, Milano, Italy
- Mazzeschi M., Unystems Luxembourg Sàrl, Luxembourg
- Kerdiles H., European Commission, Joint Research Centre, Ispra, Italy
- Rembold F., European Commission, Joint Research Centre, Ispra, Italy
- Schaffhauser T., European Commission, Joint Research Centre, Ispra, Italy
- Salamon P., European Commission, Joint Research Centre, Ispra, Italy
- Grimaldi S., European Commission, Joint Research Centre, Ispra, Italy

1. Introduction

The Copernicus Emergency Management Service (CEMS[1]), implemented by the European Commission's Joint Research Centre, provides timely and accurate geospatial information on ongoing and forecasted natural hazards and man-made disasters to support decision making and actions. Its products and services support emergency response and disaster management activities, helping to reduce risks and mitigate the impact of disasters and saving lives. CEMS has three components: early warning and monitoring; on-demand mapping; exposure mapping. The early warning and monitoring component focuses on floods, drought, and wildfire.

The European and Global Drought Observatories[2] (EDO and GDO) of CEMS provide drought forecasting and monitoring information, analysis tools and analytical reports. The Observatories aim at detecting, monitoring, and predicting droughts by using a suite of indices and indicators characterising different aspects and phases of drought. In addition, EDO and GDO provide monitoring information and forecasts of warm spells, heatwaves and cold spells. In addition, JRC runs the Anomaly Hotspots of Agriculture system that provides warnings on agricultural drought affecting crops and rangelands[3].

Drought is likely the most complex climate-related natural hazards, due to its spatio-temporal evolution, its cascading impacts on all sectors, including agriculture, public water supply, energy production, transportation, tourism, human health, biodiversity, and natural systems. Drought is a climate extreme characterized by an imbalance in the hydrological cycle. It is due to a deficit in precipitation, that accumulates over time, often compounded by warm spells and heatwaves. It is influenced by land and water use and management. Drought can occur on multiple time scales, from a few weeks to several years, affecting large areas and populations worldwide. The related impacts are both direct and indirect and can persist after its end. Depending on the effect in the hydrological cycle and the impacts on society and environment, different drought phases are commonly distinguished:

1. meteorological drought, characterised by a substantial deficit in precipitation. The deficit is defined with respect to the long-term climatology;
2. agricultural drought, characterised by reduced soil moisture that results from below-average precipitation often compounded by above-normal evapotranspiration;
3. hydrological drought, that occurs when river stream flow and water storages in aquifers, lakes, and reservoirs fall below long-term mean levels.

Due to its complexity, drought monitoring relies on a set of different indices and indicators, representing different components of the hydrological cycle (e.g. precipitation, soil moisture, reservoir levels, river flow, and groundwater levels), as well as specific impacts (e.g. vegetation water stress).

---

1 https://emergency.copernicus.eu/

2 https://drought.emergency.copernicus.eu/

3 https://agricultural-production-hotspots.ec.europa.eu/

All details of drought indices and indicators used in the Copernicus Drought Observatories are available in the associated factsheets[4] and in the JRC Data Catalogue[5].

This study is part of a series of analytical reports focused on the analysis of drought events affecting Europe as well as the other regions of the world. These studies build on data and information retrieved and processed by the Copernicus Drought Observatories. The information derived from the Observatories is usually complemented with additional sections on impacts, large-scale circulation, and other relevant factors.

This study examines drought in East Africa and the Middle East/Central Asia, where scarce rainfall and elevated temperatures have impaired crops, livestock and food security since 2021. It analyses the shared climatic drivers linking the two regions.

Four regions of analysis are here defined:

- East Africa: Somalia, Ethiopia, Kenya, Djibouti, Eritrea
- Greater East Africa: Somalia, Ethiopia, Kenya, Djibouti, Eritrea, Sudan, South Sudan, Uganda, Rwanda, Burundi, Tanzania
- Iran
- Middle East/Central Asia: Iran, Iraq, Armenia, Azerbaijan, Turkmenistan, Uzbekistan, Afghanistan, Tajikistan

4 https://drought.emergency.copernicus.eu/data/factsheet.

5 https://data.jrc.ec.europa.eu/collection/drought.

2. Standardized Precipitation Index (SPI)

The SPI provides information on the intensity of the precipitation deficit (or surplus) over a defined accumulation period (e.g. from 1 to 48 months). The lower (i.e., more negative) the SPI, the more intense is the drought. SPI can be computed for different accumulation periods. The 3-month period is often used to evaluate agricultural drought and the 12-month (and longer) period for hydrological drought, when rivers fall dry and groundwater tables lower.

Figure 1 illustrates the temporal evolution of the SPI-3 over 2021-2025 in East Africa, with bi-annual maps covering the periods from March to May and October to December for each year. Indeed, these periods represent the end of the two rainy seasons in the region. The spatial distribution of SPI-3 values reveals a complex and variable pattern, characterized by alternating periods of severe drought and excessive rainfall. The period of analysis started with the onset of a drought in 2021 that reached its peak in mid-2022, marking the most severe meteorological event of the entire period. Afterwards, conditions improved. However, this respite was short-lived, as the region experienced a significant shift towards highly wetter-than-normal conditions from mid-2023 to mid-2024, with a pronounced peak in late 2023. Then, it transitioned back to drought, from late 2024 to late 2025. This drought had lower severity compared to the one of 2022, and affected: Somalia, northern Ethiopia, and Eritrea.

Figure 1. SPI-3 computed for MAM (March-April-May) and OND (October-November-December) from 2021 to 2025.

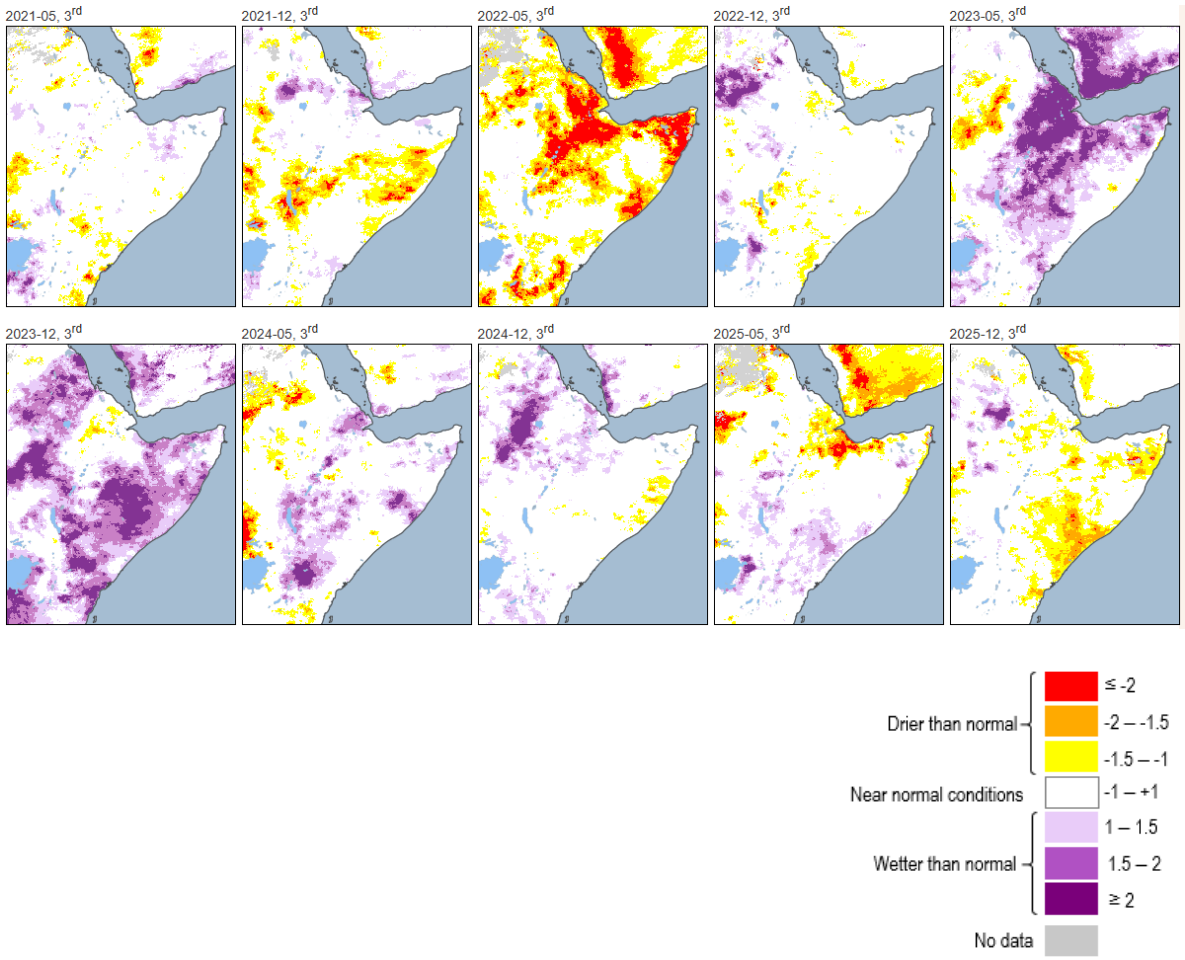

Source: JRC based on CHIRPS (Climate Hazards Group InfraRed Precipitation with Station).

Figures S1 and S2 (in the Annex) show the percentage of area in East Africa and in the Greater East Africa region (as previously defined) falling into each class of the SPI-3 from 1995 to 2025. The bar plots reveal that East Africa and the Greater East Africa region exhibit similar patterns in terms of distribution of the SPI-3 classes. There is no clear visible trend, although 2020-2025 appears to have experienced more frequent severe over-wet and dry events. The most critical drought events in both regions occurred in 1999-2000, 2009-2011, and 2022. The similarity between the two bar plots suggests that the drought patterns and their severity are comparable in the two regions.

Figure 2 illustrates the temporal evolution of the SPI-3 over the Middle East/Central Asia region, with bi-annual maps plotted in March and June of each year, coinciding with the peak (January to March) and the end (April to June) of the wet season, respectively. In contrast to the East African region, more persistent meteorological drought conditions were observed, although with variable spatial patterns. A severe drought already affected the region in March 2021, mainly Iran and Iraq, before shifting north-eastwards by June 2021, impacting the Turan Depression and Central Asia. A slight improvement in conditions characterises 2022, with less severe precipitation deficits. Similar patterns persisted in 2023. A transition occurred in 2024, with normal and even wet conditions in some areas. Nevertheless, this respite was short-lived, as the meteorological drought became extremely critical in 2025, with high severity estimated across nearly the entire region.

Figure 2. SPI-3 computed at the peak (March) and at the end (June) of the rainy season from 2021 to 2025 in the Middle East/Central Asia region.

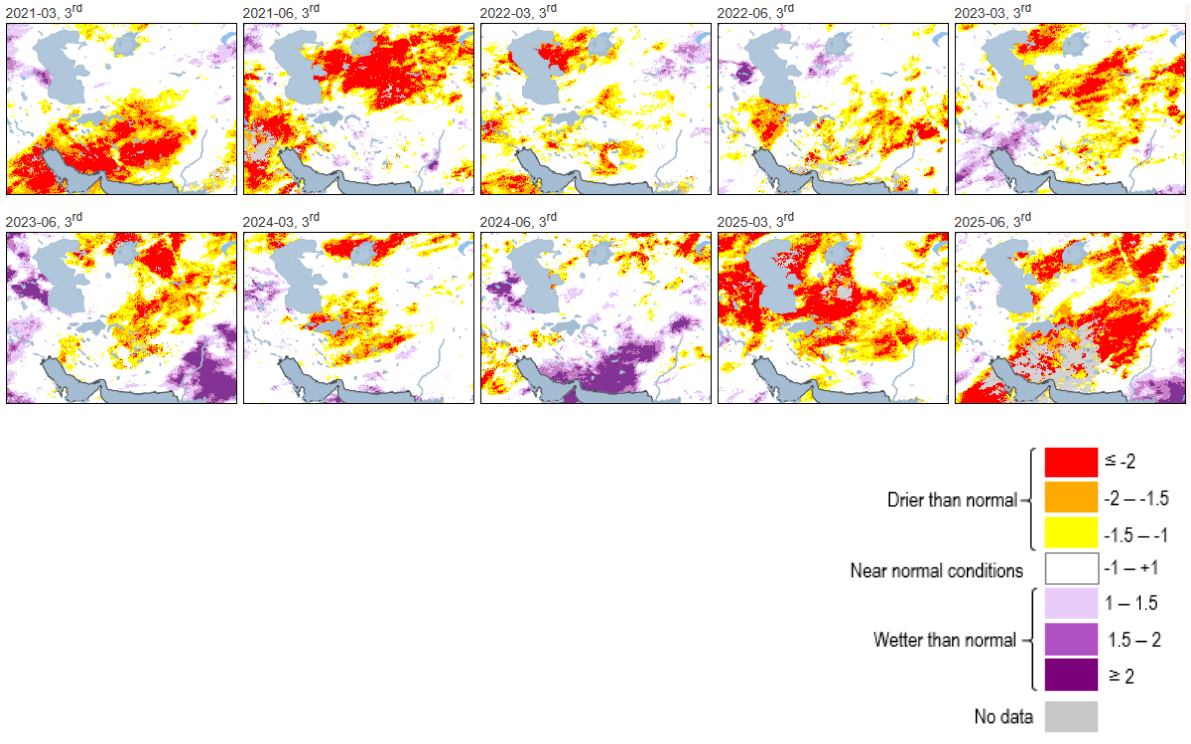

Source: JRC based on CHIRPS.

The bar plots for Iran (Figure S3 in the Annex) and the Middle East/Central Asia region (Figure S4 in the Annex) reveal a distinct pattern compared to East Africa and the Greater East Africa region. They exhibit a more pronounced tendency towards more intense and spatially broader droughts in the last 5-6 years. An increase in frequency, duration, and severity of droughts is evident, with a higher percentage of area affected by severe drought conditions. In contrast to the relatively stable pattern observed in East Africa and the Greater East Africa region, Iran and the Middle East/Central

Asia region show a marked shift towards more extreme drought events. The bar plots suggest that the region has been experiencing a significant escalation in drought severity, with more frequent and prolonged periods of water stress. The increased frequency and severity of droughts in the last 5-6 years may be indicative of a large-scale climate signal related to changes in precipitation patterns compounded by temperature increases. The spatial extent of droughts also appears to have expanded, affecting a larger percentage of the region. This tendency is of concern, as it may have significant implications for water resources, agriculture, and for the ecosystems in the region. Overall, the bar plots for Iran and the Middle East/Central Asia region highlight a pressing need for enhanced drought monitoring and management strategies, as well as adaptation measures to mitigate the impacts of increasingly frequent and severe droughts.

Figure 3 presents a comparative analysis of the SPI over a 12-month period in August (SPI-12) for the Middle East/Central Asia region and East Africa from 2011 to 2025. This timeframe was chosen to encompass the entire wet season in the Middle East and the cumulative effects of both rainy seasons in East Africa. The top panel, focusing on East Africa, reveals significant interannual variability in precipitation patterns. A worsening of conditions is evident from 2021 to 2022, when the meteorological drought reached its most severe state, affecting Somalia, Ethiopia, and Eritrea. Afterwards, a marked transition occurred, with a shift towards normal conditions in 2023, followed by severely wet conditions in 2024, which resulted in extensive flooding. By 2025, the region returned to near-normal conditions. This sequence of events highlights the complex and dynamic nature of precipitation patterns in East Africa, with significant implications for climate-resilient decision making and early warning systems.

Figure 3. SPI-12 computed at August (cumulative rainy seasons) from 2021 to 2025 in East Africa (top panel) and the Middle East/Central Asia region (bottom panel).

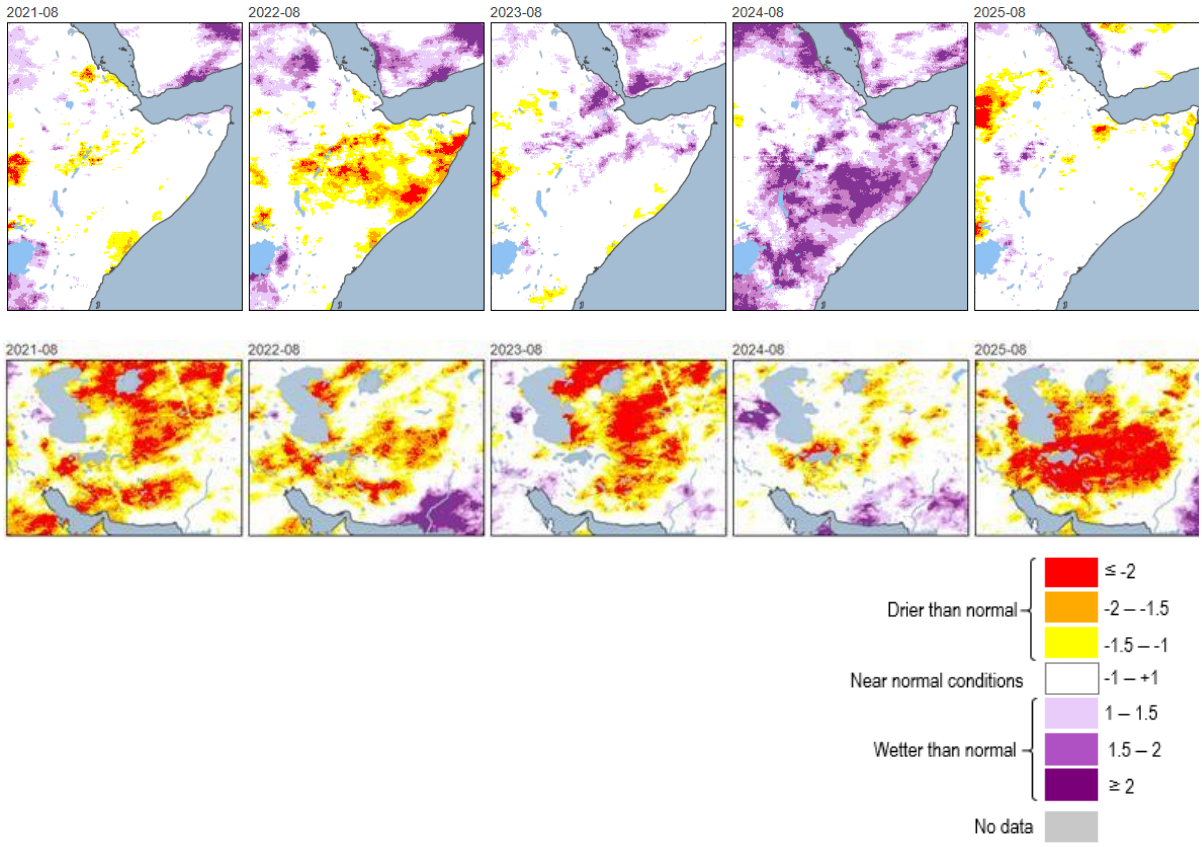

Source: JRC based on CHIRPS.

3. Temperature and the Standardized Precipitation Evapotranspiration Index (SPEI)

The timeseries of maximum and minimum daily temperature anomalies in East Africa and the Middle East/Central Asia region (Figure 4) show, besides a clear warming trend, that the period between 2021 and 2025 experienced continuous positive monthly anomalies, being also the warmest 5-year period for both maximum and minimum daily temperatures since 1981.

Figure 4. Monthly timeseries of maximum (top panel) and minimum (bottom panel) daily temperature anomalies (with respect to 1991-2000) in East Africa (left panel) and the Middle East/Central Asia region (right panel). Data are from ERA5 (ECMWF (European Centre for Medium-Range Weather Forecasts) Reanalysis version 5).

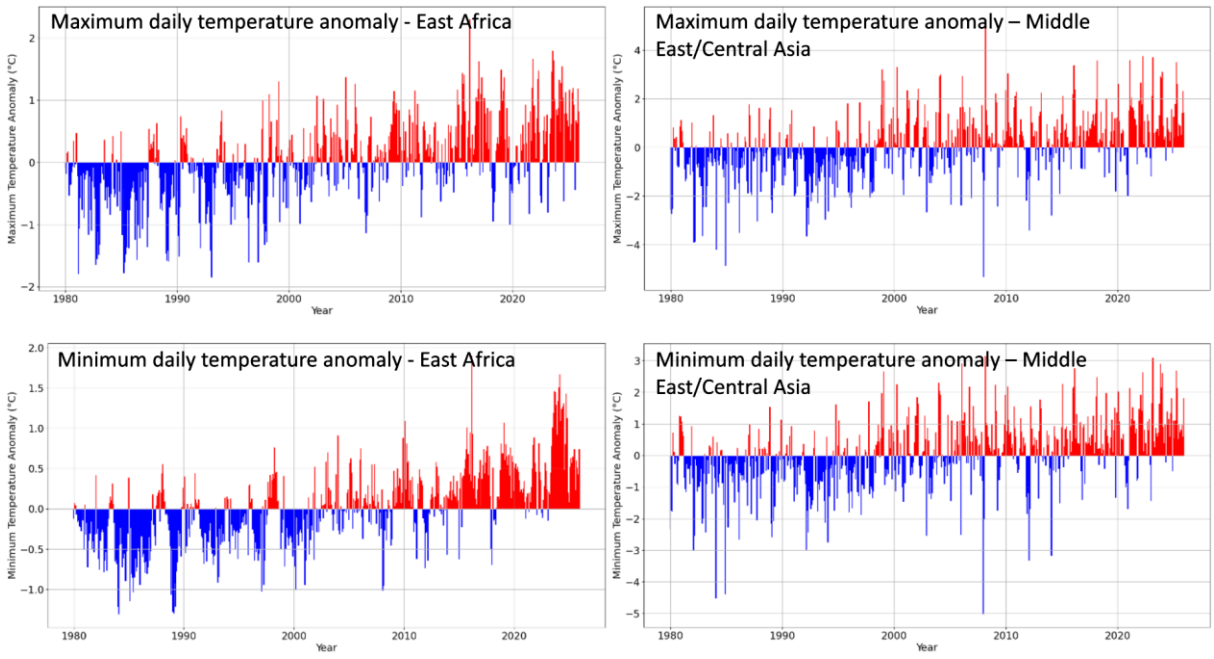

Source: JRC based on ERA5.

SPEI accounts for both precipitation and evapotranspiration (potential evapotranspiration, PET, is here computed with the Hargreaves-Samani[6] method) to estimate anomalies of the climatic water balance (precipitation minus potential evapotranspiration) with respect to the climatological average over a given period. Thus, SPEI provides an estimation of the combined effects of precipitation deficit and warmer-than-usual conditions. Here SPEI is based on ERA5 data, while SPI formerly discussed is based on CHIRPS data. This may induce some differences between the two datasets.

Figure 5 illustrates the temporal evolution of the Standardized Precipitation Evapotranspiration Index (SPEI-3) over East Africa, with bi-annual maps plotted in May and December of each year,

[6] See Hargreaves, G. H. and Samani, Z. A.: Estimating potential evapotranspiration, J. Irrig. Drain E.-ASCE, 108, 223–230, 1982 and Hargreaves, G. H. and Samani, Z. A. 1985. Reference crop evapotranspiration from ambient air temperature, American Society of Agricultural Engineers, 12 pp., available at: http://libcatalog.cimmyt.org/download/reprints/97977.pdf.

coinciding with the end of the region's two rainy seasons, from 2021 to 2025. The SPEI-3 reveals a more pronounced drought worsening trend from mid-2021 to late 2022, with the entire East Africa experiencing extremely dry conditions by the end of 2022. This suggests that the drought had a significant impact on the region's water balance, with temperature anomalies exacerbating the effects of precipitation deficits. However, a transition occurred from late 2022 onwards, with a shift from moderate dry conditions to wetter-than-normal conditions in 2023 and mid-2024, although the northwestern region, including Sudan and South Sudan, remained extremely dry. Following this improvement, a new drought event emerged from late 2024 to late 2025, initially affecting Somalia and then spreading to Eritrea, before severely worsening and impacting a larger area, including Somalia, Kenya, and southern Ethiopia, by late 2025. As SPEI-3 accounts for evapotranspiration, it can reveal the complex interplay between precipitation and atmospheric evaporative demand, providing a more comprehensive understanding of drought dynamics in the region.

Figure 5. SPEI-3 computed for MAM and OND (rainy seasons) from 2021 to 2025 in East Africa.

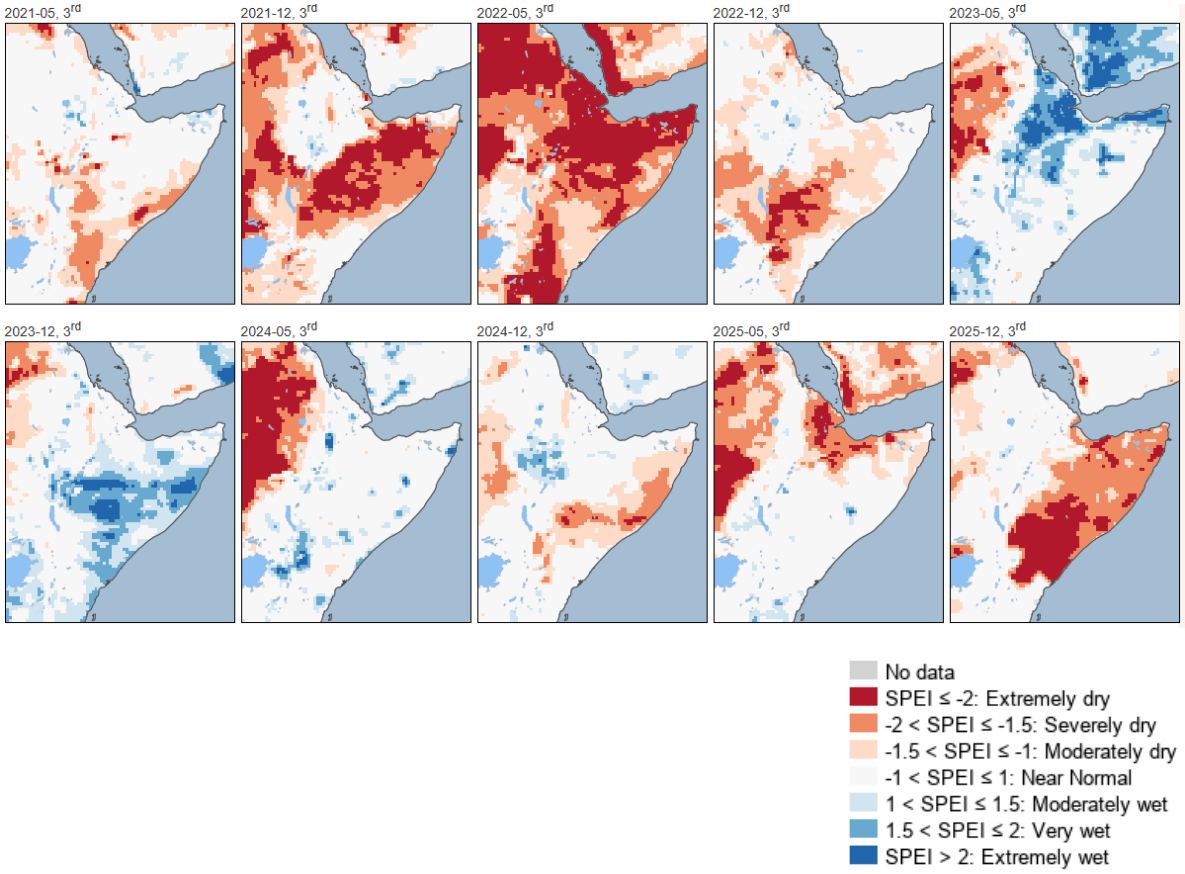

Source: JRC based on ERA5.

The bar plots of SPEI-3 for East Africa (Figure S5 in the Annex) and for the Greater East Africa region (Figure S6 in the Annex) reveal a notable increase in drought events and in their severity from 2020 to 2025. Unlike the previous analysis of SPI-3, which showed a relatively stable pattern, the SPEI-3 bar plots exhibit a more defined trend towards more frequent and intense droughts in the recent years. This suggests that rising temperatures in the region contributed to the higher severity of drought events. Warming temperatures may, indeed, exacerbate drought conditions. This trend is of concern, as it may have significant implications for water resources, agriculture, and ecosystems.

Figure 6 illustrates the temporal evolution of the SPEI-3 over the Middle East/Central Asia region, with bi-annual maps plotted in March and June of each year, coinciding with the peak and the end of the wet season, respectively, from 2021 to 2025. The SPEI-3 pattern shows similarities with the one of SPI-3, with a severe drought affecting the region in 2021, initially impacting Iran and Iraq, and subsequently spreading over the Turan Depression and Central Asia. In 2022, the drought conditions improved; however by March 2023, the Turan Depression was again severely affected by drought. From mid-2023 to mid-2024, a transition towards normal or even wet conditions occurred, particularly in southern Iran, indicating a temporary improvement in the water balance. Nevertheless, by 2025, drought conditions re-emerged, albeit in a more sparse and fragmented manner, across the Middle East and Central Asia, with a slight worsening tendency.

Figure 6. SPEI-3 computed at the peak (March) and at the end (June) of the rainy season in Middle East/Central Asia from 2021 to 2025.

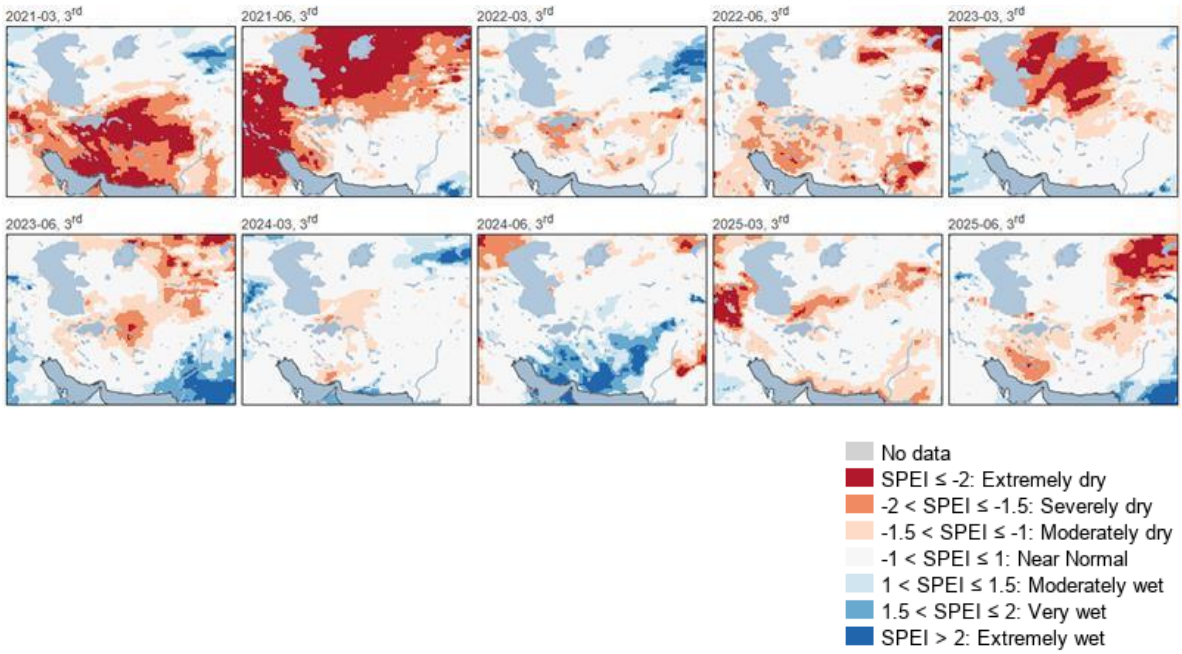

Source: JRC based on ERA5.

The bar plots of the SPEI-3 for Iran (Figure S7 in the Annex) and the Middle East / Central Asia region (Figure S8 in the Annex) reveal a pronounced tendency towards increased drought severity and frequency from 2020 to 2025. The existing trend of declining precipitation in the region is exacerbated by rising temperatures. The bar plots show a marked increase in the frequency and severity of drought events, with Iran being particularly affected. The country's bar plot indicates a significant spike in severe drought conditions in recent years, confirming that Iran has been the most affected country of the region in 2024-2025. The combination of declining precipitation and rising temperatures has triggered critical drought conditions in the region, with severe implications for water resources, agriculture, and ecosystems.

Figure 7 presents a comparative analysis of the SPEI-12 computed at August from 2021 to 2025 for East Africa and the Middle East/Central Asia region. This timeframe was chosen to capture the cumulative effects of the entire wet season in both regions. In East Africa, a severe worsening of drought conditions is evident from 2021 to 2022, with a subsequent shift in the its spatial pattern. In 2023/24, drought moved northwestern, affecting Sudan. Somalia, Kenya, and Ethiopia experienced wet conditions, particularly in 2024. In 2025, however, a new drought event emerged,

involving almost the entire region of interest. In contrast, the Middle East/Central Asia region exhibited more stable dry conditions, with only a brief relief phase observed in 2024. In the other years, conditions were very dry, with the widest extent of drought observed in 2021 and again in 2025. The comparison between the two regions highlights the distinct drought trajectories, with East Africa experiencing a more variable and dynamic pattern, while the Middle East/Central Asia region being characterized by a more persistent and widespread drought.

Figure 7. SPEI-12 computed at August (cumulative rainy seasons) from 2021 to 2025 in East Africa (top panel) and the Middle East/Central Asia region (bottom panel).

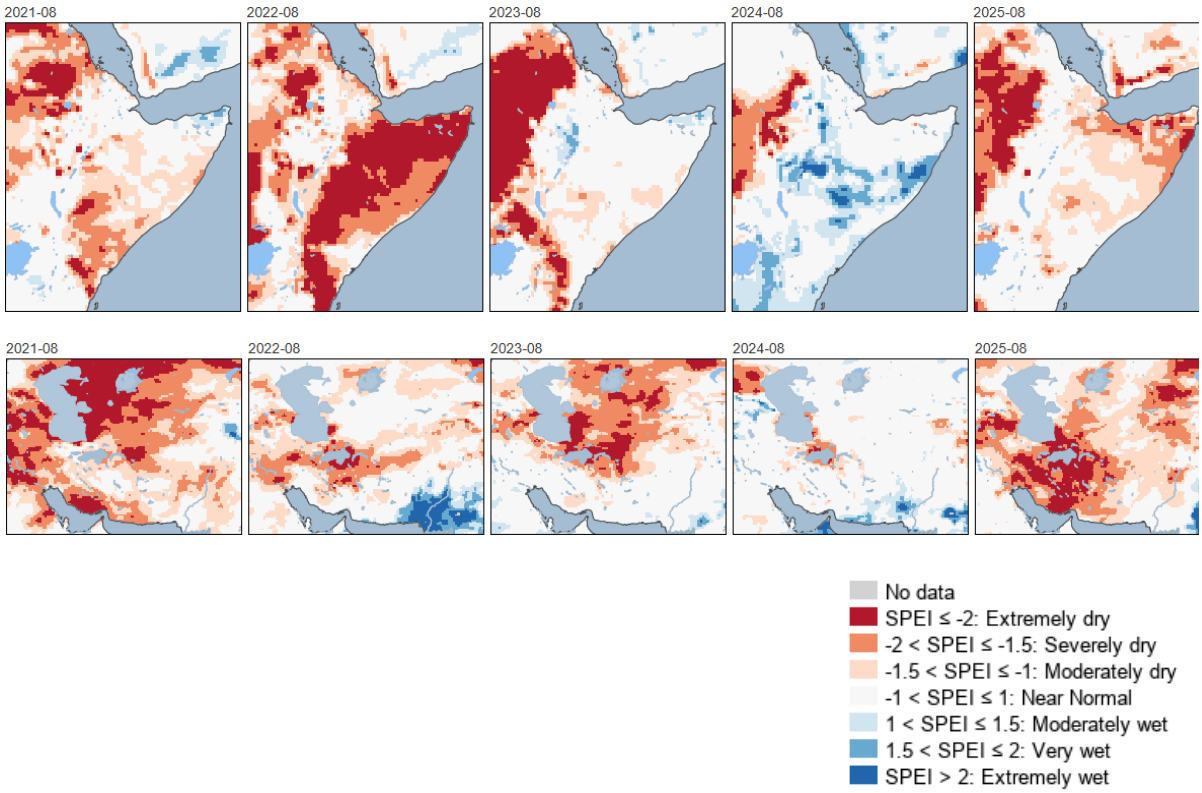

Source: JRC based on ERA5.

The bar plots of SPEI-12 from 1995 to 2025 (Figures S9-S12 in the Annex) provide a comprehensive overview of drought conditions across the four regions of analysis. They reveal more pronounced dry anomalies over the last 5-6 years, pointing to both its severity and its persistence since 2020, with a significant impact on hydrological systems.

However, some notable differences emerge between the regions. For instance, in the year 2000, the drought was less severe in East Africa compared to the Middle East/Central Asia region. Conversely, around 2010, the drought was more persistent in East Africa.

From 2015 to 2020, the drought conditions were more severe in East Africa, with a notable peak in drought severity. In contrast, the Middle East/Central Asia region experienced a significant peak in drought severity in 2020, highlighting the variability and regional differences in drought patterns over time.

The more evident signal in SPEI-12 compared to SPEI-3 may suggest that the current drought is related to hydrological aspects, such as soil moisture depletion, groundwater recharge, and water storage, rather than just being driven by precipitation deficits. This implies that the impacts of the

drought on water resources, agriculture, and ecosystems may be more profound and long-lasting, requiring a more comprehensive and sustained response.

To further evaluate the spatio-temporal dynamics of the recent drought events over the Middle East/Central Asia region and East Africa, a variant of the meteorological drought tracking method[7] is applied from January 2020 to December 2025. While the original methodology to compute the meteorological drought tracking relies on SPI-3, this variant is based on a combination of the SPEI-1 and SPEI-3. This improvement can simultaneously capture short-term anomalies driven by, e.g., evaporative demand as well as longer scale ones associated, for instance, with precipitation deficits.

Figure 8. Temporal evolution and spatial location of the six most relevant drought events in the Middle East/Central Asia region and East Africa during the period 2020-2025.

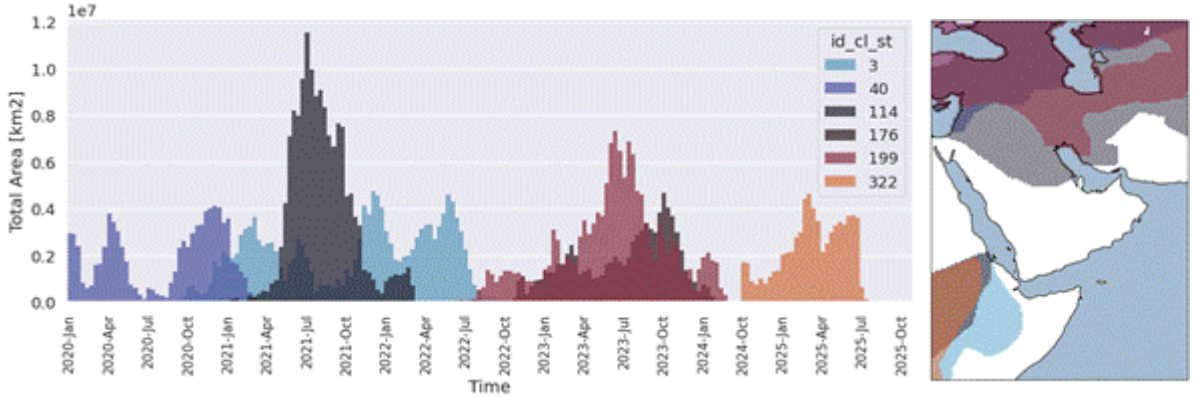

Source: JRC based on ERA5.

This analysis (Figure 8) reveals a sequence of drought events evolving over the Middle East/Central Asia region and East Africa.

- 2021–2022 A massive drought event (identified in dark grey, ID 114) rapidly developed in the Middle East/Central Asia region and peaked in mid-to-late 2021. It covered a vast area exceeding at its maximum extent over 10 million km^2. This aligns with the severe meteorological drought observed in Iran and Iraq that subsequently shifted north-eastwards into the Turan Depression.
- Another significant, localized event in the Middle East/Central Asia region (purple, ID 40) occurred from early 2020 to early 2021, less significant in terms of spatial coverage (with a peak of about 4 million km^2) than the event ID 114.
- 2021–2022 During the early 2021, a distinct and severe drought event (light blue, ID 3) emerged over East Africa, showing three distinct peaks: a first between the first quarter of 2021, a second during late 2021, and a third one during the second quarter of 2022. Spatially, this event was localised mostly over Somalia, Ethiopia and Eritrea. This tracks the onset of the devastating multi-season drought that led to widespread crop failures, historic low soil moisture, and severe vegetation stress across East Africa.

[7] https://journals.ametsoc.org/view/journals/hydr/24/3/JHM-D-22-0115.1.xml

— 2022-2023 By late 2022, a significant drought event developed over the Middle East/Central Asia region (reddish-brown, ID 199). The event peaked during mid-2023, perfectly correlated with the re-emergence of severe SPEI-3 drought conditions observed in the Turan Depression after a brief period of relief during the second quarter of 2022.

— 2024–2025 From late 2024 throughout 2025, a highly persistent and expanding drought event (orange, ID 322) dominated the drought tracking timeseries. Spatially, this event heavily impacted East Africa, spreading across western Ethiopia, Sudan, and Kenya. This confirms the emergence of a renewed, widespread drought phase in the region that followed the short-lived wet anomalies of early 2024, leading to the severe water balance deficit.

As highlighted by the pattern of drought events over the Middle East/Central Asia region and East Africa, the results of the drought tracking analysis indicates that drought has been more intensively concentrated in two distinct areas, as shown in Figure 9.

Figure 9. Cumulative drought intensity over the Middle East/Central Asia region and East Africa in 2020-2025.

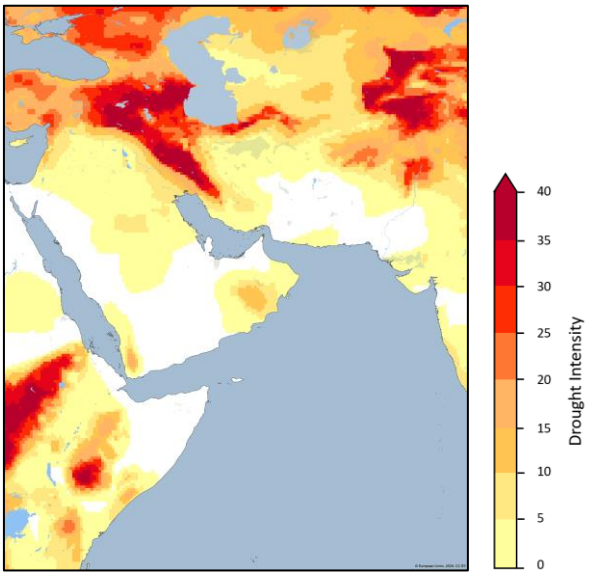

Source: JRC based on ERA5.

Figure 9 illustrates the total sum of the intensity of drought events between 2020 and 2025, highlighting the areas most critically affected by persistent and severe drought conditions. In the Middle East/Central Asia region, the most severe intensities form a broad, dark-red band stretching from northern and central Iran, up through Turkmenistan, northern Afghanistan, and parts of Uzbekistan and Tajikistan. Concurrently in East Africa, extreme drought intensities are deeply concentrated over the Horn of Africa, particularly devastating southern Somalia, western Ethiopia, and eastern Kenya. These intensity hotspots align perfectly with the regions exhibiting the most pronounced long-term SPEI-12 anomalies and historical soil moisture depletion.

In summary, the modified tracking approach underscores that while both regions have experienced recurrent crises, the drought episodes have operated on distinct, alternating timelines. The inclusion of evapotranspiration via SPEI confirms that the compounding effect of positive temperature anomalies has been a primary driver of the intensity and spatial expansion of these drought events.

4. Soil moisture

The Soil Moisture Index Anomaly (SMA) is a standardized index that estimates the deviations from normal conditions of the root-zone water content. It is an index derived from a hydrological model (LISFLOOD) associated with the difficulty of plants in extracting water from the soil.

In 2021-2025, the soil moisture anomaly pattern exhibits similarities with the SPI and SPEI indicators (Figure 10), although with a time-lag in some cases. In May 2021, soil moisture conditions were still close to normal, but by December 2021, moderate dry conditions developed, and by May 2022, extremely dry conditions spread across almost the entire region. The drought persisted until late 2022, when it slowly began to recede, although it continued to affect southern Ethiopia and Somalia. From late 2022 to mid-2024, the region gradually transitioned towards wet conditions, with Somalia, Kenya, and Ethiopia experiencing the most significant improvement in soil moisture. However, from late 2024 onwards, drought conditions began to worsen again, reaching severe levels over southern Somalia, Kenya, and southern Ethiopia by late 2025. The soil moisture anomaly patterns highlight the complex and dynamic nature of drought in East Africa, with significant implications for agricultural productivity, water resources, and ecosystem health.

Figure 10. SMA computed at the end of each MAM and OND rainy season from 2021 to 2025 in East Africa.

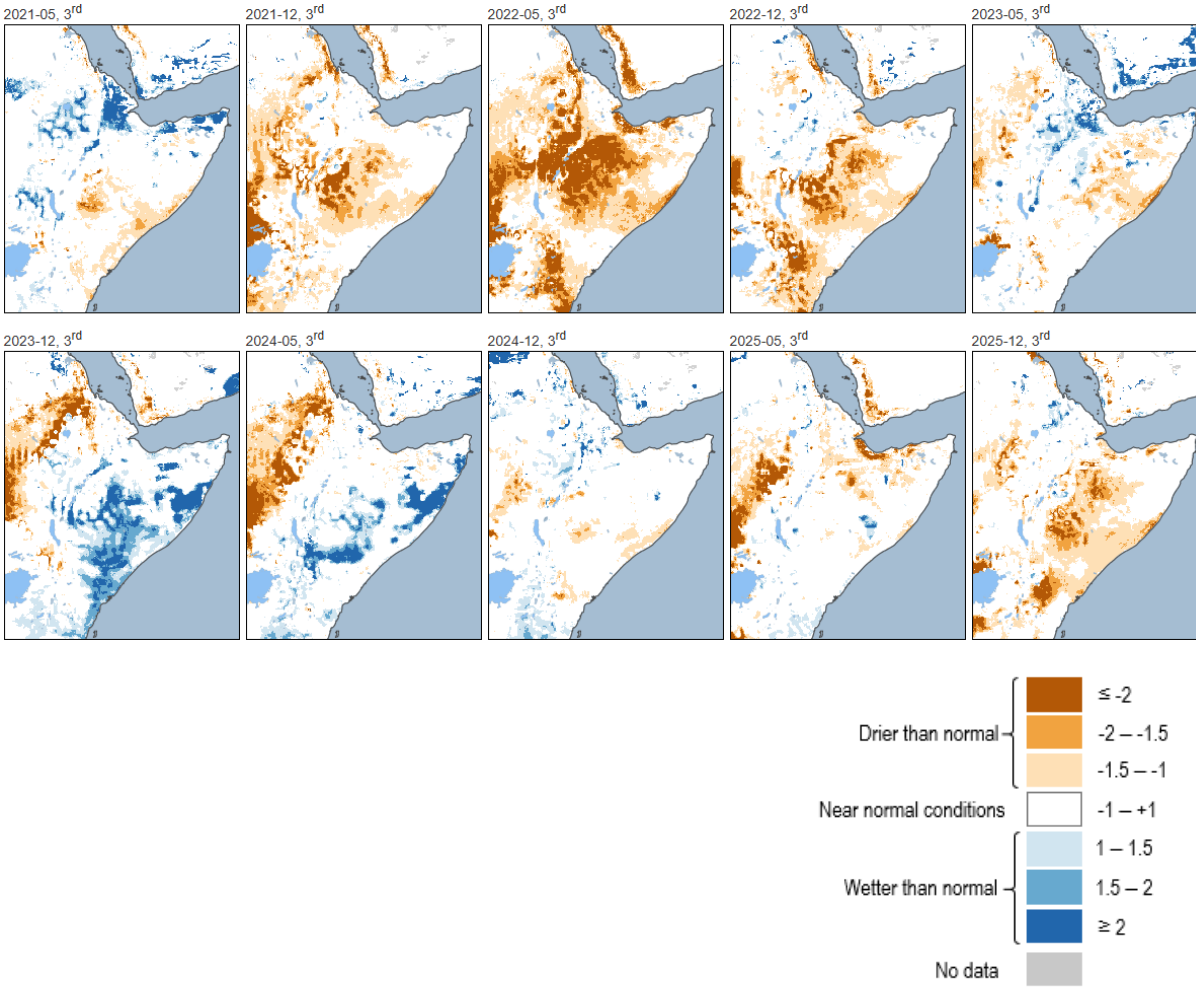

Source: JRC based on OS LISFLOOD hydrological model.

In the period 1995-2025 the general temporal evolution of soil moisture anomaly is remarkably similar to the one of the SPEI-12 data (Figures S13-S14 in the Annex). In terms of percentage of area affected by drought in East Africa and in the Greater East Africa region, the former one shows higher values, consistent with the fact that the countries within this region were more severely hit by the drought. This also suggests that the drought had a more pronounced impact on the smaller East Africa, which are entirely encompassed within the larger Greater East Africa region. The Greater East Africa region exhibits persistent and continuous drought, but characterized by lower percentage of affected area. This indicates that while drought conditions have been present in the region over the years, they have not been as widespread and severe as in East Africa.

Drought events following 2020 are more significant in terms of spatial extent, with a notable increase in the percentage of affected area. The transition from the over-wet period in 2020 to a prolonged and widespread dry period in 2021-2025 is particularly striking. The discontinuity in soil moisture conditions after 2020 is evident, with a shift from wet to extremely dry conditions that have persisted over the past few years. This suggests that drought had a profound impact on soil moisture levels, leading to a significant depletion of water resources and exacerbating the effects on agriculture, ecosystems, and human populations.

Figure 11 shows the temporal evolution of soil moisture anomalies in the Middle East/Central Asia region, with bi-annual maps plotted in March and June of each year, coinciding with the peak and end of the wet season, respectively, from 2021 to 2025. In contrast to East Africa, the soil moisture anomaly patterns in the Middle East/Central Asia region exhibit more stable conditions, with persistent dry conditions throughout the period. The worst conditions are estimated in 2021, with very dry soil moisture anomalies prevailing across the region. A slight improvement is detected in 2022, 2023, and 2024, although conditions remained generally dry. However, in 2025 soil moisture anomalies worsened again. In the central part of the region, particularly northern Iran, the highest persistence of drought is estimated, with consistently dry conditions throughout the period. In contrast, the southern region, mainly southern Iran, shows the highest variability, with periods of wetter-than-normal conditions interspersed with dry spells. This spatial variability highlights the complex and heterogeneous drought sequence in the Middle East/Central Asia region, with different areas experiencing distinct drought trajectories. In these regions also cryosphere-related and snow processes play a relevant role, shifting and changing the soil moisture patterns. These patterns suggest that drought conditions are influenced by a combination of climate drivers and local factors that can modulate drought and lead to varying levels of severity and persistence.

Figure 11. SMA at the peak (March) and at the end (June) of the rainy season from 2021 to 2025 in the Middle East/Central Asia region.

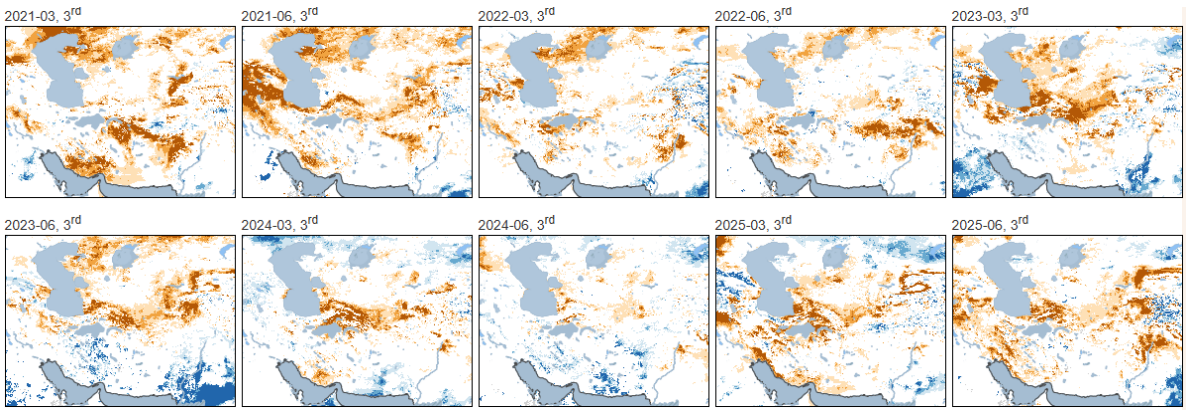

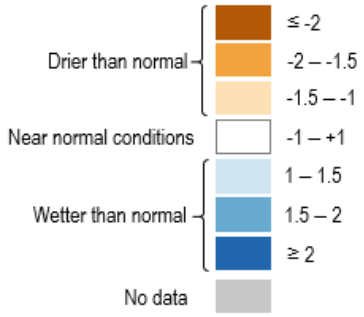

Source: JRC based on OS LISFLOOD hydrological model.

The temporal evolution of SMA in the period 1995-2025 (Figures S15 and S16 in the Annex) reveals homogeneous condition across the larger area, with limited differences between Iran and the broader Middle East/Central Asia region. Several negative peaks are visible in the timeseries, which are more pronounced compared to East Africa. For example, around 2000 a quite prolonged dry peak is evident, indicating a significant drought event that affected the region. Other dry peaks are visible in 2008 and 2018. The period 2021-2025 stands out as exceptional in terms of severity, persistence, and extent. The soil moisture anomaly during this period is characterized by an unprecedented level of dryness, with a significant percentage of the affected area. This suggests that the current drought event is one of the most severe and widespread on record, with potentially devastating impacts on agriculture, water resources, and ecosystems in the region.

5. Hydrology

Figure 12 shows the annual Runoff or Water Equivalent (ROWE) anomalies across East Africa for 2021–2025 (with respect to the 1991–2020 baseline; mm y^{-1}). In 2021 and 2022, widespread negative anomalies dominate the Ethiopian Highlands and some Kenian and Ugandan regions around Lake Victoria, impacted by La Niña conditions. However, the effects of the drought in 2021 and 2022 in the Horn of Africa are not visible in the GloFAS (Global Flood Awareness System) runoff data, neither as absolute nor as standardized anomalies. The region has a flat terrain and is characterized by ephemeral streams, no major perennial streams, and many areas with below 1 mm climatological runoff values. While in parts of the Ethiopian Highlands the negative runoff anomalies became even worse following the lack in precipitation, increasingly positive anomalies and partly wetter conditions are visible in 2023 and 2024 along the Rift Valley, coastal Kenya, and parts of Somalia. In 2025, the negative anomaly pattern re-establishes itself across much of the domain and most prominently again in northern Ethiopia, Somalia and around Lake Victoria indicating renewed hydrological drought stress. Throughout all years, the Ethiopian Highlands emerge as the most persistently and severely impacted cluster, reflecting both the high elevation variability and the strong sensitivity of highland runoff to the El Niño-Southern Oscillation (ENSO) and the Indian Ocean Dipole (IOD) forcing.

Figure 12. East Africa runoff anomalies (with respect to 1991–2020) from 2021 to 2025.

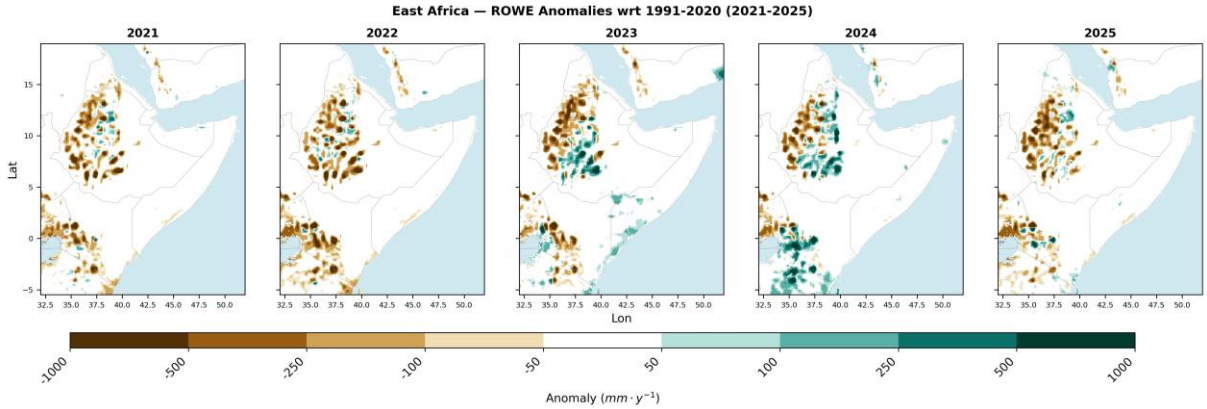

Source: GloFAS.

Figure 13 shows the annual the runoff anomalies across the Middle East for 2021–2025. In 2021, broadly negative anomalies dominate the region, with deficits spanning Iraq, Iran, the Levant, and the Arabian Peninsula, consistent with the La Niña-driven suppression of precipitation across the region. The pattern generally persists in 2022, particularly across the Zagros mountain range and western Iran, which are among the most hydrologically active zones in the Middle East given their role in Tigris–Euphrates headwater runoff. Isolated positive anomalies appear in the south of the domain in 2022, likely reflecting localised convective events rather than a coherent large-scale signal. In 2023, negative anomalies continue across the domain, however, the large negative belt in the West is resolved and not present anymore as a response to the 2023 positive IOD and El Niño forcing. By 2024, the negative signal weakens visibly across multiple parts of the domain, with near-neutral to slightly positive anomalies becoming more widespread. The positive runoff anomalies in 2023 and 2024 are in line with the SPI results as well as the positive soil moisture anomalies. Moreover, the generally wet 2024 was subject to significant flood events in its first half in Afghanistan and South of Iran. In 2025, the negative runoff anomaly belt in the West re-

established together with generally drier conditions following the negative IOD and La Niña co-occurrence.

Figure 13. Middle East runoff anomalies (with respect to 1991–2020) from 2021 to 2025.

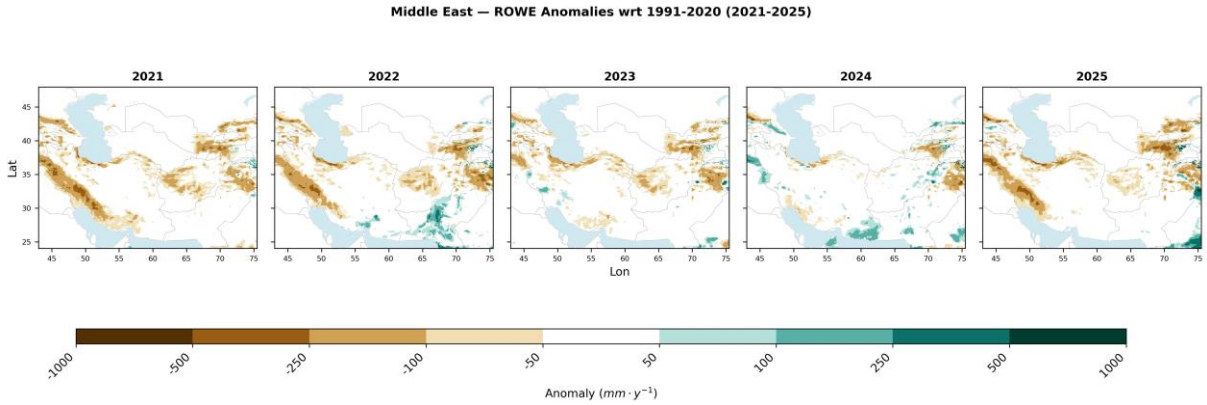

Source: GloFAS.

Figure S17 (in the Annex) shows the standardised monthly discharge anomalies (σ, relative to the 1991–2020 baseline) for the Middle East (panel a) and East Africa (panel b) from 1980 to 2025. Each panel includes a monthly discharge anomaly heatmap, an overlaid annual discharge anomaly time series, and the seasonal discharge cycle plots for 2021–2025 versus climatology in absolute values (km^3/month). Both regions exhibit high inter-annual variability with no clear long-term trend, albeit a minor tendency for negative discharge anomalies in recent years. In the Middle East, the most extreme negative anomaly in the record occurs around 2021, with the annual mean approaching −1.2σ, consistent with the severe drought conditions across the domain. 2024 shows a partial recovery toward a positive anomaly, consistent with the weakening negative spatial SPI pattern mainly occurring during late summer and autumn in the Middle East. However, the strong positive standardized anomalies in these periods are only partly reflected in the absolute values of the Middel East, as the dominant rivers remained less affected, which were vice versa strongly contributing to the Middle East absolute flow reductions visible in 2021 and 2025.

The analysis over East Africa on the other hand suggests above-average discharge anomalies in the early 1980s and mid-1990s, followed by prolonged near-normal and slightly negative discharge anomalies from approximately 2000 to 2019. Similar transitions from wet to dry conditions can be found in 1999/2000 and 2020/2021 in line with a positive IOD and El Niño conditions, yet with different magnitudes. All the years from 2021 to 2025 except 2024, show suppressed flows relative to the climatology, with coloured lines consistently falling below the black climatology curve during large parts of the annual cycle.

6. Large-scale drivers and hydrology

Ocean variability is a major driver of hydroclimatic variability in East Africa and the Middle East/Central Asia region at seasonal and annual timescales[8]. To identify oceanic drivers of SPI and SPEI variability, we sampled from a large climate model ensemble (150 members) the states that resemble the evolution of the observed SPI (SPEI) over the period 1960-2019. Figure S18 (in the Annex) shows an example of the evolution of the observed SPI-12 in both regions and the one created by sampling the model analogues closest to observations[9].

After having selected the best analogues for SPI each year, the sea surface temperature anomalies of those models are confronted with the observations by estimating the temporal correlation coefficient between them during the same period (1960-2019). Although not being a direct quantification of causality, this analysis indicates whether those selected model states (in which SPI -SPEI- are closest to the observed state) have a statistical association with observations in terms of sea surface temperature anomalies. In other words, this allows us to find regions of the oceans which are statistically associated with the SPI in East Africa and the Middle East/Central Asia region. Figure 14 shows the maps of sea surface temperature correlation between observations and the analogues selected through SPI-3 and SPEI-3 (OND and MAM seasons) in East Africa and for SPI-12 and SPEI-12 in East Africa and the Middle East/Central Asia region. There is a clear statistical association in the tropical Pacific (e.g. ENSO) and the Indian (e.g. IOD) Oceans, particularly clear for the short rains period (OND) and for SPI-12 in both regions, stronger in the Middle East/Central Asia region than in East Africa at the annual timescales. The large resemblance of the patterns indicates that both regions share important common drivers of hydroclimatic variability at seasonal to annual timescales, and this variability stems primarily from tropical oceans.

---

[8] Meehl, G.A., Richter, J.H., Teng, H. *et al.* Initialized Earth System prediction from subseasonal to decadal timescales. *Nat Rev Earth Environ* 2, 340–357 (2021). https://doi.org/10.1038/s43017-021-00155-x.

[9] Acosta Navarro, J. C., Aranyossy, A., De Luca, P., Donat, M. G., Hrast Essenfelder, A., Mahmood, R., Toreti, A., and Volpi, D.: Seamless seasonal to multi-annual predictions of temperature and Standardized Precipitation Index by constraining transient climate model simulations, Earth Syst. Dynam., 16, 1723–1737, https://doi.org/10.5194/esd-16-1723-2025, 2025.

Figure 14. Sea surface temperature temporal correlation between observations and the model analogues selected by sampling the model members that are closest in terms of SPI-3 (left) and SPEI-3 (right) states in East Africa for the short rains (OND, first row), long rains (MAM, second row), SPI-12 (left) and SPEI-12 (right) in East Africa (third row) and the Middle East/Central Asia region (fourth row).

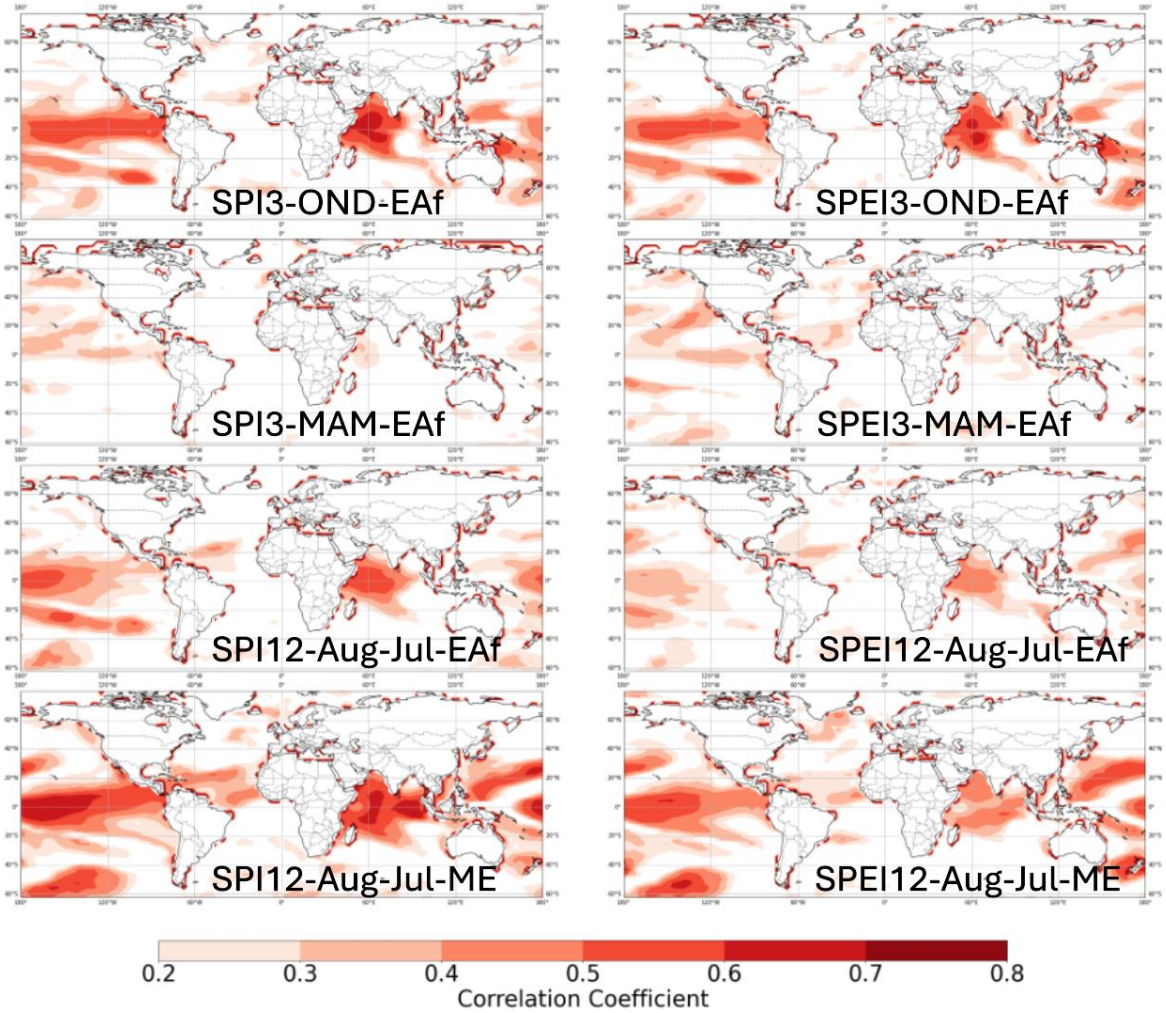

Source: JRC based on CMIP6 data.

East Africa and the Middle East/Central Asia region tend to experience drier-than-usual conditions when the ENSO and/or the IOD are in their negative phase. During the last five years, both ENSO and IOD were primarily in negative phases during roughly 2021-2022 and 2025 (Figure S19 in the Annex), when drought conditions were strongest in both regions. Despite the influence of oceanic drivers, a clear upward trend in drought intensity and recurrence is also present in both regions possibly linked anthropogenic climate change[10].

Figure 15 shows the absolute runoff anomalies in East Africa together with the global Dipole Mode Index (DMI) and the Oceanic Niño Index (ONI) time series. The smoothed anomaly (bold black line) reveals near-neutral conditions through the 1990s, a prolonged negative trend from approximately

[10] Kimutai, J., Barnes, C., Zachariah, M., Philip, S.Y., Kew, S.F., Pinto, I., Wolski, P., Koren, G., Vecchi, G., Yang, W. and Li, S., 2025. Human-induced climate change increased 2021–2022 drought severity in horn of Africa. *Weather and Climate Extremes*, *47*, p.100745.

2000 to 2020, and a sharp positive reversal around 2020–21. The teleconnection fingerprint in East Africa shows a tendency of positive IOD events (red shading) being associated with elevated runoff anomalies, most notably in 1994, 1997–98, and 2019–20. The 1997-1998 runoff anomaly was likely affected by the "double forcing" of positive ONI and positive DMI. La Niña episodes (e.g. 1988–89, 1999–2001, 2010–12, 2020–22, 2024 onward) broadly correspond to suppressed or negative runoff anomalies. During 2021–22, runoff anomalies are clearly negative, consistent with the prolonged La Niña episode and the absence of positive IOD forcing, a condition unfavourable for East Africa short rains. A recovery is visible in the raw runoff signal (grey line) around 2023–24, coinciding with the concurrent strong positive DMI and emerging El Niño conditions, yet this response remains modest. More precisely, the smoothed anomaly does not rise above zero, suggesting that despite the favourable teleconnection state the runoff response was short-lived and did not translate into a sustained hydrological recovery. By 2024–25, as La Niña conditions re-establish and DMI returns to near-neutral, runoff anomalies tend to be negative again, reinforcing the ongoing drought signal across the region.

Figure 15. Monthly runoff anomalies (with respect to 1991-2020) in East Africa and global teleconnection time series. (a) Monthly time series of the DMI; (b) Regional runoff anomaly (mm/month) with 12-month smoothed mean (bold black) and DMI-shaded background where blue indicates negative phases and red positive phases of the corresponding index; (c) Monthly ONI time series. The reference period 1991–2020 is marked by the vertical dotted lines.

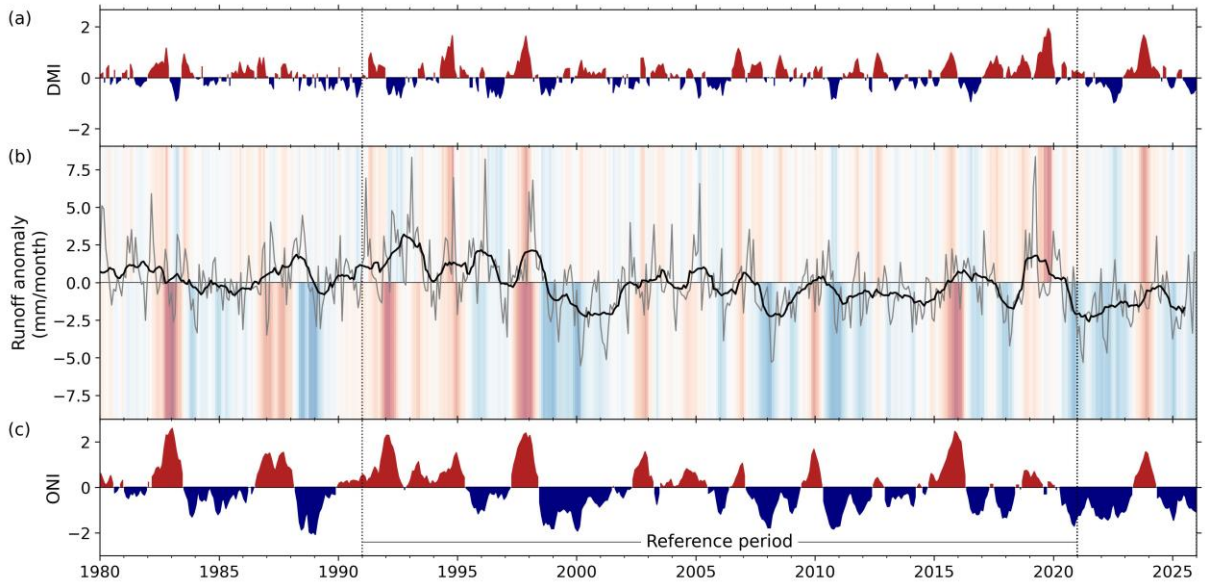

Source: GloFAS.

Runoff anomalies in the Middle East together with the global DMI and the ONI time series show high inter-annual variability with no pronounced long-term trend, oscillating around neutral throughout the reference period (Figure 16). The DMI shading in panel (b) points to a discernible imprint on the Middle East runoff. The strong positive DMI phases (red shading) are associated with several elevated runoff anomaly spikes, most clearly around 1997-98, 2019 and 2023, while extended negative DMI as well as La Niña phases correspond to below-average runoff. La Niña exception is the 1988-1989 period. The most striking feature is the sharp positive runoff peak around 1998-1999, coinciding with the strong El Niño and positive DMI, and pushing elevated runoff anomalies to the highest values in the 45-year period. The smoothed signal (bold black line) mostly remains close to zero, with a modest but sustained negative departure during 2006-2010s and from 2021 to 2023. The current period (2024–25) shows anomalies just below zero, indicating

marginally below-average but not critically deficient runoff conditions. The 2021-23 negative runoff anomalies are broadly consistent with the prevailing La Niña conditions. Around 2023–24, the anomalies rise significantly and become partly positive (both smoothed and raw signal) suggesting a more sustained hydrological response to the concurrent positive IOD and El Niño forcing, though not as sharp as the double forcing response seen in in 1997-98. By 2024–25 anomalies return toward neutral.

Figure 16. Monthly runoff anomalies (with respect to 1991-2020) in the Middle East and global teleconnection time series. (a) Monthly time series of DMI; (b) Regional runoff anomaly (mm/month) with 12-month smoothed mean (bold black) and DMI-shaded background; (c) Monthly ONI time series. The reference period 1991–2020 is marked by the two vertical dotted lines.

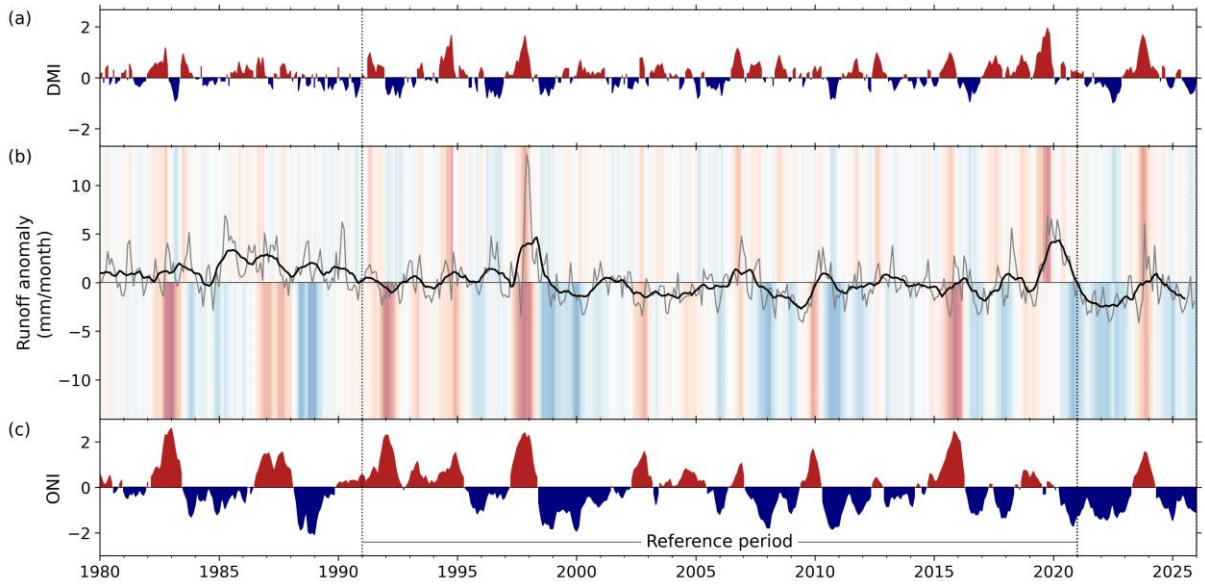

Source: GloFAS.

7. Vegetation and crops

The satellite-based fraction of Absorbed Photosynthetically Active Radiation (fAPAR) represents the fraction of solar energy absorbed by leaves due to photosynthesis. It is a measure of vegetation health and biomass. Negative fAPAR anomalies with respect to the long-term average are associated with a reduction in biomass and often with negative impacts on vegetation.

Figure 17 illustrates the temporal evolution of the fAPAR anomalies (computed as Z-score) in May and December of each year (coinciding with the end of the region's two rainy seasons) from 2021 to 2025 in East Africa. The fAPAR patterns reveal the onset of drought impacts on vegetation in southern Somalia and Kenya as early as mid-2021. Then, conditions rapidly deteriorated with widespread poor vegetation status observed across almost the entire region by May 2022. The severe drought conditions persisted until late 2022, with significant impacts on vegetation health and productivity. However, from 2023 to mid-2024, vegetation conditions improved quickly, with healthy and well-developed vegetation observed across the region, except for some initial signals of drought in southern Somalia in late 2024. Unfortunately, this recovery was short-lived, as drought conditions re-emerged in December 2025, severely affecting most of Somalia, Kenya, and south-western Ethiopia. The fAPAR indicator highlights the close relationship between vegetation health and drought conditions, with significant implications for pastoralism, agriculture, and ecosystem services in the region.

Figure 17. VIIRS (Visible Infrared Imaging Radiometer Suite) satellite-derived fAPAR anomalies computed at at the end of each MAM and OND rainy season from 2021 to 2025 in East Africa.

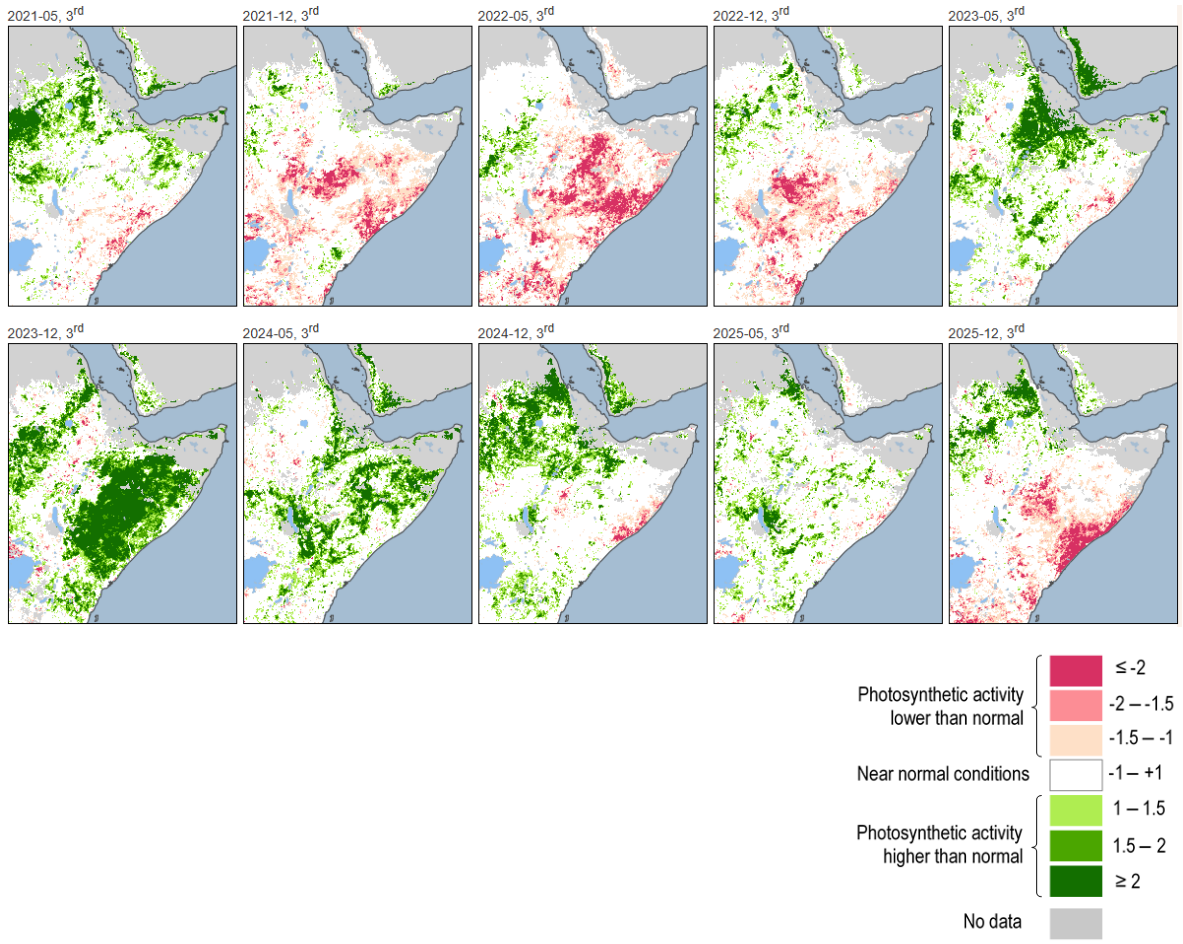

Source: JRC based on VIIRS.

The temporal evolution of fAPAR (Figures S20 and S21 in the Annex) is based on a shorter series compared to the other indicators, as it starts in 2012. Focusing on the critical period 2021-2025, the bar plots show that East Africa exhibits a wider percentage of affected area compared to the Greater East Africa region, indicating that countries in East Africa were more severely impacted by drought and vegetation stress (Figures S20 and S21 in the Annex).

Since 2020, the bar plot displays more extreme values in both higher and lower photosynthetic activity, suggesting increased variability in vegetation health. Prior to this, the only notable event occurred in 2017-2018. This pattern implies that the recent period (2021-2025) is marked by more frequent and intense droughts in East Africa.

The percentage of area in each fAPAR class at each timestep provides insight into the spatial extent of vegetation stress. During the 2021-2025 period, widespread vegetation stress and drought impact are estimated. In contrast, the Greater East Africa region (which fully include East Africa) exhibits a relatively smaller proportion of area in the lower classes, suggesting less severe impact in the other countries.

Figure 18 illustrates the temporal evolution of fAPAR anomalies (computed as Z-score) in March and June of each year (coinciding with the peak and the end of the wet season) in the Middle East/Central Asia region from 2021 to 2025. it is notable that a significant portion of the region is affected by missing data likely due to the extensive presence of arid and semi-arid regions, and this may impact the interpretation of the results. Focusing on the covered regions, the fAPAR patterns exhibit a more stable behaviour compared to East Africa. Northern Iran and Central Asia show a trend of deteriorating vegetation conditions from early 2021 to mid-2023, with the worst conditions observed in March 2023. A partial recovery is visible in March 2022, but this is short-lived, and conditions continued to decline. However, from March 2024 to March 2025, a slow and continuous improvement in vegetation conditions is evident, suggesting a recovery from the previous drought. Unfortunately, June 2025 shows a reversal of this tendency, with poor vegetation conditions re-emerging, mainly in Central Asia.

Figure 18. VIIRS Satellite-derived fAPAR anomalies at the peak (March) and at the end (June) of the rainy season from 2021 to 2025 in the Middle East/Central Asia region.

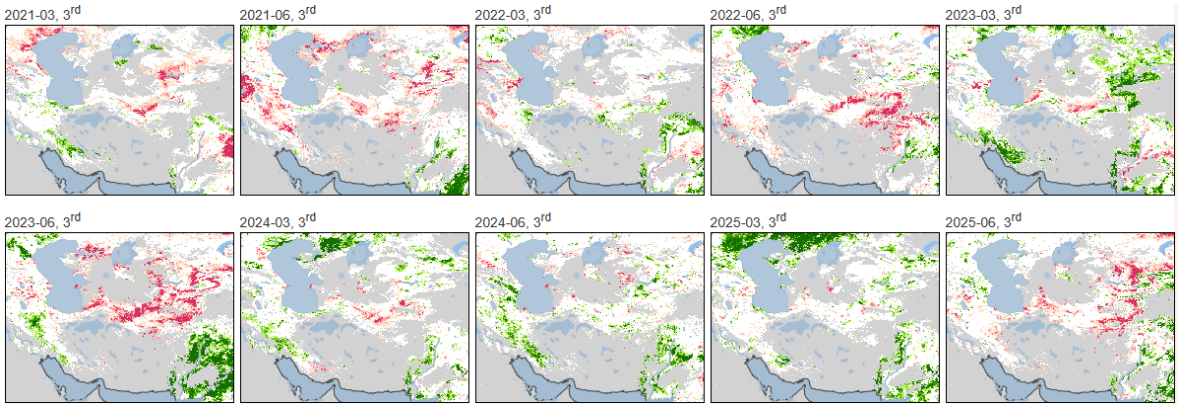

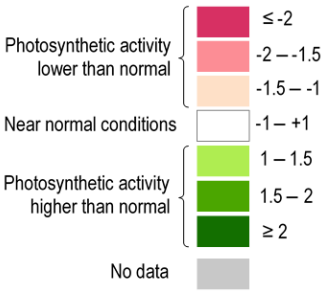

Source: JRC based on VIIRS.

Despite the data gaps in fAPAR, the bar plots still provide valuable insights into the temporal evolution in these regions (Figures S22 and S23 in the Annex). The period from 2021 to 2025 stands out as the most critical, with more frequent and severe periods of poor vegetation conditions. This suggests that the recent years have been particularly challenging for vegetation health in both Iran and the Middle East/Central Asia region.

In the wider Middle East/Central Asia region, the impact of vegetation stress is more visible, with a larger proportion of area exhibiting lower fAPAR values, especially during the 2021-2025 period. This may be attributed to the diverse landscape, which includes areas with more favourable conditions for vegetation growth, making the effects of drought and stress more apparent.

In contrast, Iran's bar plot is largely characterized by missing data, making it difficult to assess vegetation health. However, where data is available, the bar plot suggests that the vegetation was affected, particularly in 2018, when a noticeable decline in fAPAR values is visible. The recent period (2021-2025) shows even higher vegetation stress.

By looking at the ASAP warnings in the period under analysis, we can provide a more detailed analysis of drought effects on cropland and rangelands. ASAP automatically assigns warnings to sub-national administrative level. Figure 19 and 20 shows the ASAP warnings crops and rangeland in East Africa from 2021 to 2025. Ethiopia had several regions with ASAP warnings in each season from 2021 to the end of 2022. In 2023 and 2024, the country experienced overall positive crop and rangeland productivity from an agro-climatic point of view, except for minor drought impacts in Beneshangul Gumuz visible in May 2024. In Kenya, the main crop areas were not affected by significant agricultural drought events in the period 2021-2025, whereas the marginal areas in the coastal area of southeast Kenya experienced impacts throughout five consecutive crop seasons from 2021 to 2023. Parts of Central Kenya were affected in 2021 and 2022 and then experienced no major drought problem until the short rains of 2025.

Many crop areas in the region are also pastoral areas, which explains the similar dynamics of the pasture drought warnings (Figure 20). Rangeland areas also suffered droughts in 2021, 2022 and 2025, e.g., in North/East Somalia, in North/East Kenya and in Southeast Kenya.

Figure 19. ASAP warnings (cropland) from 2021 to 2025 at the end of each MAM and OND rainy season in East Africa.

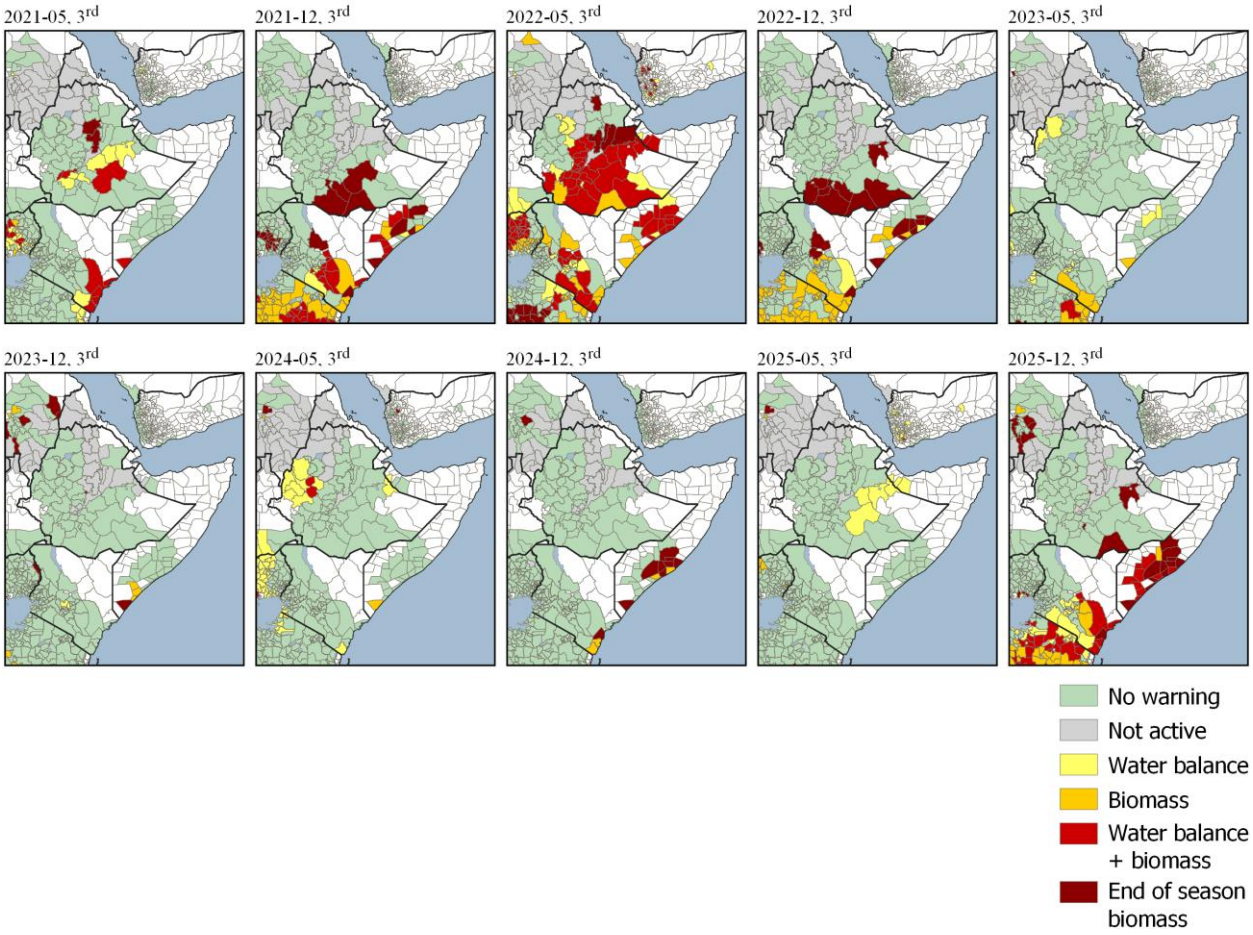

Source: JRC-ASAP

Figure 20. ASAP warnings (rangeland) from 2021 to 2025 at the end of each MAM and OND rainy seasons in East Africa.

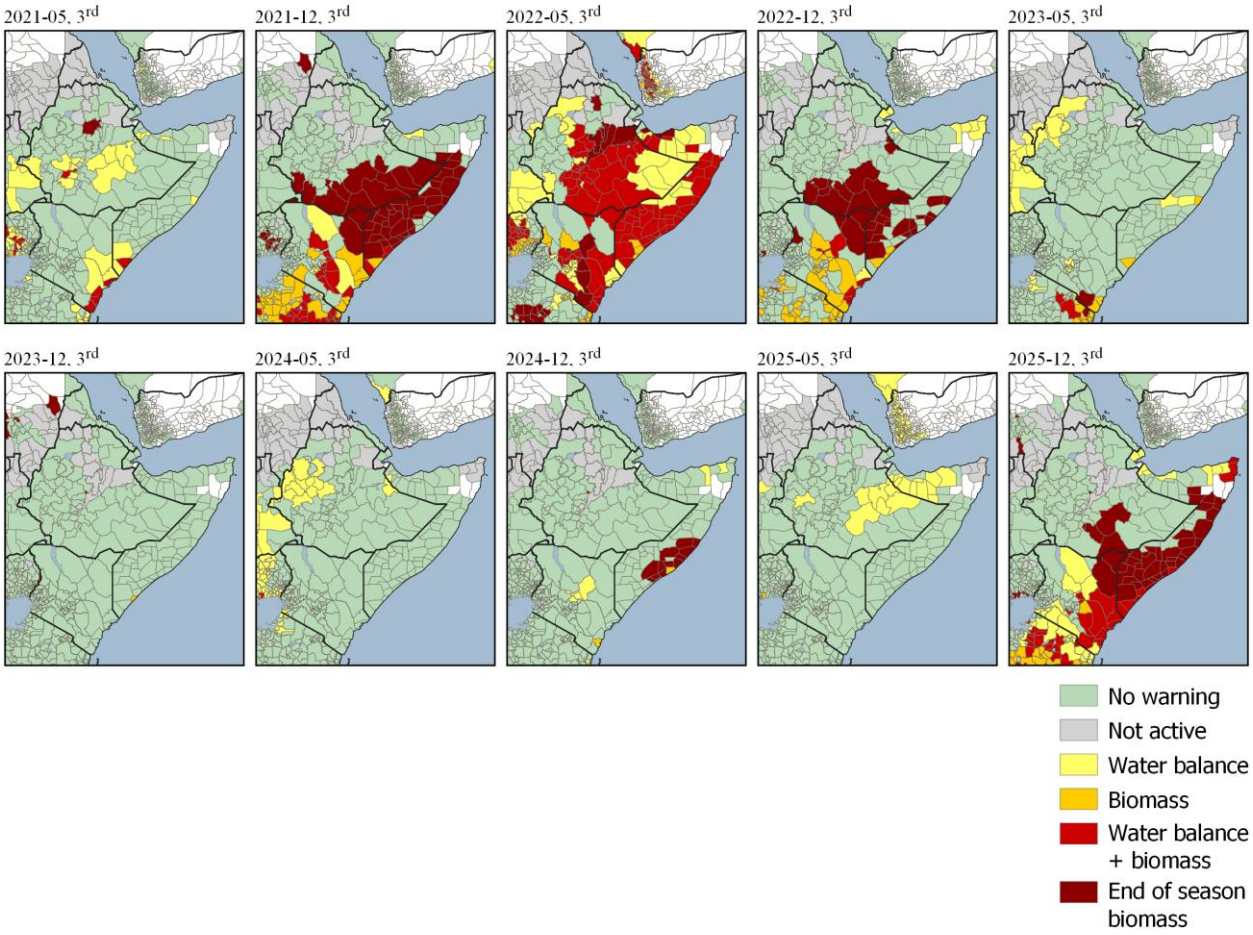

Source: JRC-ASAP

It is interesting also to observe the dynamic of warnings of 2021-2025 as compared to previous periods. For example, the time series of crop warnings for Kwale in southeastern Kenya (Figure S24 in the Annex) clearly shows how bad the 2021-2025 period was compared with the previous 5-year periods. Figure 21 shows that the agricultural areas of southeastern Kenya were exposed to drought in 2021-2025 longer than in the previous 5 years, whereas pastoral vegetation shows higher drought conditions frequency in 2021-2025 (compared with 2016-2020) in northeastern Kenya. In contrast, crops in western Kenya were less exposed to drought conditions in the last five years as compared with the previous period. The same holds for some pastoral areas in the South (e.g. Kitui county) and in the North (Turkana County).

In Ethiopia, most of the country was more frequently exposed to drought conditions in the last five years as compared with the previous 5-year period, both in cropland and in rangelands. Tigray, which experienced a major conflict and humanitarian emergency in 2020-2022, is the area in Ethiopia which experienced highest positive drought frequency as compared with the previous period, which further complicated recovery after the conflict.

In south-central and north-west Somalia higher drought frequency in the period 2021-2025 (than in the previous period) are detected. Improvement can be seen in the pastoral areas of Puntland and in significant parts of the Mudug pastoral area, as well as in parts of Somaliland.

Figure 21. Change in ASAP warning frequency (% of active ten-day periods) at warning level ≥ 2 between 2021–2025 and 2016–2020 in East Africa, for cropland (left panel) and rangeland (right panel).

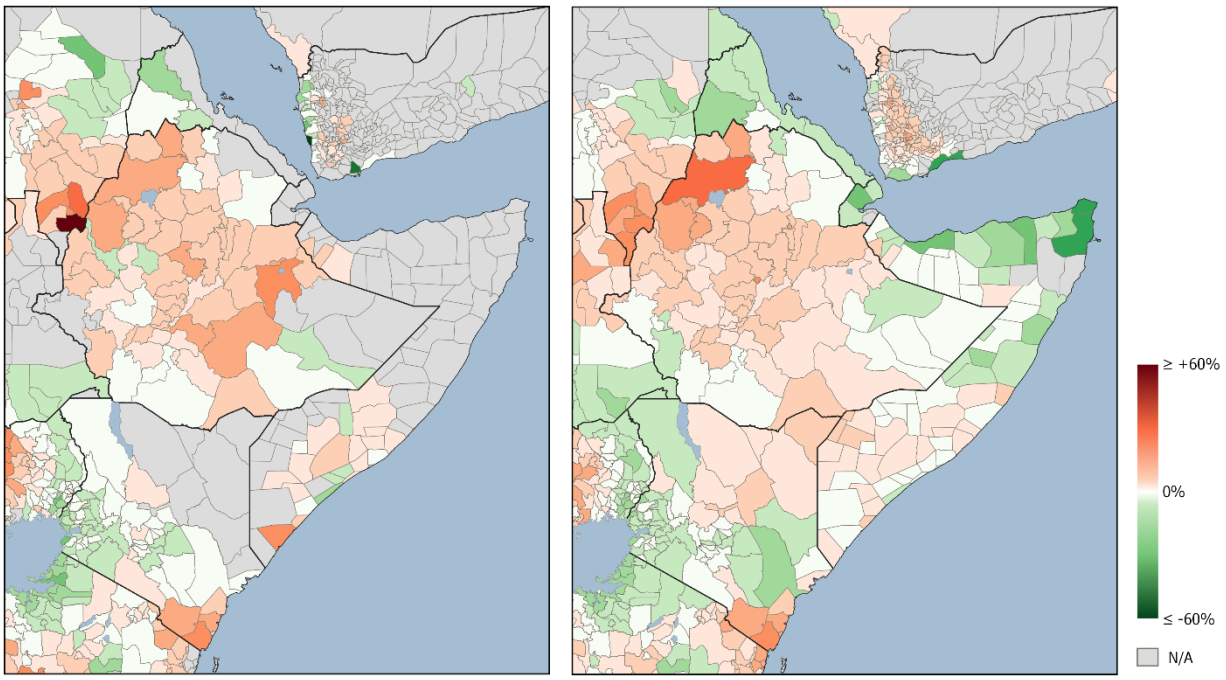

Source: JRC-ASAP

In the Midde East/Central Asia region, ASAP warnings are present in all years, except in June 2024, and for most administrative units, with a higher frequency in a region centred on Turkmenistan and including northeastern Iran, western Afghanistan and Uzbekistan for both cropland (Figure 22) and rangeland (Figure 23).

Figure 22. ASAP warnings (cropland) from 2021 to 2025 at the peak (March) and at the end (June) of the winter cereals season in the Middle East/Central Asia region.

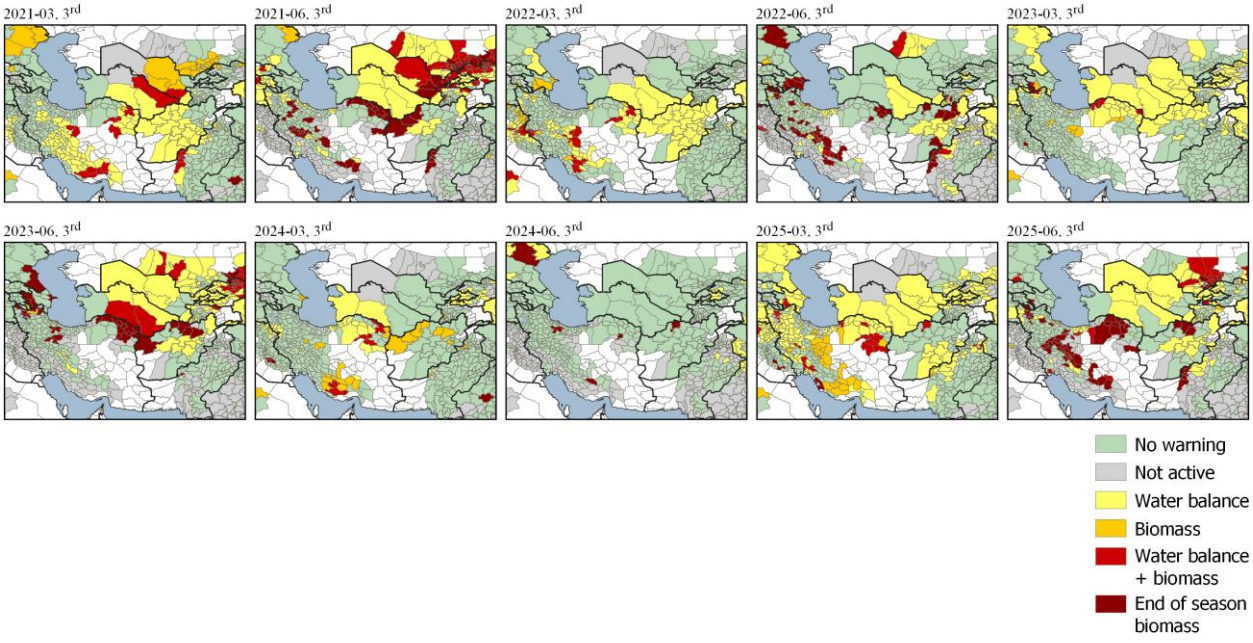

Source: JRC-ASAP

Figure 23. ASAP warnings (rangeland) from 2021 to 2025 at the peak (March) and at the end (June) of the rangelands season in the Middle East/Central Asia region.

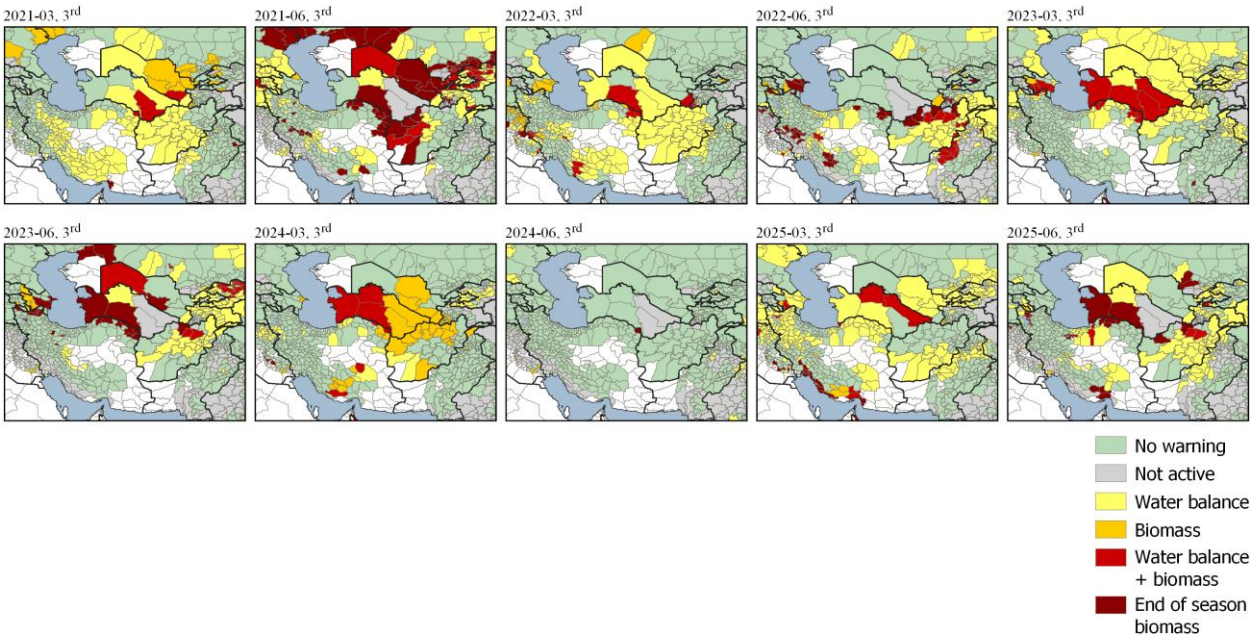

Source: JRC-ASAP

Figure 24. Changes in ASAP warning frequency (% of active ten-day periods) at warning level ≥ 2 between 2021–2025 and 2016–2020 in the Middle East/Central Asia region, for cropland (left panel) and rangeland (right panel).

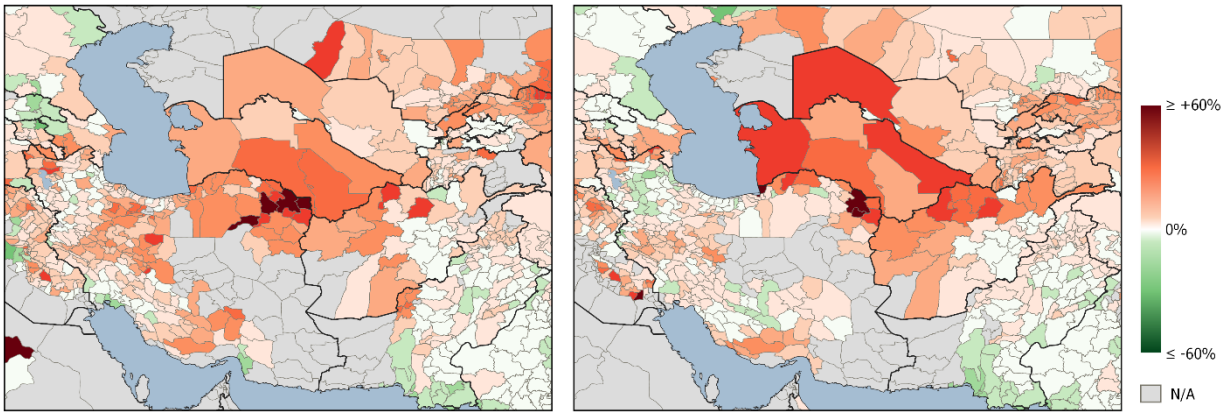

Source: JRC-ASAP

Figure 24 shows an increase in the frequency of ASAP warnings of level 2 and higher, i.e. warnings indicating a crop or rangelands biomass deficit with or without water balance deficit, between 2016-2020 and 2021-2025. Vegetation biomass deficit results often from water stress caused directly by rainfall deficit for rainfed crops and pastures or indirectly by government measures limiting irrigation. In Iraq, for instance, the government banned rice in the main producing areas in 2018, 2022, 2023, 2025, and for the first time in November 2025 limited the area devoted to wheat and barley irrigated with surface water to 250,000 ha (i.e. half of the usual area). Similarly, restrictions may be induced by lack of irrigation water coming from neighbour countries (e.g. the Pamir and Tien Shan mountains in Tajikistan and Kyrgyzstan provide water to the Amu Daria and Syr Daria rivers which flow to Turkmenistan, Uzbekistan, Kazakhstan. Less often, vegetation

biomass deficit is caused by excess rainfall and flooding. Figure 24 shows that the frequency of dry conditions increased in the region centred on Turkmenistan and going from northeast Iran to south Uzbekistan and north-west Afghanistan, but also in Kyrgyzstan, South Kazakhstan, centre-west Iran and eastern Iraq.

In Iran, the impacts of drought vary due to compensation by irrigation in some areas (Figure S25 in the Annex). In Khorasan, the first barley producing province and an important wheat producing area bordering Turkmenistan and Afghanistan, rainfall deficit occurred from January to May in all five years since 2021 and resulted in below average winter cereals biomass, suggesting that rainfed crops dominate in this province. In contrast, Khuzestan in the west, which is the first wheat producing province, shows above average crop biomass in all five years despite poor rainfall in 2021, 2025 and the 2nd part of the 2022 winter crops season. This is due to the use of irrigation despite the current water crisis[11].

In Mazandaran, the main rice producing province bordering the Caspian Sea, crop conditions are average to above average in all five years including 2025, which had poor rainfall during the whole year (450 mm in 2025 versus a long-term average of 720 mm per year). Here again, irrigation supported the rice production.

In Fars, the 2nd wheat producing province in the centre-south, rainfall was below average in 2021, 2024 and 2025, above average in 2023 and mixed in 2022 (close to normal followed by moderate deficit). Winter crop conditions are slightly below average in 2021, 2024 and 2025, well below average in 2022, which is surprising as 2022 is far from being the driest year, and as expected, above average in 2023.

In many cases, irrigation supported crop production. However, there is growing concern on how long irrigation water will continue to be available, as shown by the water crisis of November 2025 with 19 out of the 31 provinces in severe drought[12].

In Afghanistan, in the last five years, SPI-3 in Jawzjan was always negative (below average) between January and April and not surprisingly, winter crops biomass was below average (Figure S26 in the Annex). Actually, this province was systematically identified by ASAP as having poor performance every year between 2021 and 2025, possibly due to a reduction in the planted area, whereas in the previous two decades (2001-2020), poor years were less frequent (Figure S27 in the Annex). In contrast, in Kunduz and to some extent Hirat, below average rainfall (in particular in 2023 for Kunduz) did not result in below average crop biomass thanks to irrigation. The issue is to assess whether irrigation will still be possible in the coming years if the decreasing precipitation trend continues, reducing snow cover and leading to groundwater depletion.

In Turkmenistan, in the 2021 to 2025 period, moisture conditions were drier than average during the winter cereals season (January to June) for all years except at the end of the 2024 season (Figure S28 in the Annex). The driest season was 2023 with SPI-3 remaining below –1.5 from the end of January to the end of May (which corresponds to a rainfall deficit from November to May). Despite below average rainfall for all five years, cereals biomass was below average only in 2021 and well below average in spring 2023. According to the ASAP assessment of May 2023, the region

[11] see https://iramcenter.org/en/overview-of-the-water-crisis-in-khuzestan_en-705.

[12] https://carnegieendowment.org/emissary/2025/11/iran-water-crisis-warning-climate?lang=en.

received the lowest total rainfall of the last 32 years for the period October 1 - May 20, which may have led to a reduction in the sown area of winter wheat.

In Uzbekistan, SPI-3 was below the long-term average for part of the winter cereals season for all five years, except 2024. Crop biomass was surprisingly above average in 2025 despite the dry conditions, close to average in 2024 and below average in 2021 (Figure S29 in the Annex).

In Pakistan, despite drier than average conditions during the Rabi crops (winter cereals) season in 2020-2021, 2022-23 and 2024-25, biomass of winter cereals was above the long term average for all years, thanks to irrigation (Figure S30 in the Annex). In the five years under analysis, crop production was more affected by excess water than by rainfall deficit.

To explore better the reported impacts, we analyse the official crop statistics of production, harvested area and yield from FAOSTAT (Food and Agriculture Organization Statistical Database[13]). The following figures show the evolution from 2016 to 2024 (last available year) for: Kenya, Somalia, Ethiopia and Tanzania (East Africa); Iran, Afghanistan, Turkmenistan, Uzbekistan and Pakistan (Middle East/Central Asia).

We compare 2021-2024 with 2016-2020 in terms of mean production, harvested area and yield of up to three main cereals to detect tendencies that could result from the increase in dry conditions.

Figure 25. Production, harvested area and yield of maize, sorghum and wheat for the period 2016-2024 in Kenya.

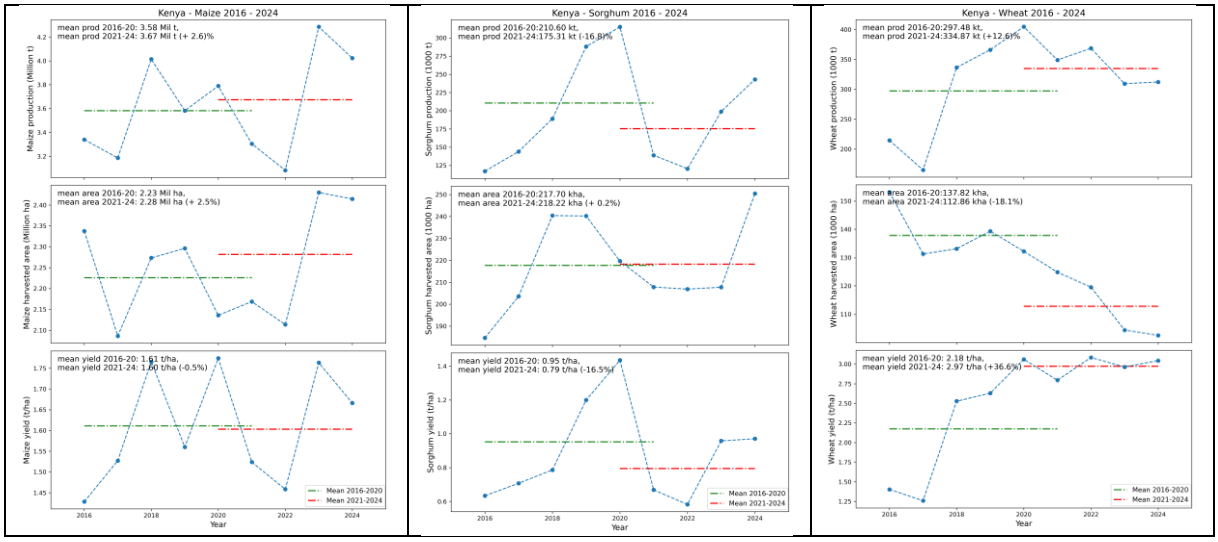

Source: JRC based on FAOSTAT data.

In Kenya, maize average production, area and yield remained similar (around 3.6 million t, with less than 3% difference) in the two periods, while sorghum average production decreased by 17% in 2021-2024 due to a decline in yield (Figure 25). As for wheat, the area decrease of 18% was

13 https://www.fao.org/faostat/en/#data/QCL.

largely compensated by the yield increase of 36%, which resulted in an increased production (+13%).

Figure 26. Production, harvested area and yield of maize and sorghum for the period 2016-2024 in Somalia.

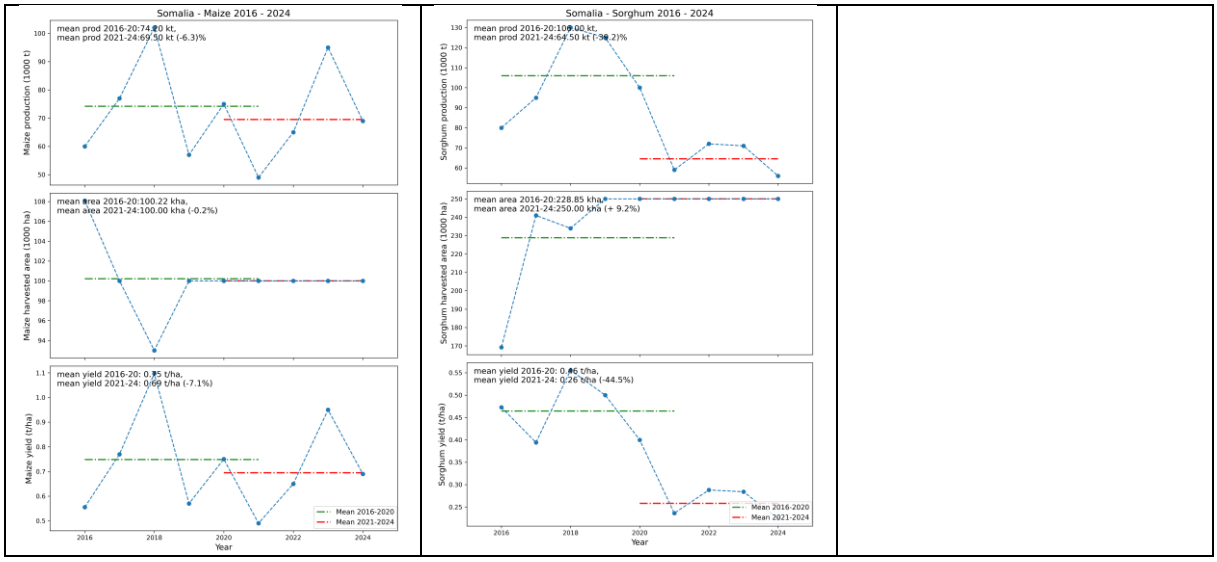

Source: JRC based on FAOSTAT data.

In Somalia, sorghum production strongly decreased by about 40% between 2016-2020 and 2021-2024, most likely as a result of the dry conditions. Maize production remained similar, i.e. around 70,000 t (Figure 26). This is probably due to the fact that maize is partly irrigated, while sorghum is mostly rainfed. The unchanged area from 2019 to 2024 for both maize and sorghum suggests missing survey data.

Figure 27. Production, harvested area and yield of maize, rice and sorghum for the period 2016-2024 in Tanzania.

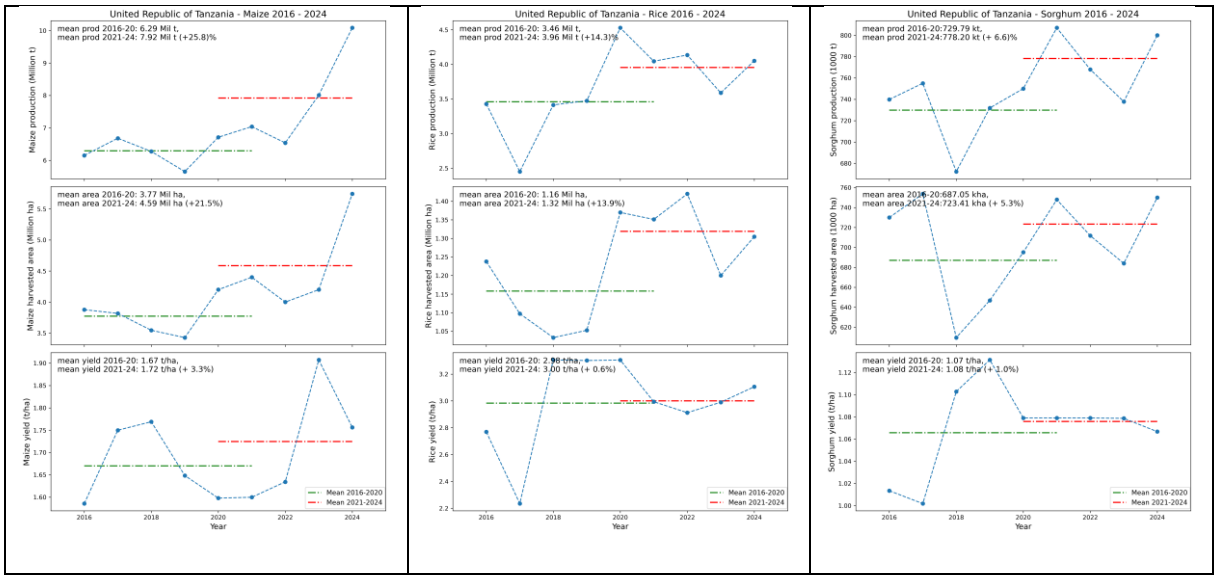

Source: JRC based on FAOSTAT data.

In Tanzania, the 2021 –2024 average production, area and yield of the three crops (maize, rice and sorghum) are similar or better than their respective 2016-2020 averages, due to the increase in harvested area mainly (maize harvested area increased from 3.8 to 4.6 million ha, i.e. 21%).

Figure 28. Production, harvested area and yield of maize, wheat and sorghum for the period 2016-2024 in Ethiopia.

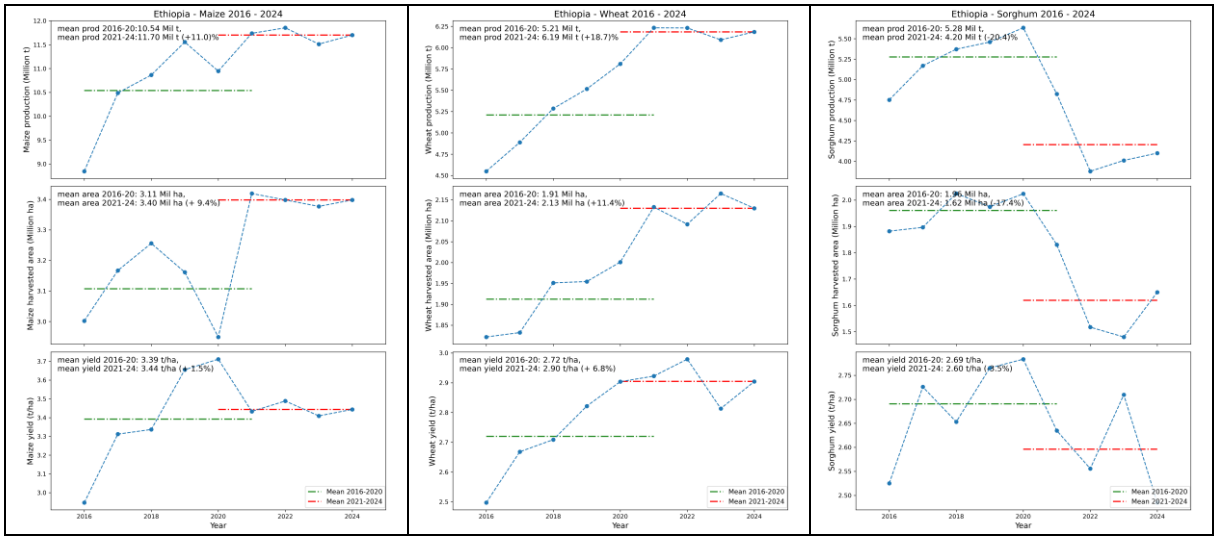

Source: JRC based on FAOSTAT data.

In Ethiopia, between 2016-2020 and 2021-2024, production increased for maize (+11%) and wheat (+19%) but decreased for sorghum (-20%), as shown in Figure 28. As for maize, the driver of production increase was clearly the crop area increase (9%). Concerning wheat, both yield and area increased by 7% and 11%, respectively; while for sorghum (that is a subsistence crop in rural areas) both yield and area decreased by 8.5% and 17%, respectively. The impacts of dry conditions on wheat and maize are not visible in the official yield and area statistics; while sorghum production is low from 2022 to 2024, which is somewhat unexpected as 2023 and 2024 were favourable.

Figure 29. Production, harvested area and yield of wheat, barley and rice for the period 2016-2024 in Iran.

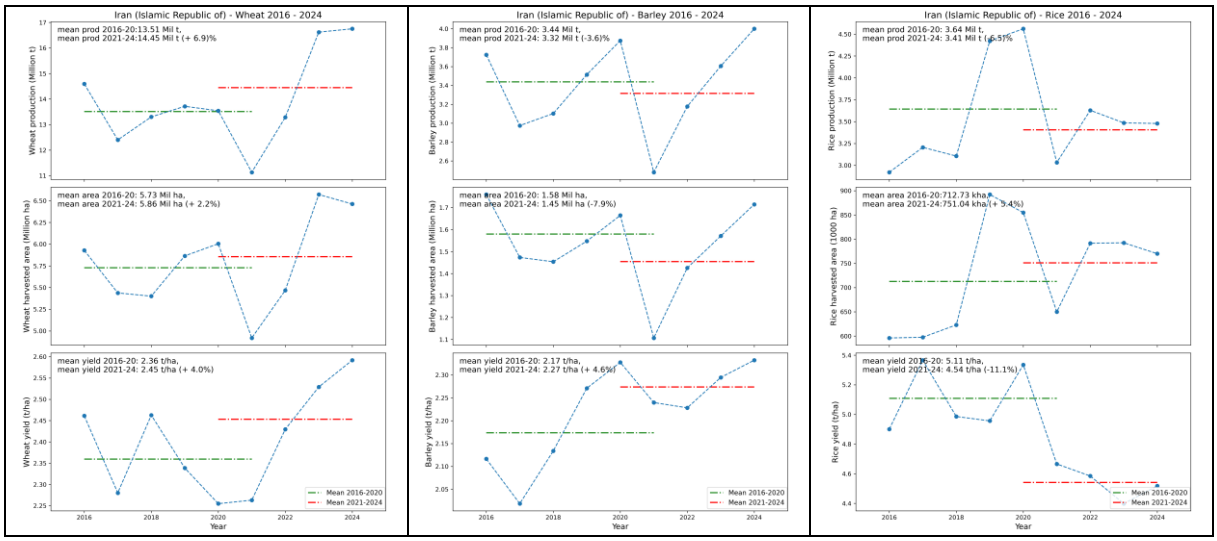

Source: JRC based on FAOSTAT data.

In Iran, between 2016-2020 and 2021-2024, wheat production slightly increased (by 7% on average) due to increased yield (+4%) as shown in Figure 29. Barley production remained stable (-4%) and rice production slightly declined (-6.5%). Despite the increased frequency of dry conditions, Iran has managed to maintain its cereals production thanks to irrigation (including underground water extraction).

Figure 30. Production, harvested area and yield of wheat and rice for the period 2016-2024 in Afghanistan.

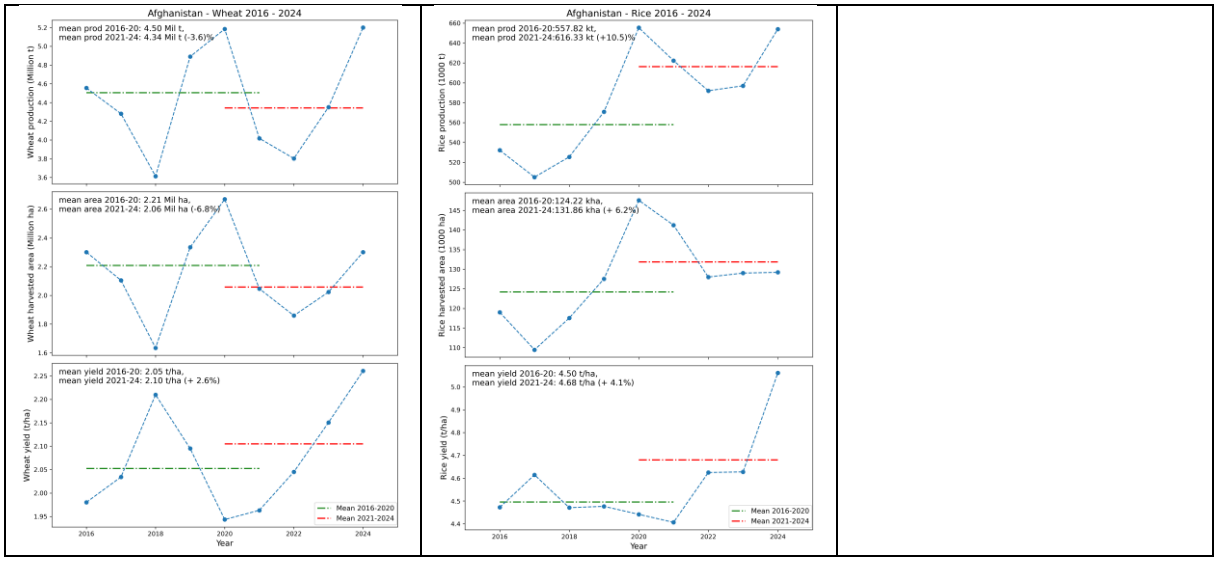

Source: JRC based on FAOSTAT data.

In Afghanistan, between 2016-2020 and 2021-2024, wheat production remained stable around 4.4 million t, while rice production increased (+10%) as a result of area and yield increase (+6% and +4% respectively). These statistics are in contrast with the increasing frequency of dry conditions affecting this country, in particular its northwest, possibly thanks to irrigation.

Figure 31. Production, harvested area and yield of wheat and rice for the period 2016-2024 in Turkmenistan.

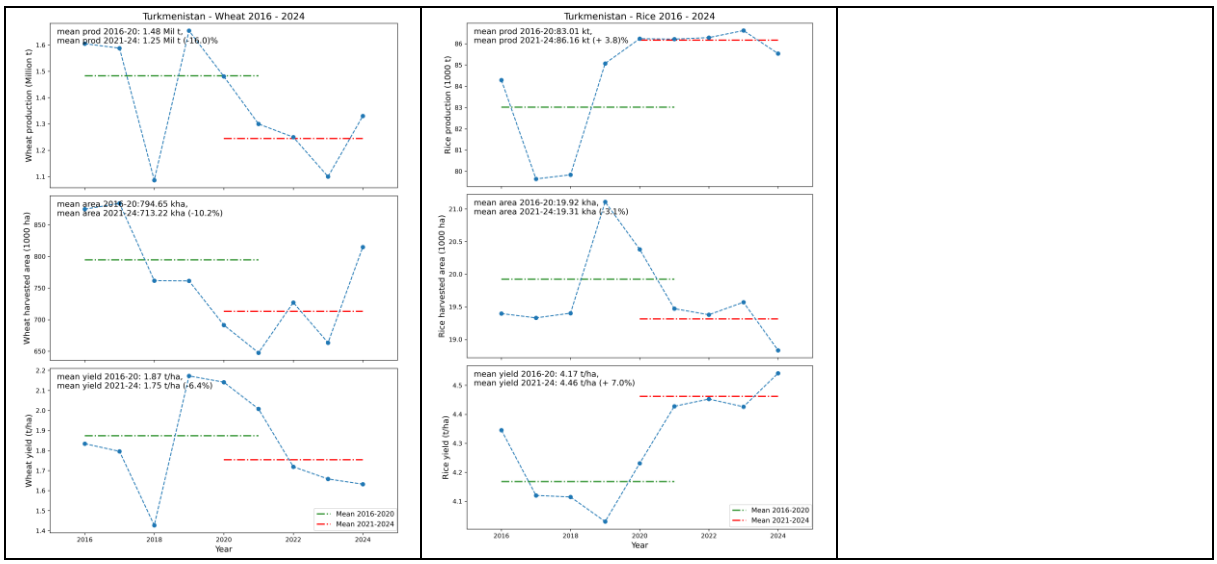

Source: JRC based on FAOSTAT data.

In Turkmenistan (Figure 31), between 2016-2020 and 2021-2024, the production of the main cereal (wheat) decreased by 16% due to the decrease in both harvested area (-10%) and yield (-6.5%), possibly as a result of a reduction in the water available for irrigation and soil salinization. Irrigated rice production is modest and slightly increased by 4% thanks to yield increase (+7%).

Figure 32. Production, harvested area and yield of wheat, maize and rice for the period 2016-2024 in Uzbekistan.

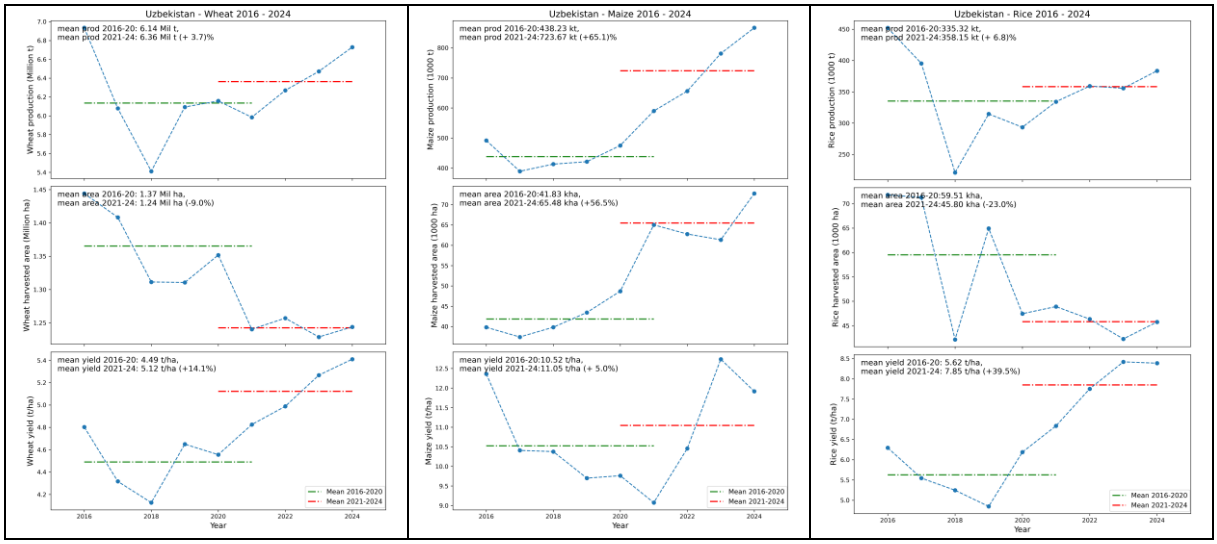

Source: JRC based on FAOSTAT data.

In Uzbekistan, between 2016-2020 and 2021-2024, the production of the main cereal (wheat) increased (+3.7%) thanks to a 14% yield increase which compensated the 9% decrease in area. Regarding summer crops, maize production increased (+65%) thanks to a 56% area increase. Rice production slightly increased (+7%) despite a 23% area decrease compensated by a 40% yield increase (Figure 32).

Figure 33. Production, harvested area and yield of wheat and rice for the period 2016-2024 in Pakistan.

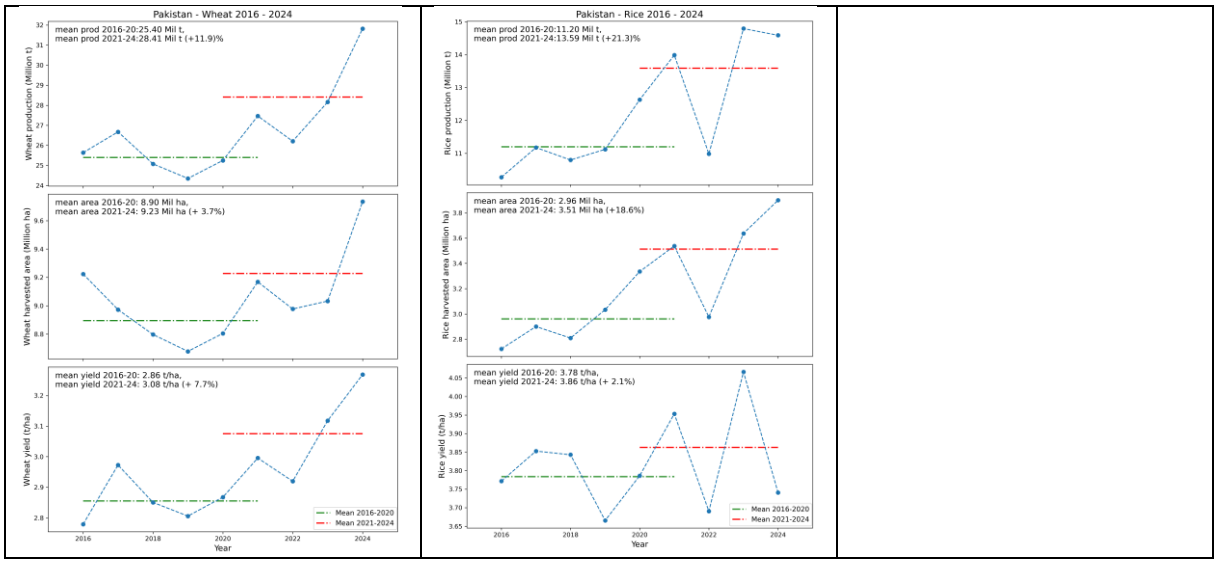

Source: JRC based on FAOSTAT data.

In Pakistan, between 2016-2020 and 2021-2024, the production of the two main cereals, namely wheat and rice, increased by 12% and 21%, respectively, thanks to an increase in harvested area (especially for rice which gained 18% while wheat gained 3.7%) and yield (nearly +8% for wheat, +2% for rice).

Overall, crop production in the 2021-2024 period[14] decreased (with respect to 2016-2020) mostly in central Asia, in an area centred on Turkmenistan and going from northeast Iran to south Kazakhstan and northwest Afghanistan. In other countries, it remained either stable (Afghanistan) or even increased (Iran, Uzbekistan, Pakistan). These tendencies may be attributable to irrigation, which seems to be still feasible in these countries. On the contrary, irrigation started to be strongly limited in Iraq (with ban on rice cultivation in 2018[15], 2022, 2023[16] and 2025[17] and halving of the wheat area benefitting from surface irrigation in 2025/2026[18]). In Iran, however, the unsustainable groundwater extraction is contributing to the water crisis[19], and many reservoirs were at extreme low capacity (in November 2025[20]).

In East Africa, the main areas affected by dry conditions in 2021-2025 (with respect to 2016-2020) are: Ethiopia, south-central Somalia, and south-eastern Kenya. Mixed conditions prevailed in the remaining areas.

---

14 2025 official statistics are not yet available on FAOSTAT website (https://www.fao.org/faostat/en/#data/QCL) so that the impact of the 2025 dry conditions cannot be observed on crop production yet.

15 https://english.alarabiya.net/features/2018/07/05/Iraq-bans-farming-summer-crops-as-water-crisis-grows-dire

16 https://www.arabnews.com/node/2554101/middle-east.

17 https://shafaq.com/en/Report/Drought-s-devastation-Iraq-s-rice-belt-withers.

18 https://thearabweekly.com/iraqs-dreams-wheat-independence-dashed-water-crisis#:~:text=%E2%80%9CBoth%20require%20modern%20irrigation.%E2%80%9D,river%20water%2C%E2%80%9D%20he%20said.

19 https://untoldmag.org/the-countdown-to-irans-day-zero-a-crisis-of-water-not-war/#:~:text=Mismanagement%20and%20policy%20failures,to%20the%20depletion%20of%20aquifers.&text=Projects%20like%20the%20Koohrang%20water,consumption%20agriculture%2C%20notably%20watermelon%20farming and https://carnegieendowment.org/emissary/2025/11/iran-water-crisis-warning-climate?lang=en

20 https://www.aljazeera.com/news/2025/11/12/as-the-dams-feeding-tehran-run-dry-iran-struggles-with-a-dire-water-crisis.

8. Current drought conditions

Figure 34 displays the SPI for East Africa over two different time scales. At the 3-month time scale, SPI shows that region is characterized by wetter-than-normal or near-normal conditions, indicating that the meteorological drought has fully recovered. The recent precipitation has been sufficient to alleviate short-term drought conditions. In contrast, SPI-12 shows still drought conditions in eastern Somalia, western Eritrea, and western Ethiopia. This suggests that despite the recent recovery in short-term precipitation, the long-term deficit has not been fully alleviated in these regions. The comparison between SPI-3 and SPI-12 highlights the importance of considering multiple time scales when assessing drought conditions.

Figure 34. SPI-3 (left panel) and SPI-12 (right panel) at the end of March 2026.

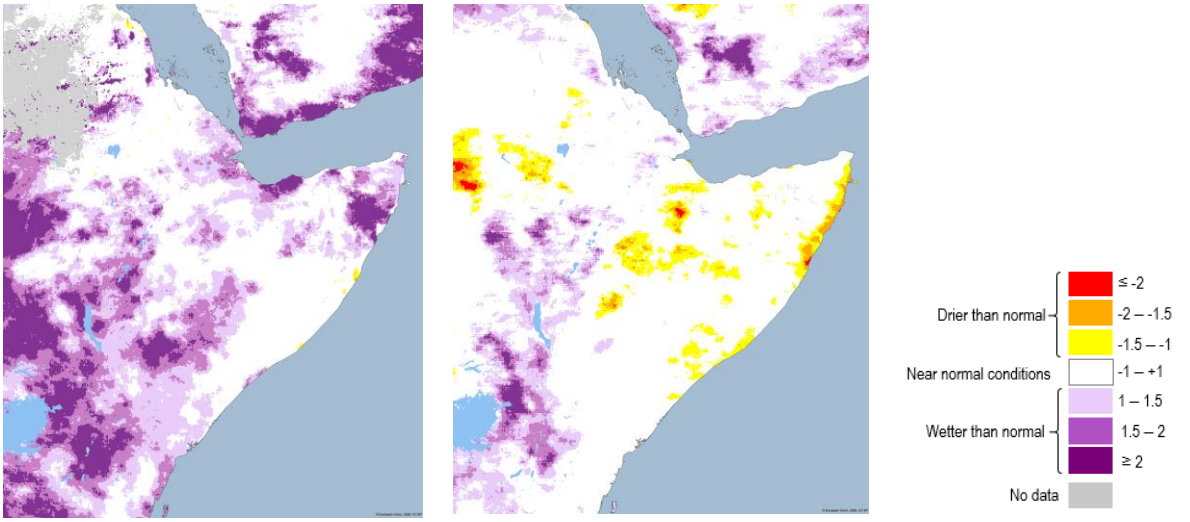

Source: JRC based on CHIRPS (Climate Hazards Group Infrared Precipitation with Station).

Figure 35 points to persistent dry conditions in eastern Iran, western Afghanistan, central Pakistan, and Tajikistan. Elsewhere, recent precipitation has been sufficient to alleviate the short-term deficit.

The SPI-12 index reveals a more critical condition. Despite some recent improvement in precipitation, several areas continue to exhibit significant drought. Northern Iran, the Turan Depression, Tajikistan, and central-eastern Afghanistan are among the regions where long-term deficits persist. These areas have not yet fully recovered from the cumulative effects of below-average precipitation over the past years.

Figure 35. SPI-3 (left panel) and SPI-12 at the end of March 2026.

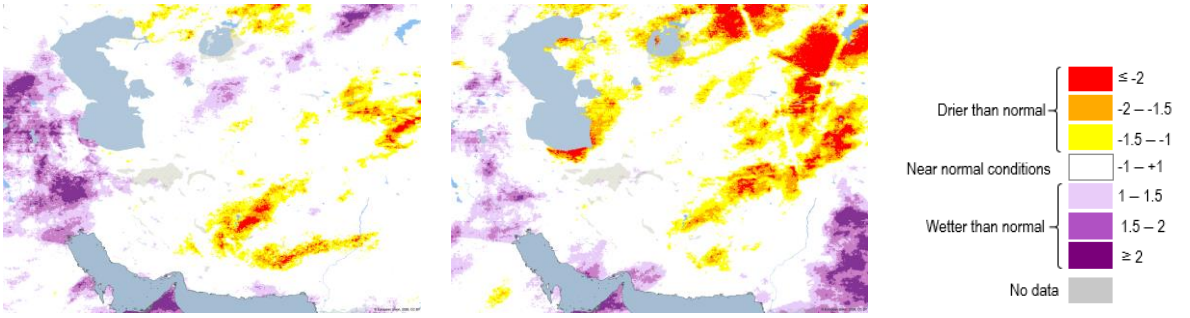

Source: JRC based on CHIRPS (Climate Hazards Group Infrared Precipitation with Station).

In March 2026, most of East Africa experienced close-to-average temperatures (baseline 1991-2020), with positive anomalies exceeding 1°C above the average over southern Sudan, Eritrea, northern and central Ethiopia, and north-eastern Somalia (Figure 36).

Figure 36. Average temperature anomaly (ERA5, ECMWF European Centre for Medium-Range Weather Forecasts, Reanalysis v5) computed for March 2026. Baseline: 1991-2020.

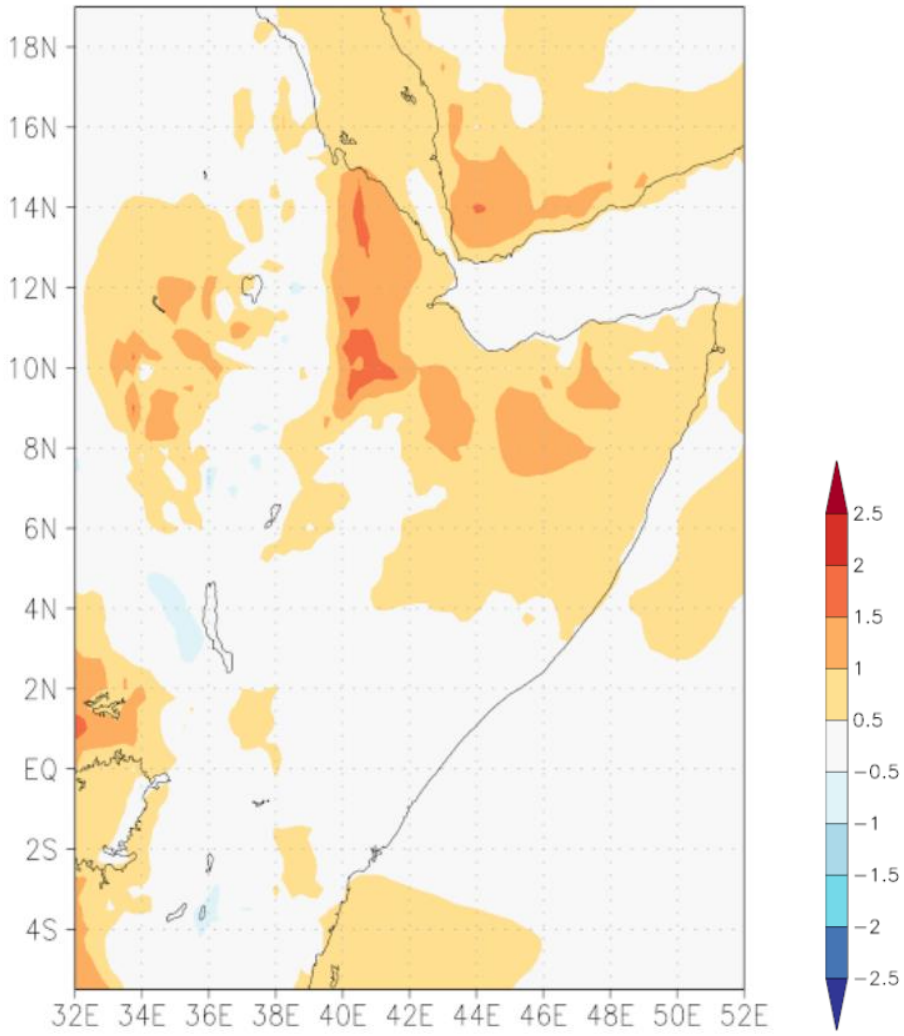

Source: the KNMI (Koninklijk Nederlands Meteorologisch Instituut) Climate Explorer [21].

On the other side in the Middle East/Central Asia region, extreme positive temperature anomalies have been observed in March 2026 exceeding 2.5°C in northern Iran, Turkmenistan, and Uzbekistan, and in any case exceeding 1°C over almost the whole region of interest (Figure 37).

[21] https://climexp.knmi.nl

Figure 37. Average temperature anomaly (ERA5, ECMWF European Centre for Medium-Range Weather Forecasts, Reanalysis v5) computed for March 2026. Baseline: 1991-2020.

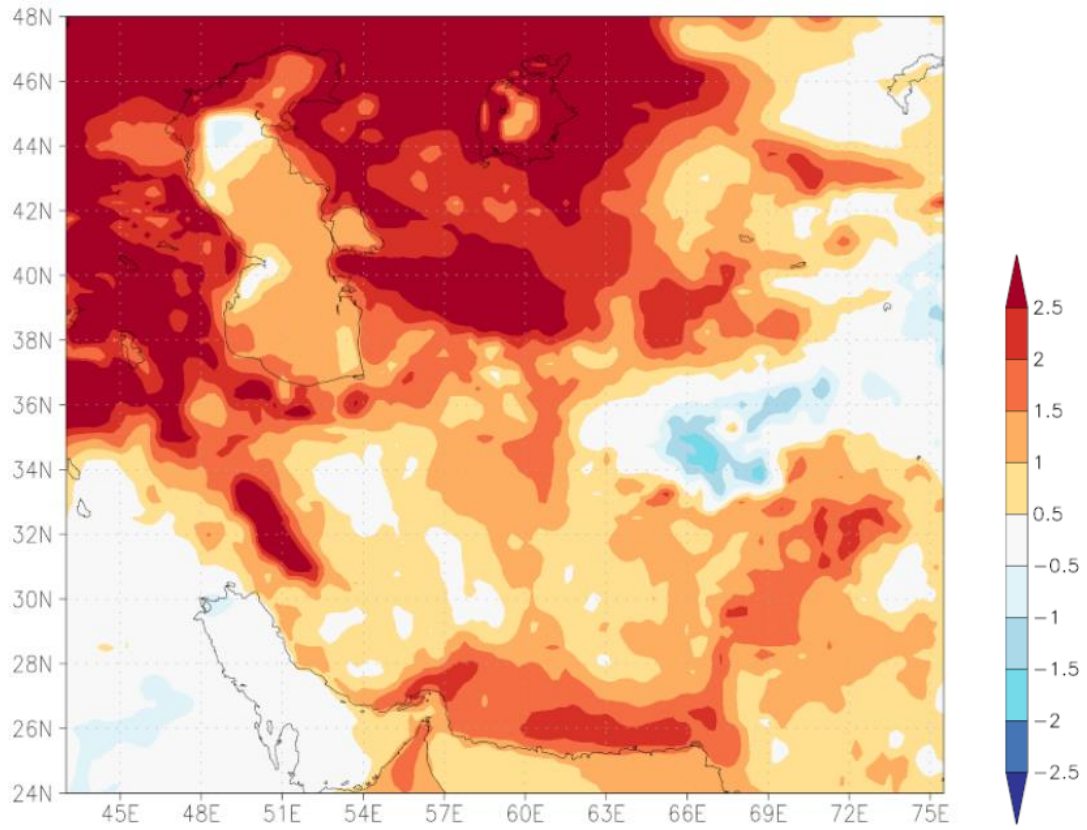

Source: The KNMI Climate Explorer.

The SPEI, shown in Figure 38, in East Africa confirms the recent reduction of the short-term deficits. In contrast, the SPEI-12 exhibits markedly drier conditions than the SPI-12 described previously. Extreme negative anomalies are evident across Somalia, Eritrea, most of Ethiopia and northern Kenya. This amplified dryness is attributable to evapotranspiration. It is also important to highlight that the two indices rely on different input datasets further contributing to the observed divergence. The juxtaposition of SPEI-3 and SPEI-12 thus reinforces the earlier conclusion that short term precipitation has recovered, while the cumulative water balance deficit over the past year remains severe.

Figure 38. SPEI-3 (left panel) and SPEI-12 (right panel at the end of March 2026.

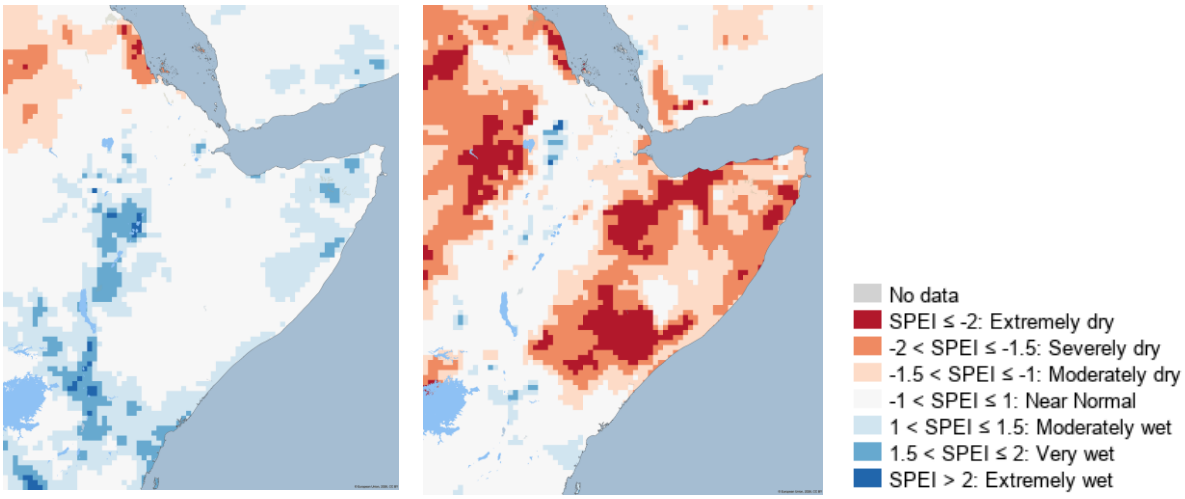

Source: JRC based on ERA5.

Figure 39 shows that the SPEI-3 is generally close to, or moderately drier than average. In contrast, the SPEI-12 reveals a pervasive, extreme dryness across the entire study area. This pronounced long-term deficit reflects the cumulative effect of reduced precipitation together with heightened evapotranspiration driven by elevated temperatures.

Figure 39. SPEI-3 (left panel) and SPEI-12 at the end of March 2026.

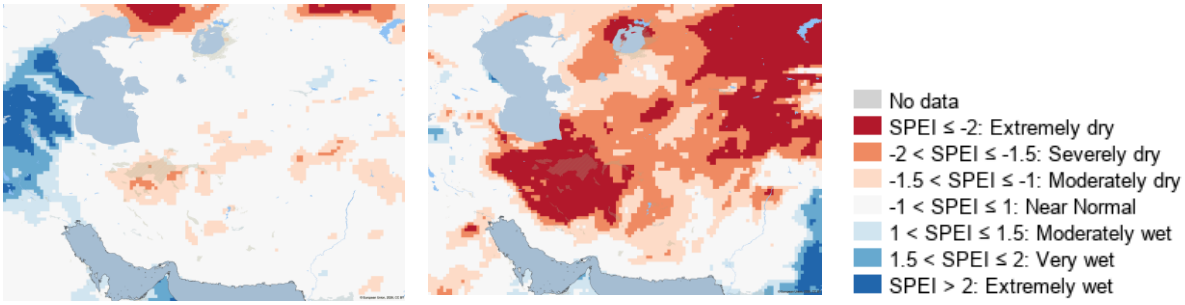

Source: JRC based on ERA5.

Concerning soil-moisture anomalies for East Africa at late March 2026, negative values are concentrated in central Ethiopia, northern Eritrea, southern Somalia, north-eastern Kenya and southern Sudan, mirroring the extreme SPEI-12 dry signals identified earlier. These residual deficits indicate that, despite the near-normal SPEI-3 conditions, the longer-term effect on soil moisture persists (Figure S31 in the Annex).

In the Middle East/Central Asia region, the spatial pattern of soil moisture anomalies is heterogeneous, reflecting the complex topography and lithology as well as the prolonged and complex drought. Strong negative values are visible in northern Iran and the eastern sectors of Afghanistan and Pakistan, confirming the severe dryness indicated by the SPEI-12. In contrast, central Iran and Afghanistan exhibit near-normal to positive anomalies, driven by recent precipitation events and meltwater from the winter snowpack (Figure S32 in the Annex).

Figure 40 displays the late March 2026 fAPAR for East Africa. Very low values occur in southern Somalia and eastern Kenya, indicating a pronounced reduction in vegetation greenness that reflects

the prolonged drought identified by the SPEI-12. The onset of the rainy season has not yet alleviated the moisture deficit in these areas. In contrast, the remaining areas show fAPAR at or above the long-term mean, pointing to near-normal or improved vegetation conditions where water availability is sufficient. In Kenya and Ethiopia, it is visible a strong regreening signal as natural vegetation quickly recovered thanks to recent precipitation. This is not directly informative about the real crop planted area. The early stage of the current rainy season will therefore be critical: a timely and sustained precipitation increase is required to reverse the vegetation stress in the most affected regions, a factor that should be closely monitored in short-term forecasts.

Figure 40. VIIRS (Visible Infrared Imaging Radiometer Suite) Satellite-derived fAPAR anomaly indicator in late March 2026.

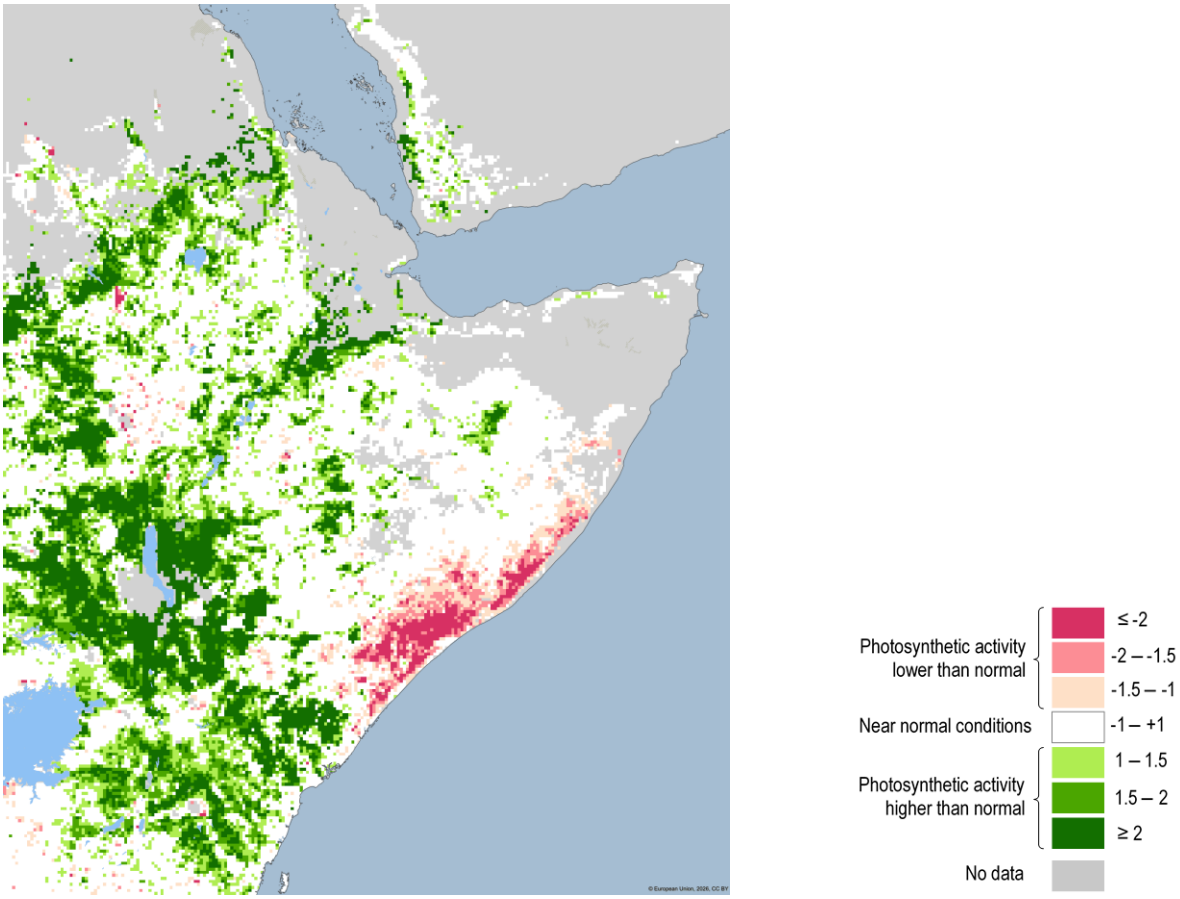

Source: JRC based on VIIRS (Visible Infrared Imaging Radiometer Suite).

Figure 41 presents the fAPAR Anomaly map for the MiddleEast/Central Asia region. Extensive data gaps are evident across the high-relief and arid zones, reflecting retrieval limitations in these complex terrains. In the grid cells where observations are available, fAPAR values cluster close to the climatological mean, indicating that vegetation greenness is largely near normal despite the heterogeneous hydroclimatic context.

Figure 41. VIIRS (Visible Infrared Imaging Radiometer Suite) Satellite-derived fAPAR anomaly indicator in late March 2026.

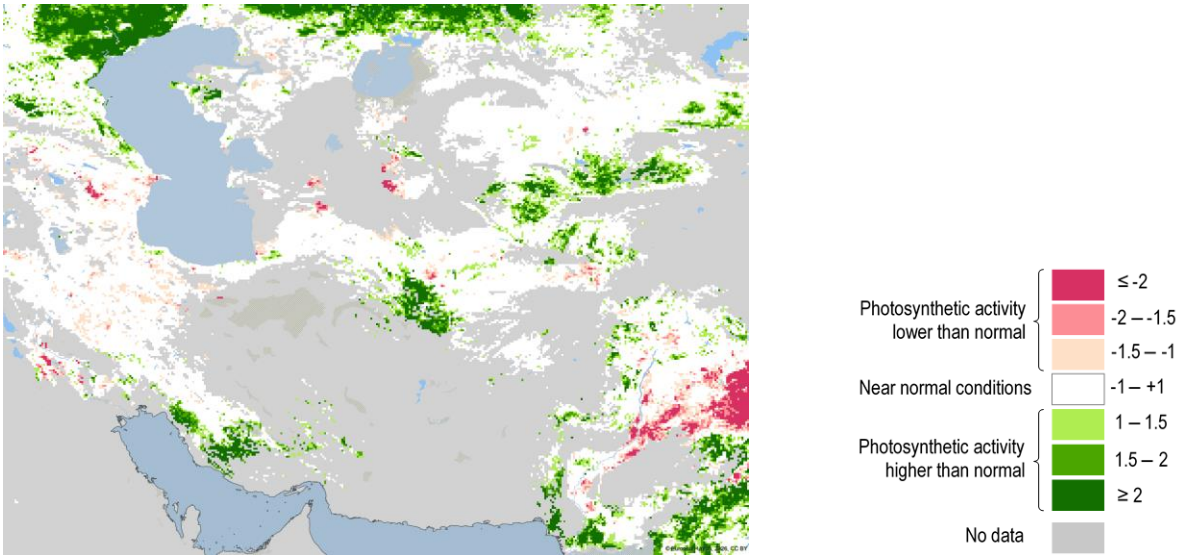

Source: JRC based on VIIRS (Visible Infrared Imaging Radiometer Suite).

9. Seasonal forecast

The Multi-system Indicator for Forecasting Unusually Wet and Dry Conditions provides early risk information at global scale. The indicator is computed from forecasted SPI-1, SPI-3, and SPI-6 derived from eight components: ECMWF (European Centre for Medium-Range Weather Forecasts), CMCC (Centro Euro-Mediterraneo sui Cambiamenti Climatici), DWD (Deutscher Wetterdienst), ECCC (Environment and Climate Change Canada), Météo France, NCEP (USA National Centers for Environmental Prediction), UKMO (UK Meteorological Office), BOM (Bureau of Meteorology, Australia).

Close-to-average conditions are forecasted from April to June 2026 by the multi-system ensemble (Figure 42) over East Africa. This forecast cover most of the rainy season and for this reason may be relevant for a potential improvement of the drought condition in the region. Additionally, it comes after a second half of March wetter than average.

Figure 42. Multi-system Indicator for Forecasting Unusually Wet and Dry Conditions, April - June 2026, based on dynamic forecasting systems from 8 centres: ECMWF, CMCC, DWD, ECCC, Météo France, NCEP, UKMO, BOM. The baseline period is 1993-2016.

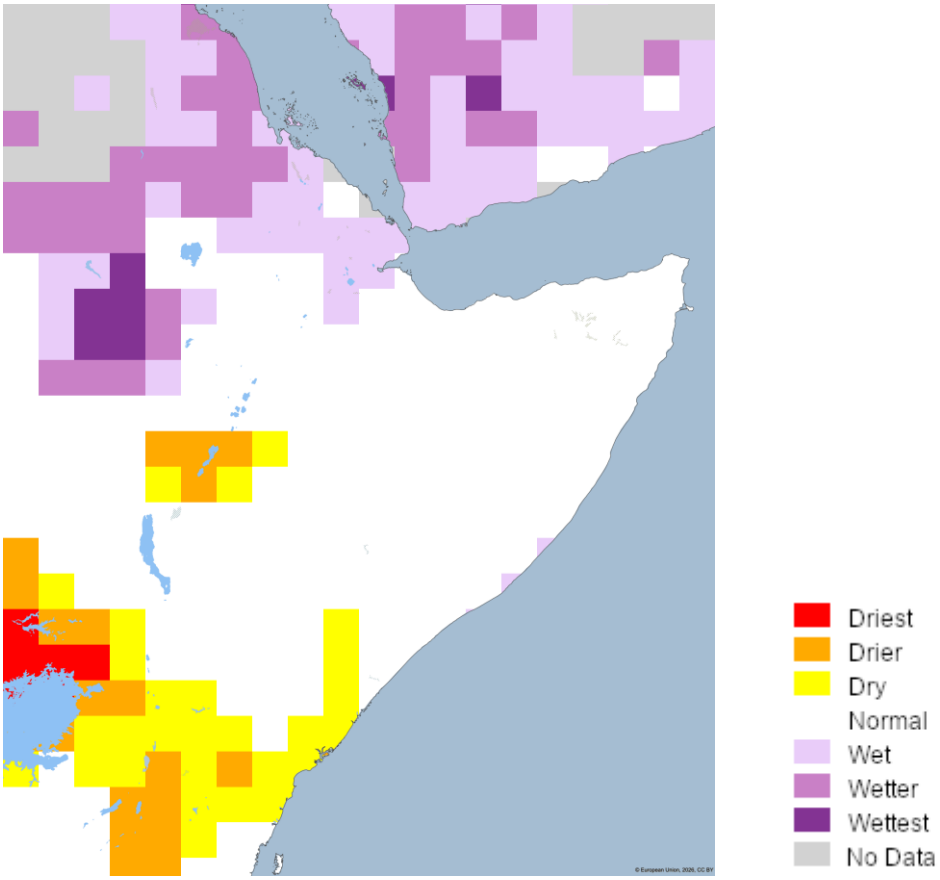

Source: JRC based on ECMWF, CMCC, DWD, ECCC, Météo France, NCEP, UKMO, BOM.

Wetter than average conditions are forecasted from April to June 2026 by the multi-system ensemble (Figure 43) over Middle East/Central Asia.

Figure 43. Multi-system Indicator for Forecasting Unusually Wet and Dry Conditions, April - June 2026, based on dynamic forecasting systems from 8 centres: ECMWF, CMCC, DWD, ECCC, Météo France, NCEP, UKMO, BOM. The baseline period is 1993-2016.

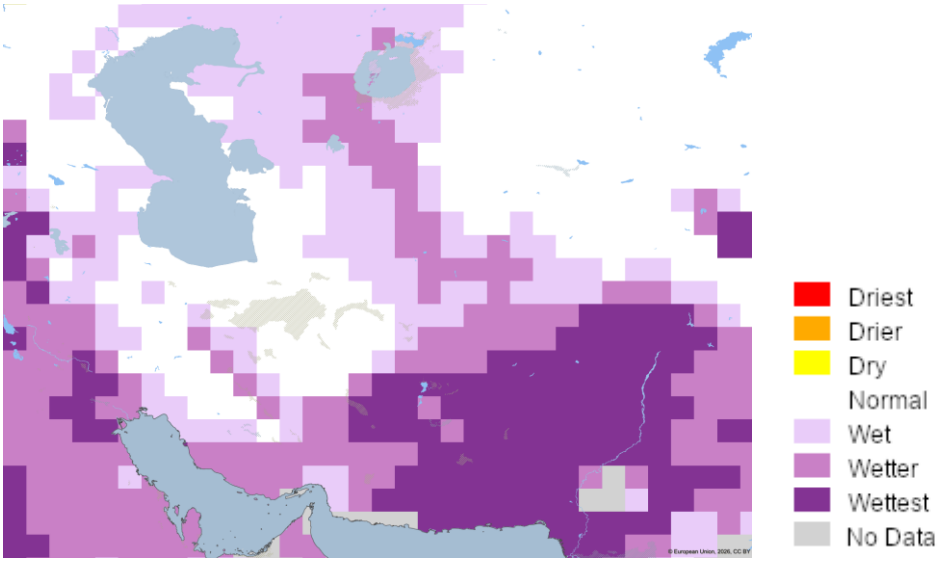

Source: JRC based on ECMWF, CMCC, DWD, ECCC, Météo France, NCEP, UKMO, BOM.

The single forecasting systems (not shown here), that compose the multi-system ensemble, point to a discrete agreement, giving a good reliability to the prediction.

The Multi-system Indicator for Forecasting Unusual Warm and Cool Conditions provides early risk information at global scale. As the previous one, this indicator is computed from forecasted temperatures derived from eight components. Warmer than average conditions are forecasted for April 2026 by the multi-system ensemble over southern regions in East Africa and northern regions in Middle East/Central Asia, while close-to-average temperatures are predicted in the northern part of East Africa and in most of the Middle East/Central Asia (Figure 44 and Figure 45, respectively).

Figure 44. Multi-system Indicator for Forecasting Unusually Warm and Cool Conditions, April 2026, based on dynamic forecasting systems from 8 centres: ECMWF, CMCC, DWD, ECCC, Météo France, NCEP, UKMO, BOM. The baseline period is 1993-2016.

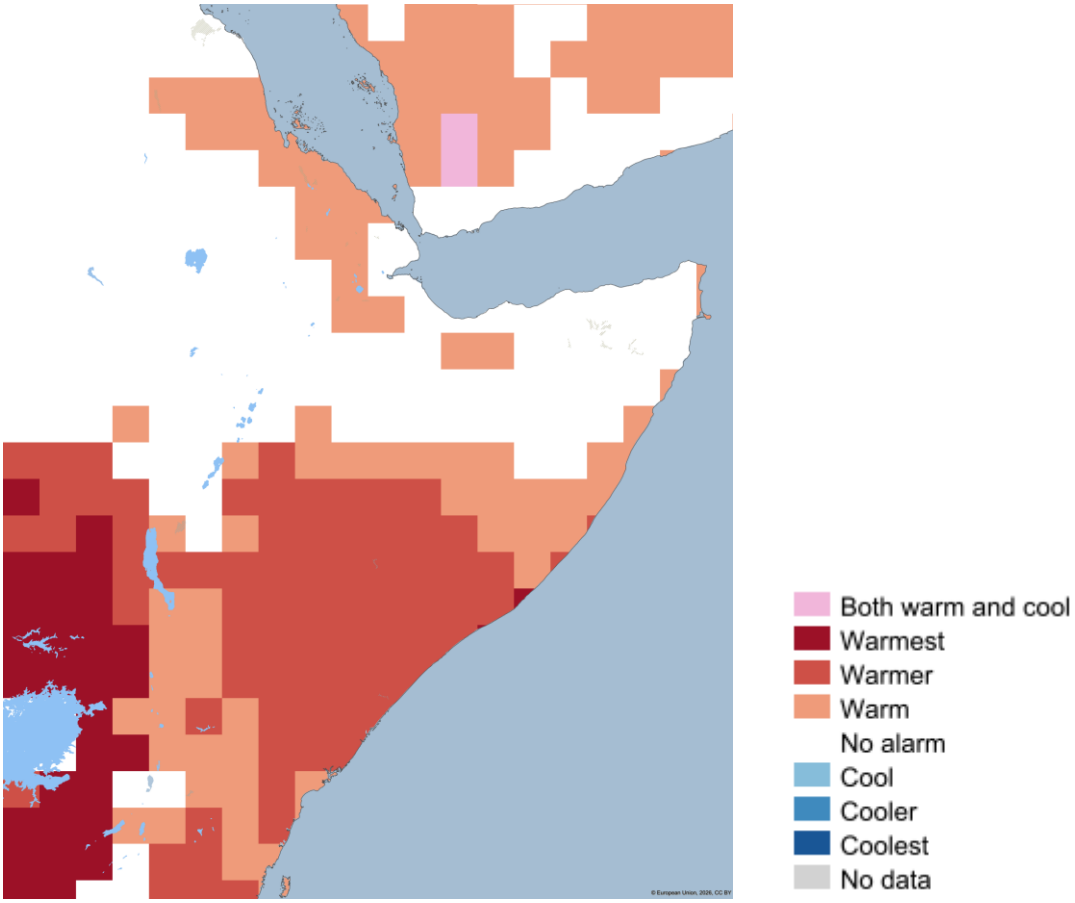

Source: JRC based on ECMWF, CMCC, DWD, ECCC, Météo France, NCEP, UKMO, BOM.

Figure 45. Multi-system Indicator for Forecasting Unusually Warm and Cool Conditions, April 2026, based on dynamic forecasting systems from 8 centres: ECMWF, CMCC, DWD, ECCC, Météo France, NCEP, UKMO, BOM. The baseline period is 1993-2016.

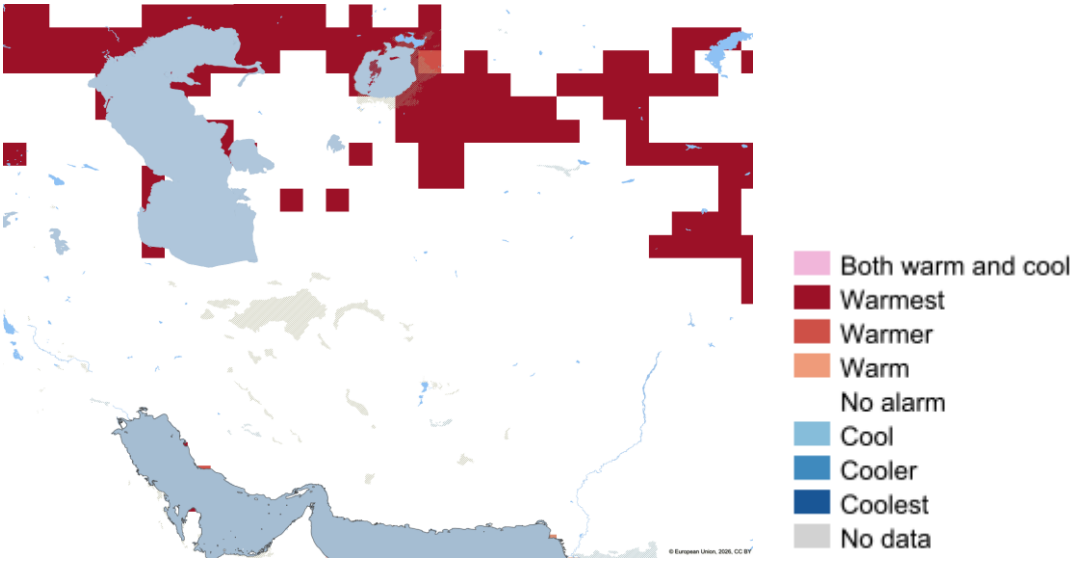

Source: JRC based on ECMWF, CMCC, DWD, ECCC, Météo France, NCEP, UKMO, BOM.

Based on the Copernicus Climate Change Service (C3S) seasonal forecasts[22] (not shown here), warmer than usual conditions and slightly wetter than usual conditions are likely to occur both in East Africa and in Middle East/Central Asia up to June 2026.

Based on the Global Flood Awareness System (GloFAS)[23], Figure 46 shows the April 2026 river flow forecasts for the major basins in East-Africa and the Middle East/Central Asia region. The majority of catchments are forecasted to deliver near normal or even higher than normal discharges, indicating a fading out phase of the drought. Notable exceptions are the Upper Nile tributaries, draining southern Sudan and South Sudan, where the model predicts persistent low flow anomalies, and eastern Uzbekistan and Turkmenistan, which also exhibit reduced discharge.

Figure 46. Seasonal forecast anomaly and uncertainty provided by the 7-month simulation covering April to October 2026, with information aggregated by basin. Different colours indicate the anomaly category, while the colour intensity shows the confidence level in the anomalies, with the lighter colours associated with higher uncertainty. The forecast anomaly and uncertainty signals are derived by comparing the EFAS (European Flood Awareness System) hydrological forecast driven by ECMWF SEAS5 (Seasonal Forecasting System 5) to the 99-value percentile climatology. The climatology is generated using ECMWF SEAS5 reforecasts over a 20-year period.[24]

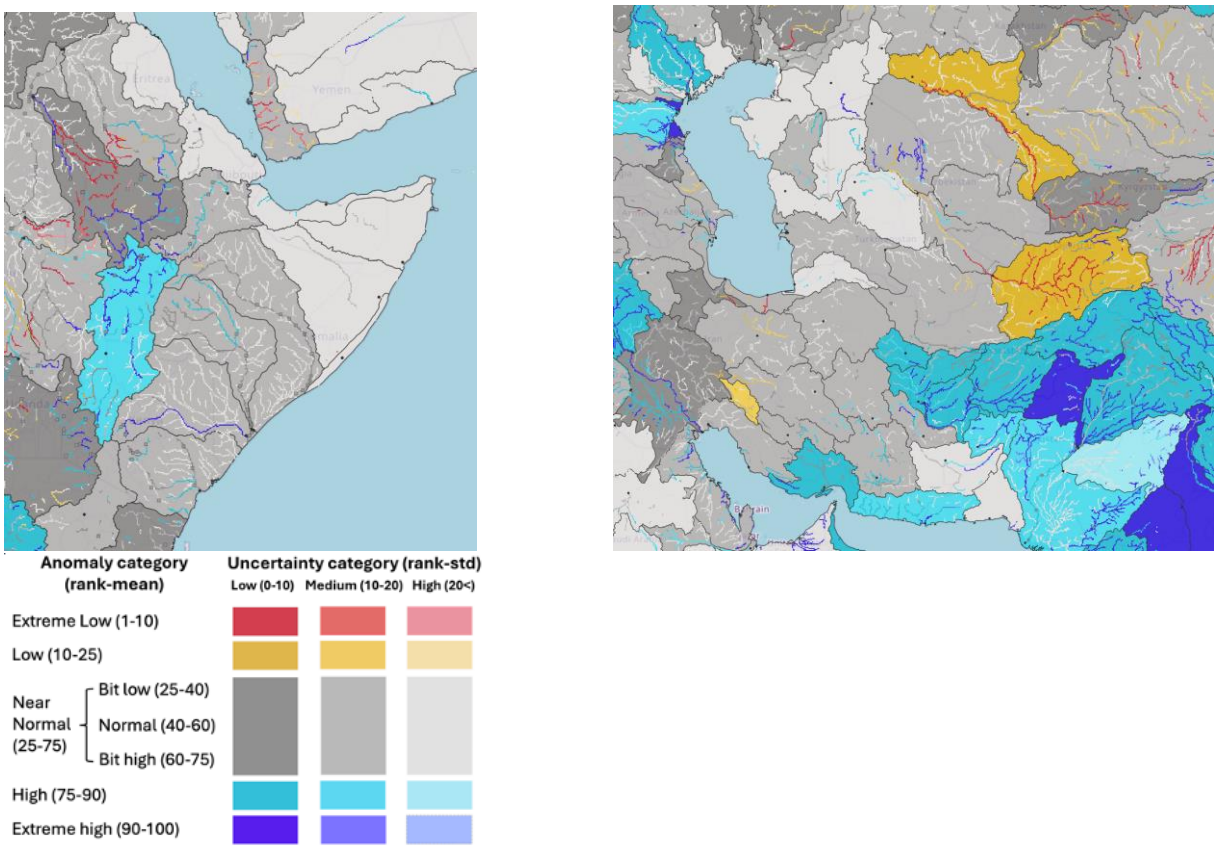

Source: GloFAS.

22 https://climate.copernicus.eu/seasonal-forecasts.

23 https://global-flood.emergency.copernicus.eu/glofas-forecasting/.

24 Source: The CEMS European Flood Awareness System (EFAS): https://www.efas.eu, documentation at EFAS sub-seasonal and seasonal forecasting - Copernicus Emergency Management Service - CEMS - ECMWF Confluence Wiki. See also technical note in Annex on page 71

10. Latest and expected impacts

10.1. East Africa

According to GEOGLAM (Group on Earth Observation Global Agricultural Monitoring) Crop Monitor bulletins of December 2025, the ongoing drought in East Africa has had severe impacts on the agricultural and livestock sectors. In Somalia, the country-wide drought conditions are expected to result in significant yield losses. The ASAP assessment of January 2026 confirms that, due to the severe drought conditions from November onwards, most Deyr season (from October to January) crops have completely failed and pastoral vegetation in Southern Somalia is rapidly degrading. Similar concerns characterise marginal agricultural areas in eastern Kenya and predominantly pastoral areas in southeastern Ethiopia. The delayed and dry start of the season has affected sowing as well as the development of the second cereal season in countries such as Uganda, Kenya, and Tanzania. Crop failure, reduced yields, low pastures availability and limited access to water are expected to cause negative impacts on crop yields and livestock productivity. Together with high levels of underlying vulnerability, concomitant economic shocks, reduced humanitarian funding, and conflicts, the situation is causing a downwards spiral for food security in the region. Overall, the recurrent droughts since 2021 and the challenging conditions for recovery are threatening the livelihood of farmers and pastoralists in East Africa, highlighting the need for urgent support and intervention to mitigate the effects of this crisis.

According to the Famine Early Warning Systems Network (FEWS NET[25]) as of January 2026, the ongoing drought in East Africa has led to a severe humanitarian crisis, with emergency-level food insecurity impacting pastoral and agropastoral areas in Somalia, Ethiopia, and Kenya. In Somalia, 4.61 million people are affected and over 135,000 are recently displaced due to a near-total failure of the late-2025 rainy season, contributing to rising livestock mortality, record-high cereal prices, and increasing acute malnutrition in children across the region. Moreover, more than 75,000 students in the whole region have been forced to leave school, as reported by OCHA (UN Office for the Coordination of Humanitarian Affairs)[26].

On 12 January, the Somali Observatory of Humanitarian Affairs (SOHA) warned for the worsening of drought, rising an alarm on the extreme emergency, emphasizing that rural communities suffer from a total collapse of essential resources[27]. Satellite imagery in the ASAP High-Resolution Viewer, shows the riverbed of the Shabelle river nearly completely dry close to Afgooye as of late February 2025[28]. More than three million Somalis have been displaced to camps, in some cases affected by malnutrition and wasting disease.[29] [30]. In Galmadug, visited at the beginning of March by the

25 https://fews.net/east-africa/alert/december-2025-0.

26 https://news.un.org/en/story/2025/12/1166654.

27 https://sooha.org/en/2026/01/12/somali-upper-house-warns-of-worsening-drought-crisis/.

28 https://agricultural-production-hotspots.ec.europa.eu/s/810dc79d.

29 https://www.ipcinfo.org/fileadmin/user_upload/ipcinfo/docs/IPC_Somalia_Acute_Food_Insecurity_Malnutrition_Jan_Jun2026_Report.pdf.

30 https://wardheernews.com/somalia-in-crisis-drought-displacement-and-the-cost-of-survival/.

Somali Disaster Management Agency (SoDMA), life-saving assistance was provided[31] [32]. In Puntland, grazing lands have degraded to dust fields, wells are intermittent or empty, livestock is severely malnourished, camels collapse under extreme heat. Transporting livestock to safer areas is too expensive for pastoral communities and families have to ration water between children and animals. In Somalia livestock represents savings, capital, and dignity. Whenever it suffers or dies, rural wealth disappears, purchasing power reduces as well as markets and trade contracts. Consequences are also perceived in urban centres, absorbing displaced families and facing additional pressure on already fragile infrastructures. This crisis cannot only be attributed to climate change but also to structural weakness, such as the lack of water storage systems. Risk of acute malnutrition for about 2 million children was also warned by UNICEF (United Nations International Children's Emergency Fund) at the end of March[33].

Critical conditions are also reported in Kenya[34], where the National Drought Management Authority (NDMA) has raised the alarm due to the worsening of drought especially in Mandera County, which has reached the Alarm Phase, with severe water shortages leading to livestock deaths and child malnutrition[35]. Other nine counties were in the Alert Phase already on 10 December 2025. 1.8 million people are estimated to be in food insecure conditions in the Arid and Semi-Arid Lands (ASALs). The national government has announced an allocation of funds to combat the severe drought, posing a major threat to livestock due to drastic shortage of forage seeds and to the pastoral communities[36]. Shortened rainy seasons have increasingly exposed pastoral communities to drought conditions, with high mortality rates registered among animals. This situation is following up the 2020-2023 livestock crisis, when millions of animals died in Kenya, Ethiopia and Somalia and strong famine in Somalia did not materialise only thanks to international aid. The Kenya National Commission on Human Rights (KNCHR) reported alleged livestock killings by multi-agency security officers engaged in an operation aimed at recovering illegally held firearms in the North Rift region[37]. KNCHR stated that the loss of animals has devastating socio-economic consequences, especially in a region already hit by drought, food insecurity and a notable increase of banditry and cattle rustling. In Turkana County, cattle raid episodes and effects of aid cuts are reported, as well as the warning raised by agencies of increasing competition for decreasing resources and the consequent risk of violence[38]. Rainfall came again at the begging of March, but very intense (more than 120% of the average monthly rainfall fell within a single day[39]) and with

---

31 https://allafrica.com/stories/202603020345.html.

32 https://radiodalsan.com/news/301593/sodma-commissioner-delivers-emergency-water-aid-to-drought-hit-af-barwaago.

33 https://www.miragenews.com/unicef-urges-global-aid-for-somalias-1645246/.

34 https://www.kenyanews.go.ke/ndma-sounds-alarm-as-drought-worsens-across-the-country/.

35 https://www.aljazeera.com/gallery/2026/2/10/severe-drought-leaves-over-two-million-kenyans-hungry-and-desperate.

36 https://www.theonlinekenyan.com/daily/2026-01-15/kenya-faces-severe-drought-government-allocates-funds-amid-livestock-threats.

37 https://www.capitalfm.co.ke/news/2026/02/knchr-condemns-killing-of-livestock-alleged-abuses-by-security-teams-in-baringo/, https://allafrica.com/stories/202602100030.html.

38 https://www.devdiscourse.com/article/law-order/3810444-drought-and-starvation-grip-turkana-amid-aid-cuts.

39 https://www.theguardian.com/environment/2026/mar/09/weather-tracker-deaths-in-nairobi-after-torrential-rain#:~:text=In%20reality%2C%20within%20the%20space,heavy%20downpours%20to%20the%20region.

disruptive flash floods which, up to 22 March and according to the authorities' communication, provoked 81 casualties in the country and 37 in the capital, Nairobi, together with high damages[40].

The drought emergency has been also affecting Ethiopia, especially its southern regions[41]. The Ethiopian Red Cross Society (ERCS) has activated the second trigger of its Drought Early Action Protocol (EAP) for the Bega season (October-November-December), due to crop yield reduction of more than 50% and the worsening of pasture conditions. In the previously cited report, OCHA states that humanitarian efforts are in place to tackle the crisis, but they are severely constrained by significant funding reductions. On 22 December 2025, only $370 million (of the $1.4 billion required by the humanitarian response) have been received, with inevitable critical gaps across lifesaving programmes. Similarly to Kenya, strong drought and flash flood episodes (10 March, with 30 people killed[42]) are reported in Ethiopia.

The critical situation has been also confirmed by ICPAC (IGAD Intergovernmental Authority on Development Climate Prediction and Applications Centre) on 14 January 2026[43] and in the already cited Climate Watch Advisory of January 2026, where maps of warning levels for crop and rangeland show water and biomass stress conditions.

International fundings and their sharp decline are key factors in the drought emergency in East Africa. On 20 February 2026, the World Food Program (WFP) warned that it could suspend its humanitarian work for food and nutrition assistance in Somalia in April, if funding will not be released (about 80,7 million euros are urgently needed). This happens during one of the most complex hunger emergencies in recent years, where about 4.4 million people are facing food insecurity and around one million people are suffering from extreme hunger[44]. 6.5 million people are expected to face food insecurity at the end of March 2026 and 1,84 million 5-year younger children are expected to suffer acute malnutrition in the whole 2026, according to the February report of the Integrated Food Security Phase Classification (IPC)[29]. WPF was already forced to reduce the number of people assisted from 2.2 million at the beginning of 2025 to 600,000 in February 2026, while other reductions or interruptions of humanitarian aid activities were reported by the UN and the Somali government in late February[29].

Fortunately, also positive news have appeared in 2026. The World Bank's Productive Safety Net Project 6 (PSNP 6 [45] [46]) - designed to improve access to better jobs, build the resilience of the poorest households, enhance food security, and build climate resilience - is expected to be approved

---

40 https://www.channelnewsasia.com/world/torrential-rains-in-kenya-kill-81-in-march-officials-6010251.

41 https://reliefweb.int/report/ethiopia/ethiopia-drought-eap-early-action-protocol-activation-18112025-eap-no-eap2022et02-operation-no-mdret033.

42 https://borkena.com/2026/03/10/ethiopia-gamo-flash-flood-landslide-accident-kills-30-people/?utm_source=ICPAC_NEWSLETTER&utm_campaign=7c61ba079c-EMAIL_CAMPAIGN_2019_02_25_06_47_COPY_01&utm_medium=email&utm_term=0_0ea0a0abaf-7c61ba079c-396049832.

43 https://x.com/IGAD_CPAC/status/2011405882416935420.

44 https://www.diariosigloxxi.com/texto-ep/mostrar/20260220144513/pma-advierte-podria-suspender-abril-trabajos-humanitarios-somalia-no-recibe-fondos.

45 https://allafrica.com/stories/202603050049.html.

46 https://documents1.worldbank.org/curated/en/099111425070037792/pdf/P511478-ba2ad2f0-3dbb-4993-b589-00b84ca54059.pdf.

in March for Ethiopia. In February, the United Arab Emirates Aid Agency dispatched 30 tonnes of food assistance to Kenya for supporting families impacted by the severe drought[47].

10.2. Middle East and Central Asia

Droughts and unsustainable water management are among the main factors in shaping the current water crisis in Iran[48]. An annual groundwater depletion of 1.7 billion cubic metre has been estimated together with land subsidence in 3.5% of the country with a large area having rates greater than 10 cm/year[49]. The situation is worsened by a number of dams built in inadequate places and by poor irrigation practices, leading to disruption of river flows, enhanced evaporation, and ecological damages[50].

According to the UNICEF Humanitarian Report of 1 January - 31 December 2025 [51], a severe humanitarian crisis is ongoing in Afghanistan, driven by decades of geopolitical and social emergencies and conflicts, widespread poverty, and climate change. In 2025, more than half of the population (nearly 23 million people, including 12 million children) required humanitarian assistance. In addition to this, 2.9 million Afghans returned to the country from Iran and Pakistan in the year, increasing pressure on assistance in a context of severe natural hazards: persistent drought conditions, recurrent floods, and even two earthquakes happened in the year. In particular, severe drought affected 3.4 million people in 12 provinces, further deteriorating the already critical food conditions. According to the Whole of Afghanistan Assessment (WoAA 2025), 67 percent of households experienced drought and widespread water scarcity in 2025. In Afghanistan, an aid programme funded by the World Bank is ongoing for building drinking water supply networks in the drought-affected central-western province of Ghazni. This aims at addressing the water crisis due to prolonged droughts, which dried wells up and forced many people to travel long distances to have access to drinking water[52].

47 https://www.urdupoint.com/en/middle-east/uae-sends-30-tonnes-of-food-aid-to-support-dr-2142150.html.

48 https://www.science.org/doi/10.1126/sciadv.adk3039 , https://www.nature.com/articles/s41467-023-42411-2.

49 https://www.science.org/doi/10.1126/sciadv.adk3039.

50 https://www.dw.com/en/iran-at-an-environmental-crossroads-paths-to-recovery/a-75523489.

51 https://www.unicef.org/afghanistan/media/13156/file/UNICEF%20Afghanistan%20Humanitarian%20Situation%20Report%20No.%2012%20%25.

52 https://www.aninews.in/news/world/asia/afghanistan-world-bank-funded-water-networks-launched-in-drought-hit-ghazni-to-benefit-1000-families20260210142057/.

List of abbreviations and definitions

Abbreviations	Definitions
ASALs	Arid and Semi-Arid Lands
ASAP	Anomaly Hotspots of Agricultural production
BOM	Bureau of Meteorology, Australia
C3S	Copernicus Climate Change Service
CHIRPS	Climate Hazards Group Infrared Precipitation with Station
CEMS	Copernicus Emergency Management Service
CMCC	Centro Euro-Mediterraneo sui Cambiamenti Climatici
DMI	Dipole Mode Index
DWD	Deutscher Wetterdienst
EAP	Early Action Protocol
ECCC	Environment and Climate Change Canada
ECMWF	European Centre for Medium-Range Weather Forecasts
EDO	European Drought Observatory (Copernicus Emergency Management Service, CEMS)
EFAS	European Flood Awareness System
ENSO	El Niño Southern Oscillation
ERA5	ECMWF Reanalysis v5
ERCS	Ethiopian Red Cross Society
ERSST	Extended Reconstructed Sea Surface Temperature
FAOSTAT	Food and Agriculture Organization Statistical Database
fAPAR	Fraction of Absorbed Photosynthetically Active Radiation

Abbreviations	Definitions
FEWS NET	Famine Early Warning Systems Network
GAUL	Global Administrative Unit Layers
GDO	Global Drought Observatory (Copernicus Emergency Management Service, CEMS)
GEOGLAM	Group on Earth Observation Global Agricultural Monitoring
GloFAS	Global Flood Awareness System (Copernicus Emergency Management Service, CEMS)
ICPAC	IGAD Climate Prediction and Application Centre
IDO	Indian Ocean Dipole Oscillation
IGAD	Intergovernmental Authority on Development
IOD	Indian Ocean Dipole
IPC	Integrated Food Security Phase Classification
JRC	Joint Research Centre
KNCHR	Kenya National Commission on Human Rights
KNMI	Koninklijk Nederlands Meteorologisch Instituut
LISFLOOD	grid-based hydrological rainfall-runoff-routing model
MAM	March-April-May season
NCEP	National Centers for Environmental Prediction (National oceanic and Atmospheric Administration, NOOA)
NDMA	National Drought Management Authority, Kenya
OCHA	UN Office for the Coordination of Humanitarian Affairs
OND	October-November-December season
ONI	Oceanic Niño Index

Abbreviations	Definitions
OS	Open Source
PET	Potential Evapotranspiration
PSNP	Productive Safety Net Project
ROWE	Runoff or Water Equivalent
SEAS	Seasonal Forecasting System
SoDMA	Somali Disaster Management Agency
SOHA	Somali Observatory for Humanitarian Affairs
SPEI	Standardized Precipitation Evapotranspiration
SPI	Standardized Precipitation Index
UKMO	United Kingdom Meteorological Office
UN	United Nations
UNICEF	United Nations Children's Fund
VIIRS	Visible Infrared Imaging Radiometer Suite
WFP	World Food Program
WoAA	Whole of Afghanistan Assessment

List of figures

Annex

Figure S1. SPI-3 from 1995 to 2025. The bar plot corresponds to the percentage of each class for each timestep in East Africa (Somalia, Ethiopia, Kenya, Djibouti, Eritrea).

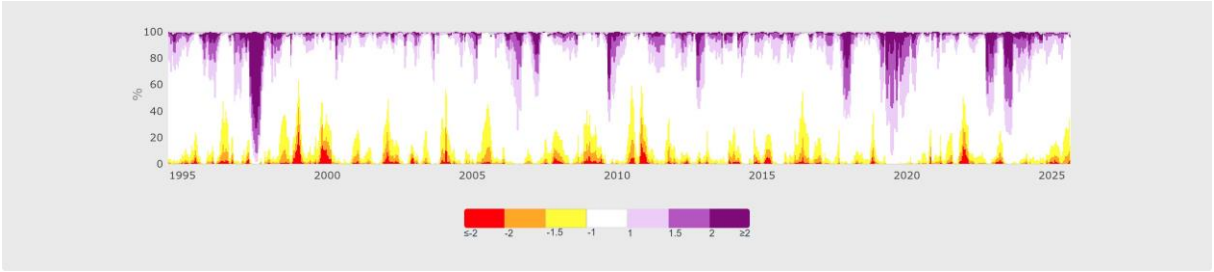

Source: JRC based on CHIRPS.

Figure S2. As Figure S1 but for the Greater East Africa region (Somalia, Ethiopia, Kenya, Djibouti, Eritrea, Sudan, South Sudan, Uganda, Rwanda, Burundi, Tanzania).

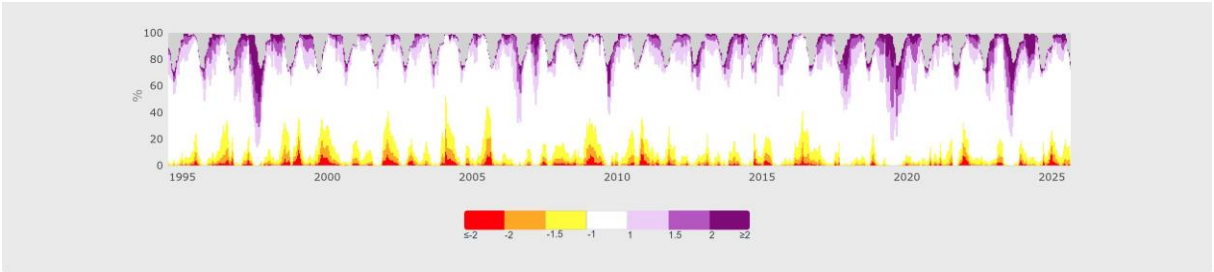

Source: JRC based on CHIRPS.

Figure S3. As Figure S1 but for Iran.

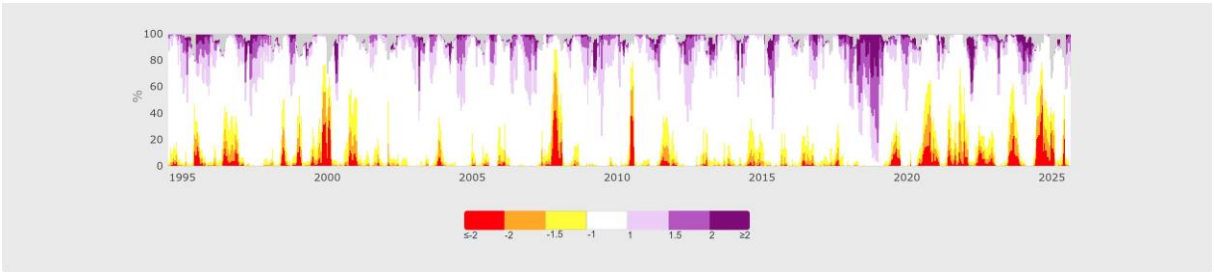

Source: JRC based on CHIRPS.

Figure S4. As Figure S1 but for the Middle East/Central Asia region.

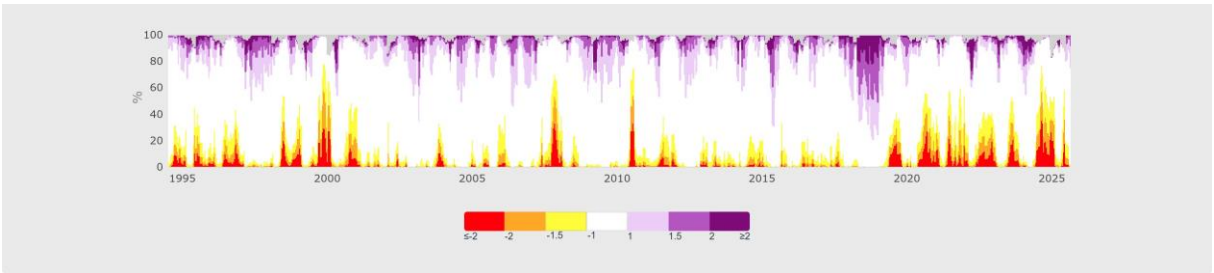

Source: JRC based on CHIRPS.

Figure S5. SPEI-3 from 1995 to 2025 timeseries. The bar plot corresponds to the percentage of each class for each timestep in East Africa (Somalia, Ethiopia, Kenya, Djibouti, Eritrea).

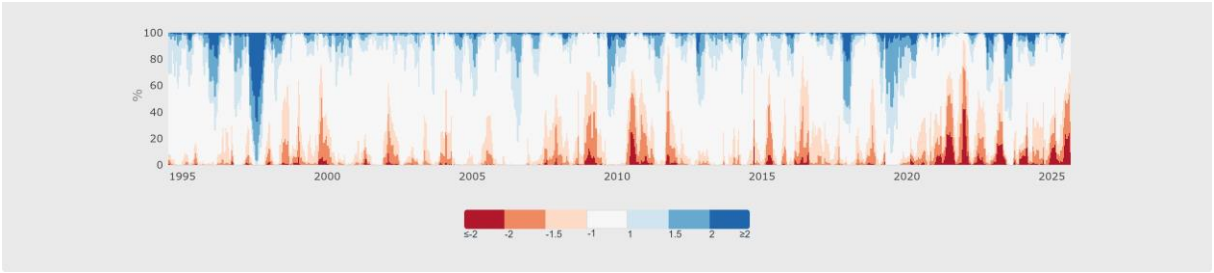

Source: JRC based on ERA5.

Figure S6. As Figure S5 but for Greater East Africa region (Somalia, Ethiopia, Kenya, Djibouti, Eritrea, Sudan, South Sudan, Uganda, Rwanda, Burundi, Tanzania).

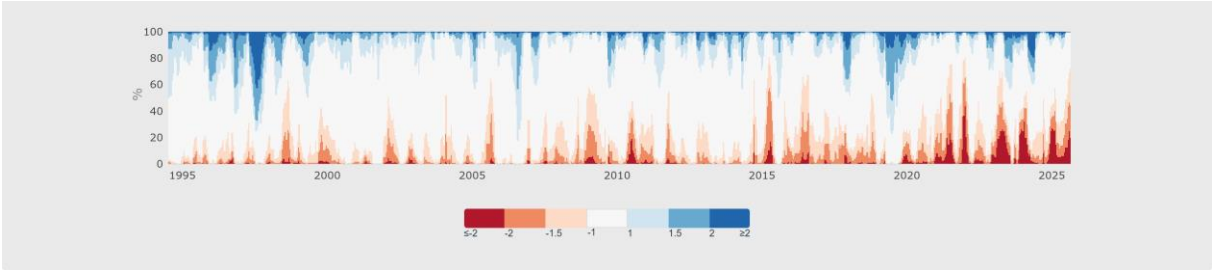

Source: JRC based on ERA5.

Figure S7. SPEI-3 from 1995 to 2025 timeseries. The bar plot corresponds to the percentage of each class for each timestep in Iran.

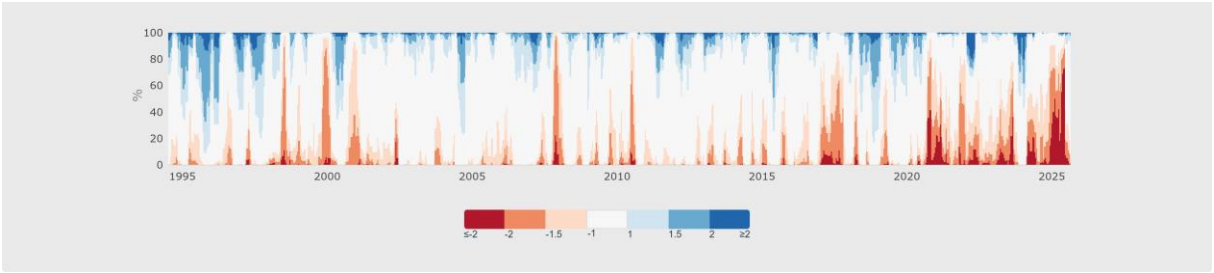

Source: JRC based on ERA5.

Figure S8. As Figure S7 but for the Middle East/Central Asia region (Iran, Iraq, Armenia, Azerbaijan, Turkmenistan, Uzbekistan, Afghanistan, Tajikistan).

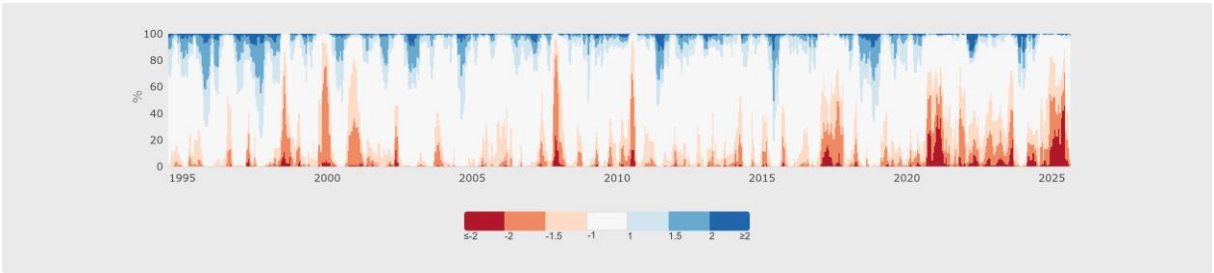

Source: JRC based on ERA5.

Figure S9. SPEI-12 from 1995 to 2025. The bar plot corresponds to the percentage of each class for each timestep in East Africa (Somalia, Ethiopia, Kenya, Djibouti, Eritrea).

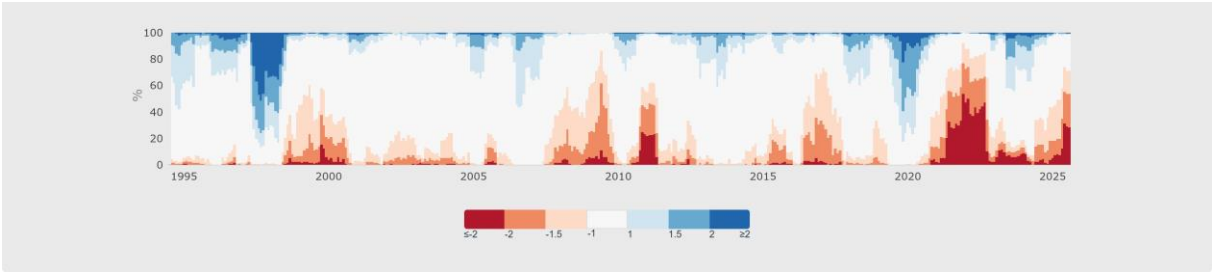

Source: JRC based on ERA5.

Figure S10. As Figure S9 but for the Greater East Africa region (Somalia, Ethiopia, Kenya, Djibouti, Eritrea, Sudan, South Sudan, Uganda, Rwanda, Burundi, Tanzania).

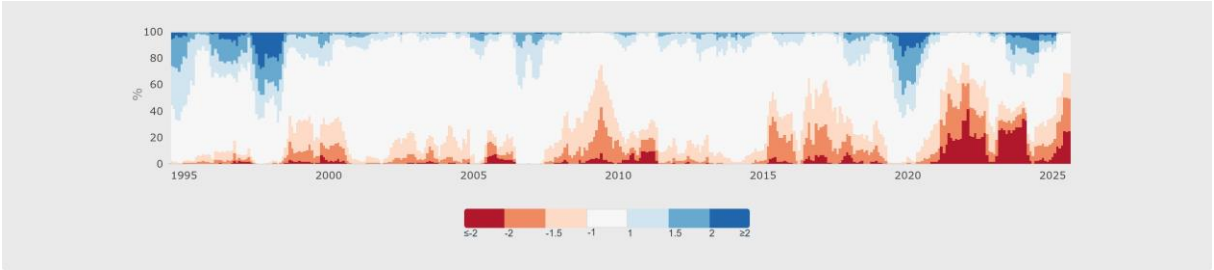

Source: JRC based on ERA5.

Figure S11. As Figure S9 but for Iran.

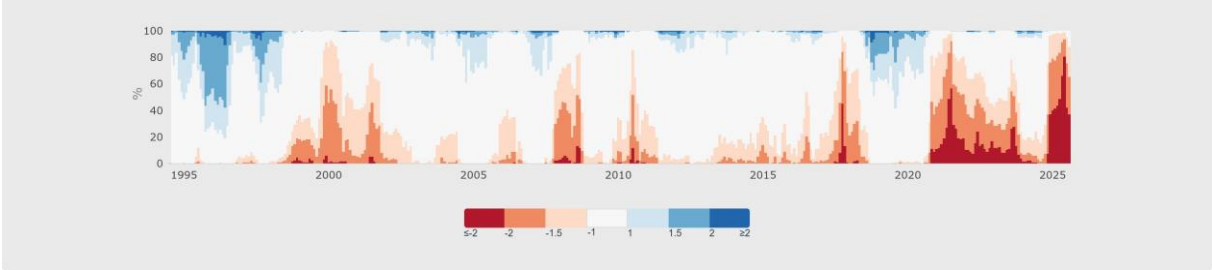

Source: JRC based on ERA5.

Figure S12. As Figure S9 but for the Middle East / Central Asia region (Iran, Iraq, Armenia, Azerbaijan, Turkmenistan, Uzbekistan, Afghanistan, Tajikistan).

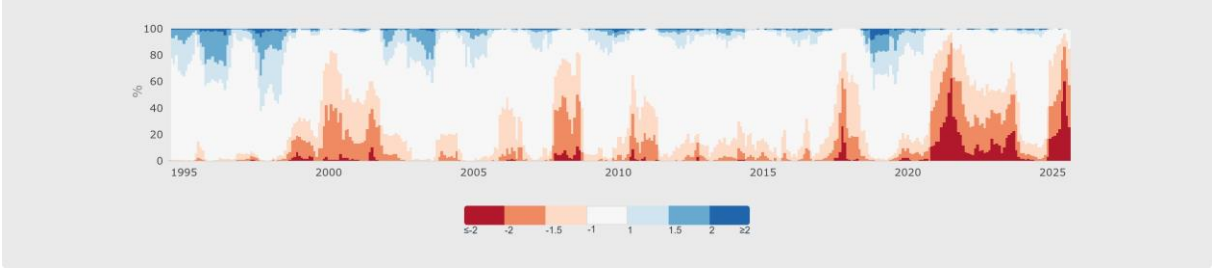

Source: JRC based on ERA5.

Figure S13. SMA from 1995 to 2025. The bar plot corresponds to the percentage of each class for each timestep in East Africa (Somalia, Ethiopia, Kenya, Djibouti, Eritrea).

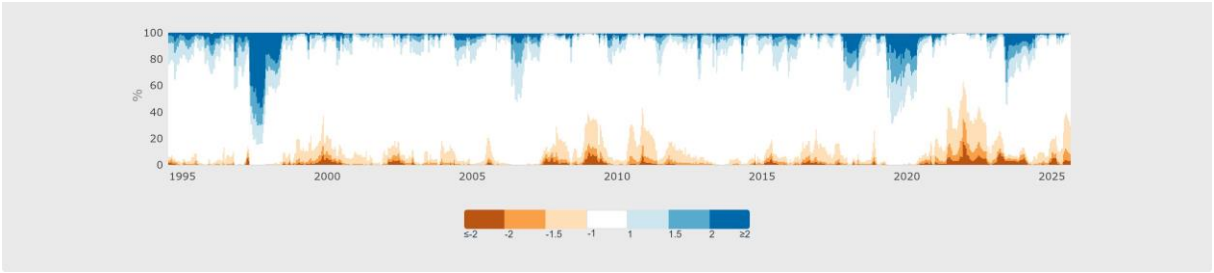

Source: JRC based on OS LISFLOOD hydrological model.

Figure S14. As Figure S13 but for the Greater East Africa region (Somalia, Ethiopia, Kenya, Djibouti, Eritrea, Sudan, South Sudan, Uganda, Rwanda, Burundi, Tanzania).

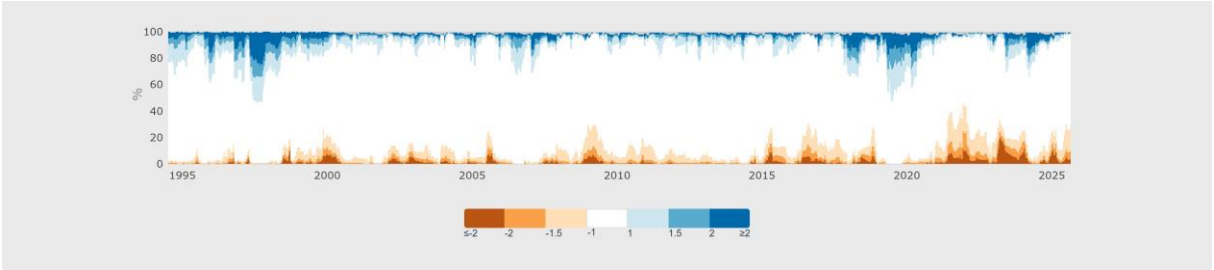

Source: JRC based on OS LISFLOOD hydrological model.

Figure S15. SMA from 1995 to 2025 timeseries. The bar plot corresponds to the percentage of each class for each timestep in Iran.

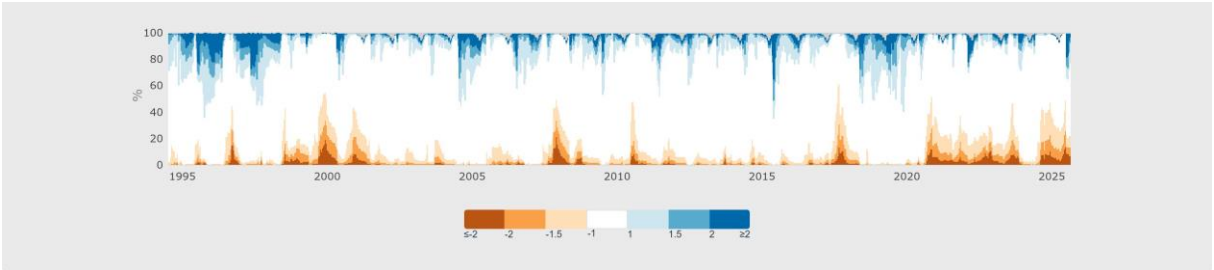

Source: JRC based on OS LISFLOOD hydrological model.

Figure S16. As Figure S15 but for the Middle East/Central Asia region (Iran, Iraq, Armenia, Azerbaijan, Turkmenistan, Uzbekistan, Afghanistan, Tajikistan).

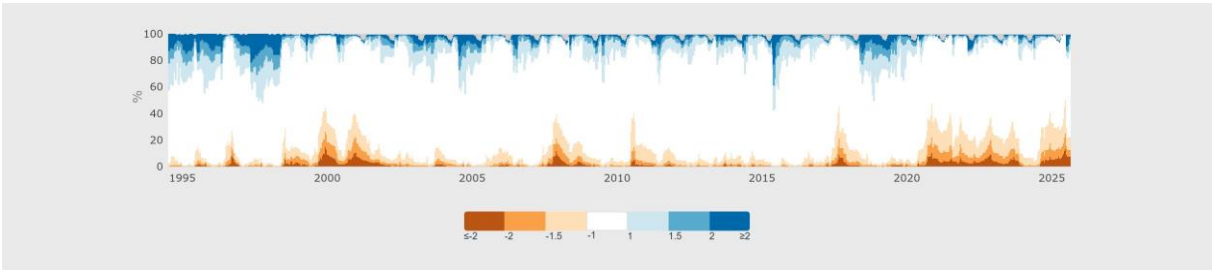

Source: JRC based on OS LISFLOOD hydrological model.

Figure S17. Standardized discharge anomalies (σ) for selected basins in (a) the Middle East and (b) East Africa with respect to the mean annual discharge of 1991-2020 (black line). Heatmap: monthly anomaly in σ. Right panels: monthly absolute discharge of climatology (black, km³/month averaged over 1991-2020) and the 2021-2025 seasonal cycles as coloured lines.

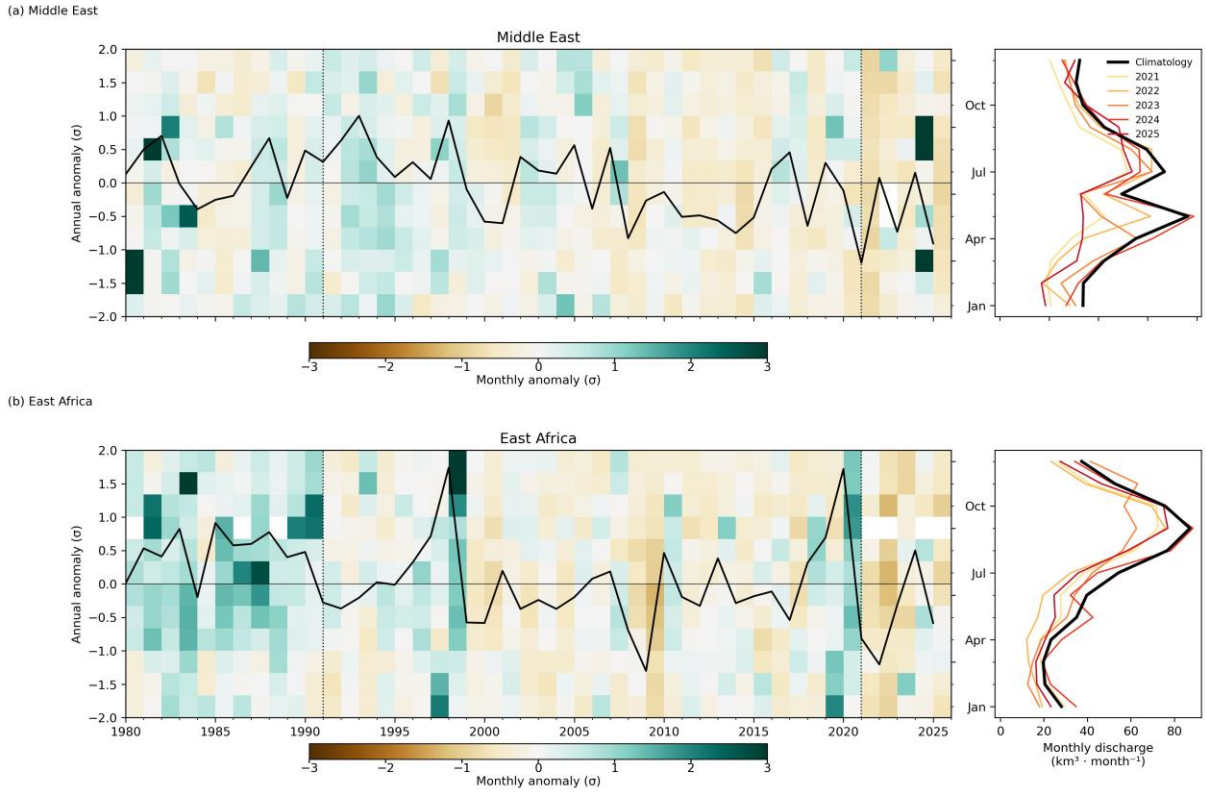

Source: GloFAS.

Figure S18. *Ensemble of selected climate model analogues (mean and range) and observed (black) SPI-12 in East Africa (left) and the Middle East/Central Asia region (right)*

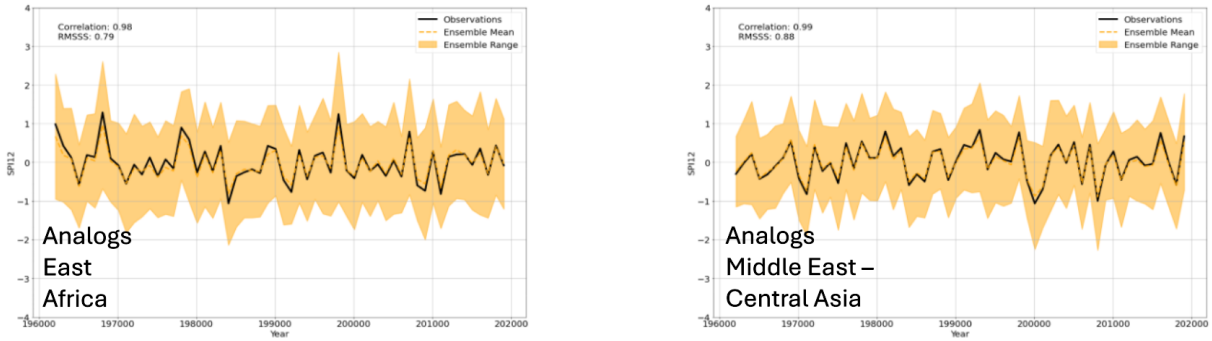

Source: JRC based on CMIP6 and ERSSTv5 data.

Figure S19. ENSO and IOD indices for the period 1980-2025. Reference dataset ERSST (Extended Reconstructed Sea Surface Temperature) v5.

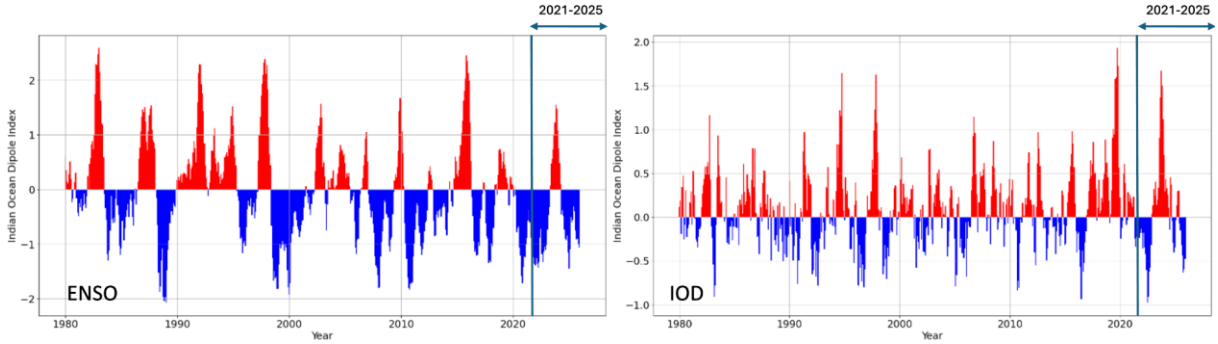

Source: JRC based on ERSSTv5 data.

Figure S20. VIIRS Satellite-derived fAPAR anomalies from 2012 to 2025. The bar plot corresponds to the percentage of each class for each timestep in East Africa (Somalia, Ethiopia, Kenya, Djibouti, Eritrea).

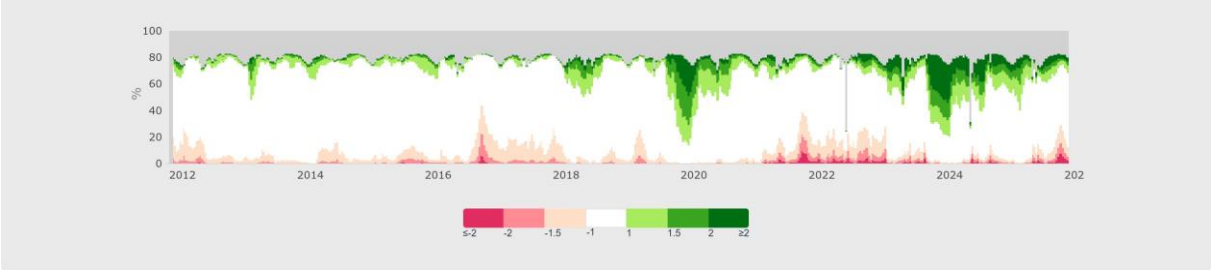

Source: JRC based on VIIRS.

Figure S21. As Figure S20 but for the Greater East Africa region (Somalia, Ethiopia, Kenya, Djibouti, Eritrea, Sudan, South Sudan, Uganda, Rwanda, Burundi, Tanzania).

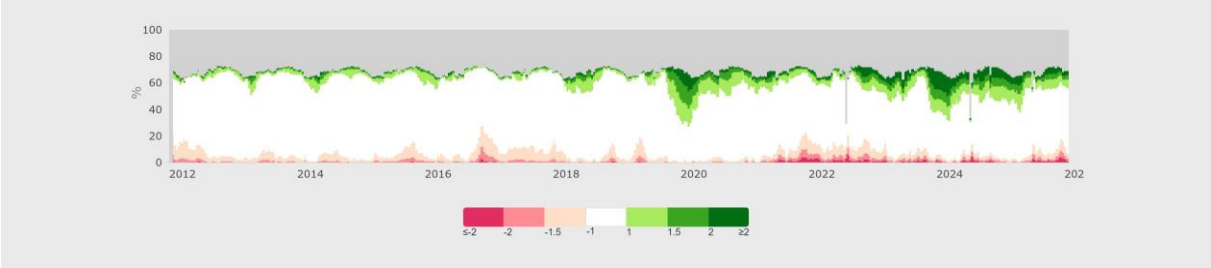

Source: JRC based on VIIRS.

Figure S22. VIIRS Satellite-derived fAPAR anomalies from 2012 to 2025. The bar plot corresponds to the percentage of each class for each timestep in Iran.

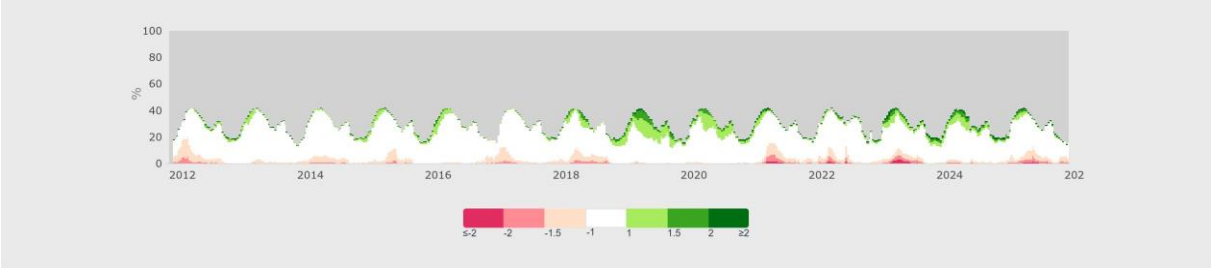

Source: JRC based on VIIRS.

Figure S23. As Figure S22 but for the Middle East/Central Asia region (Iran, Iraq, Armenia, Azerbaijan, Turkmenistan, Uzbekistan, Afghanistan, Tajikistan).

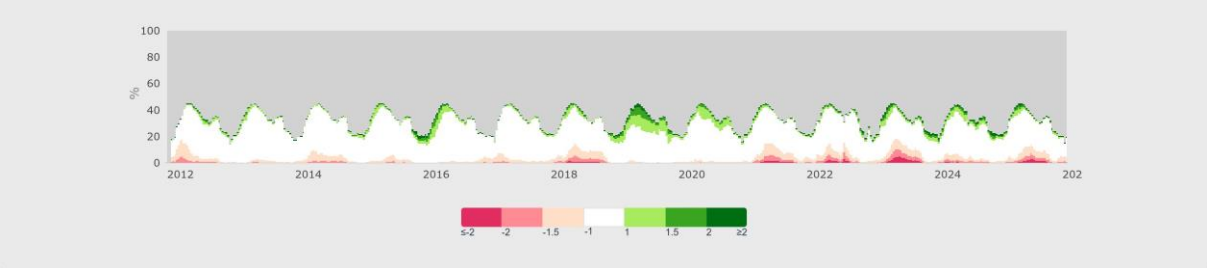

Source: JRC based on VIIRS.

Figure S24. ASAP warnings for Kwale County in Kenya and for Jowhar district in Somalia from 2001 to early 2026.

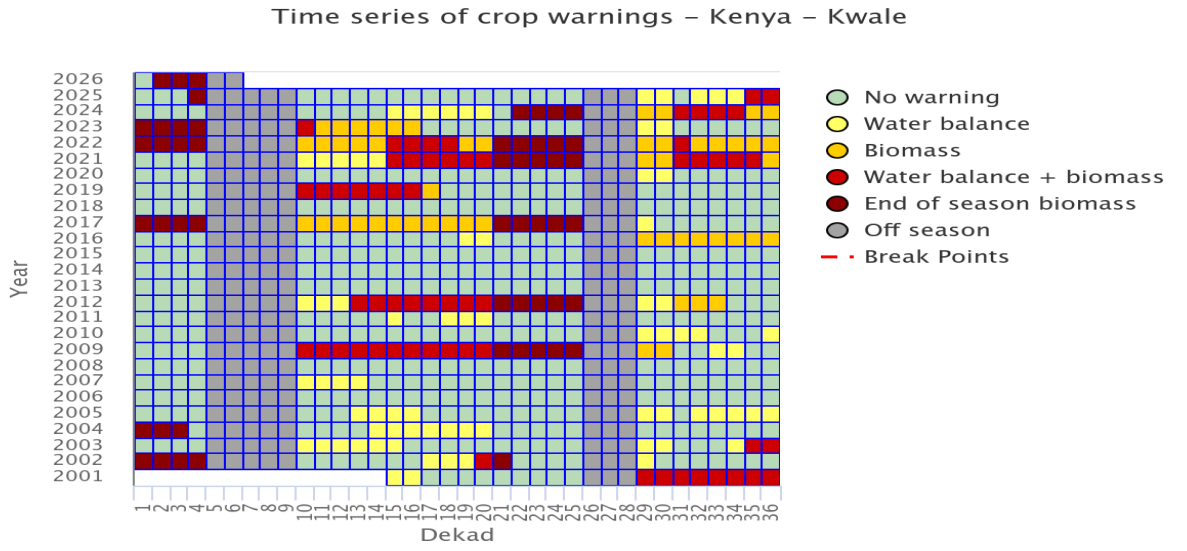

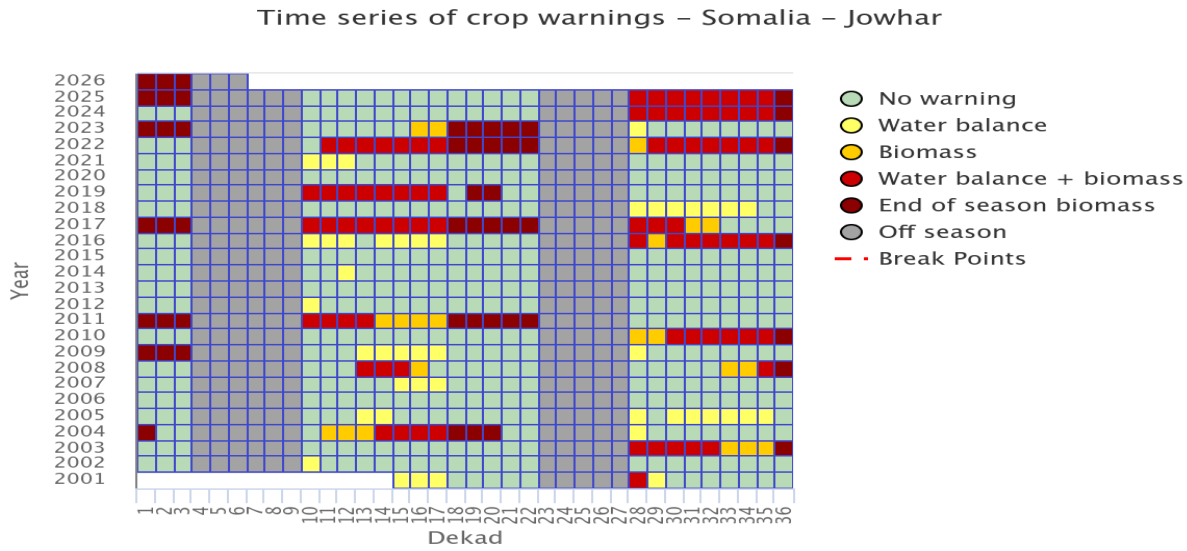

Source: JRC-ASAP

Figure S25. Evolution of SPI-3 and fAPAR from October 2020 to July 2025 in Khorasan, Khuzestan, Mazandaran and Fars provinces, Iran.

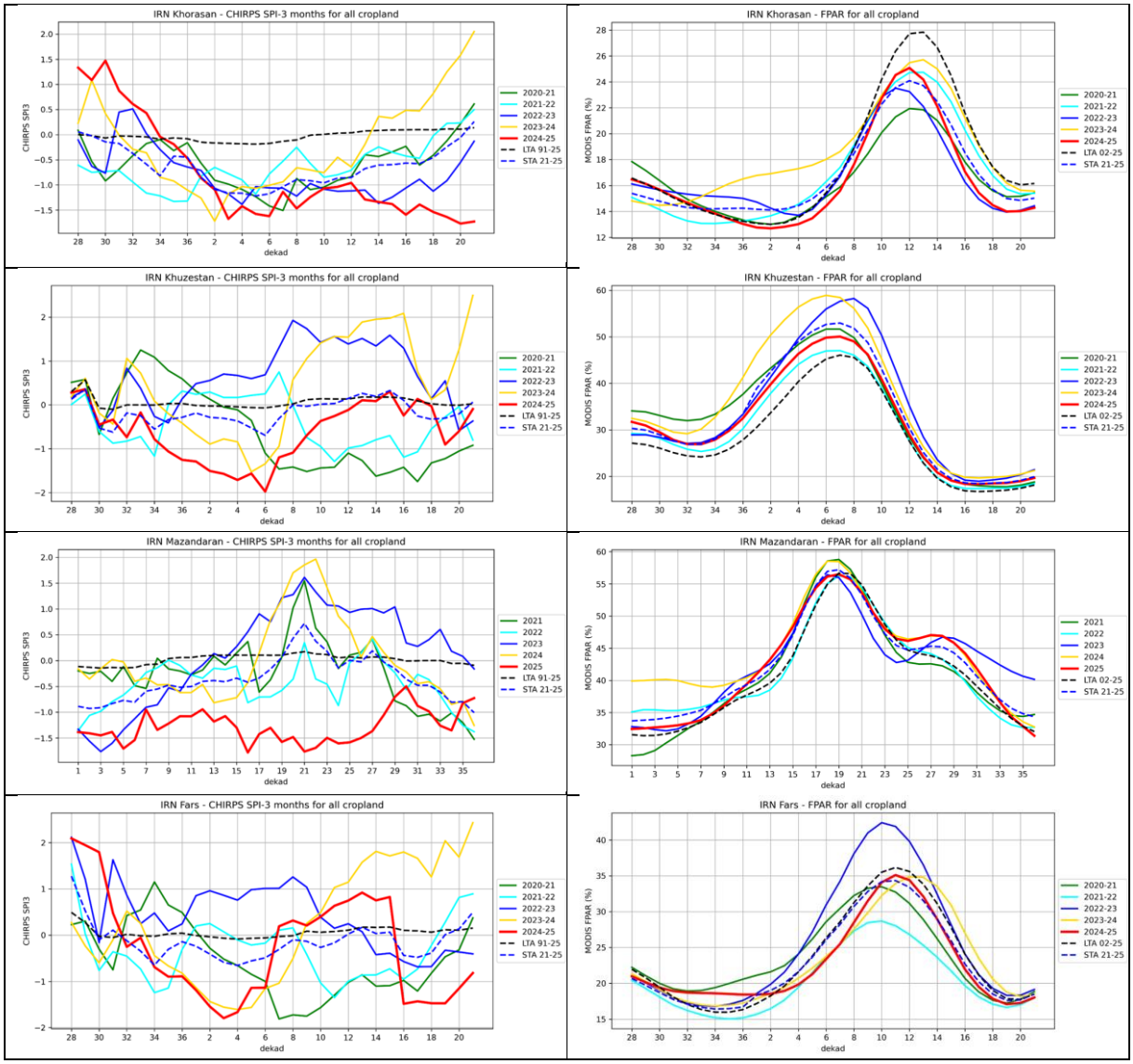

Source: JRC-ASAP

Figure S26. Evolution of SPI-3 and fAPAR from October 2020 to September 2025 in Jawzjan, Hirat and Kunduz provinces, Afghanistan.

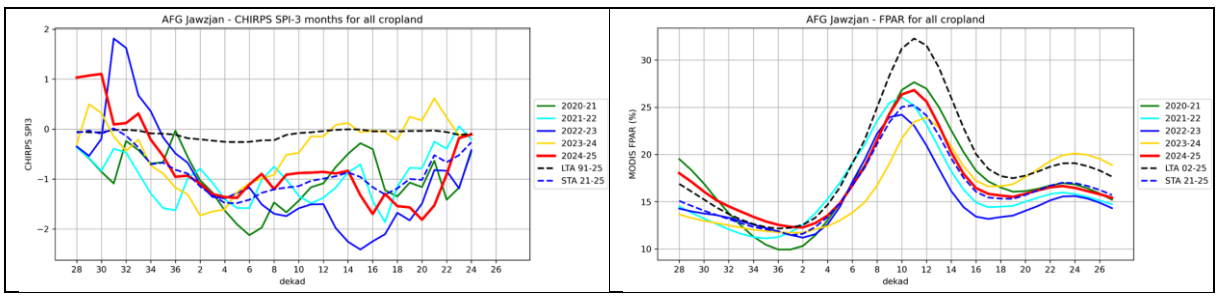

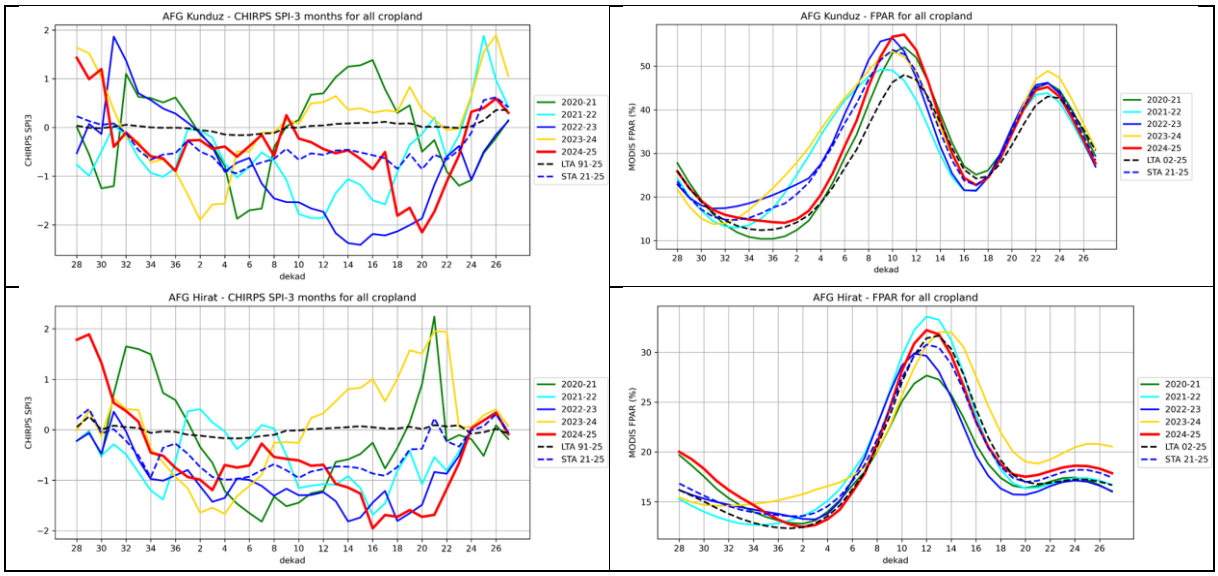

Source: JRC-ASAP

Figure S27. ASAP warnings for Jawzjan (left panel) and Kunduz (right panel), Afghanistan.

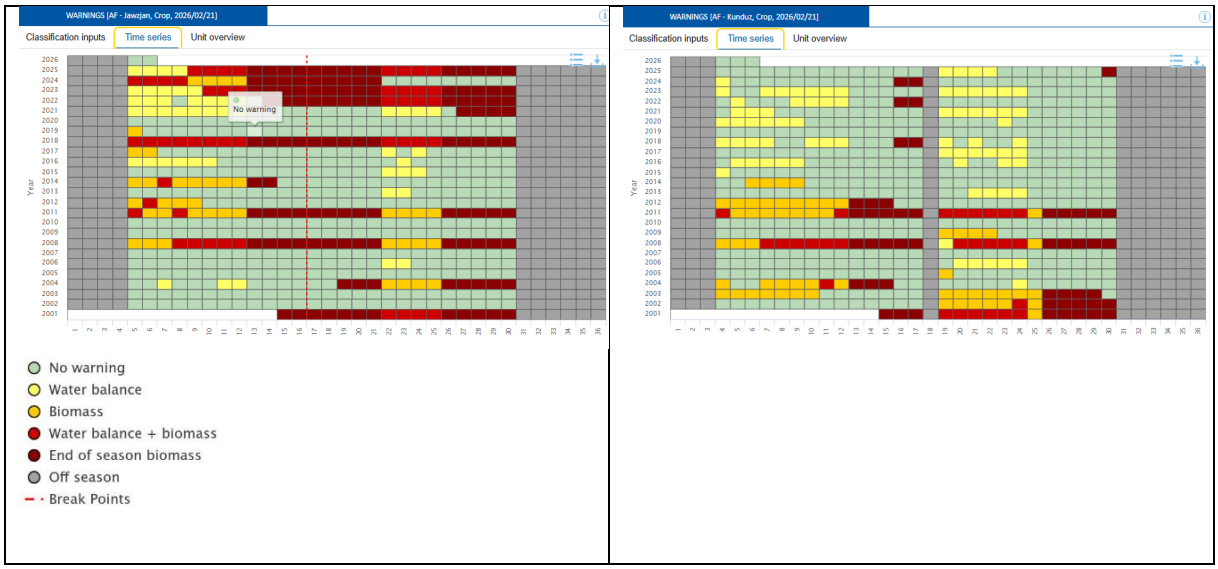

Source: JRC-ASAP

Figure S28. Evolution of SPI-3 and faPAR from January 2021 to December 2025 in Ahal province, Turkmenistan.

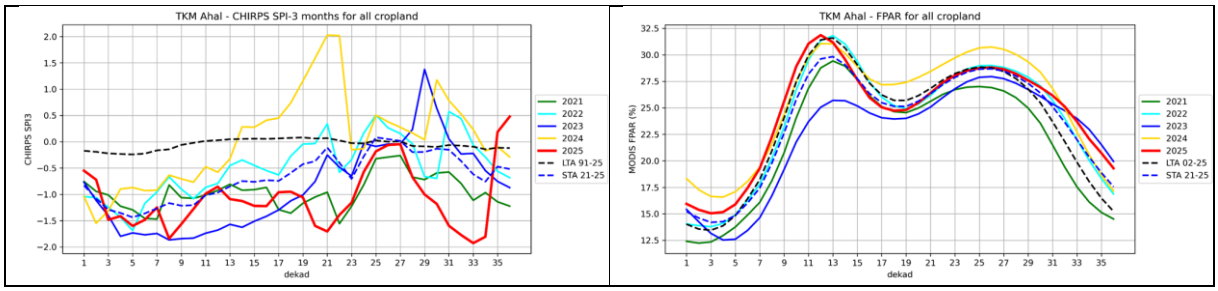

Source: JRC-ASAP

Figure S29. Evolution of SPI-3 and fAPAR from January 2021 to December 2025 in Kashkadarya province, Uzbekistan.

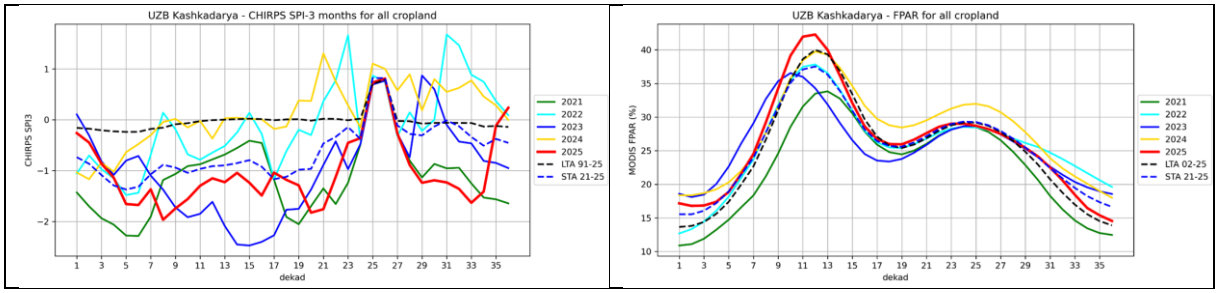

Source: JRC-ASAP

Figure S30. Evolution of SPI-3 and fAPAR from November 2020 to October 2025 in Sindh province, Pakistan.

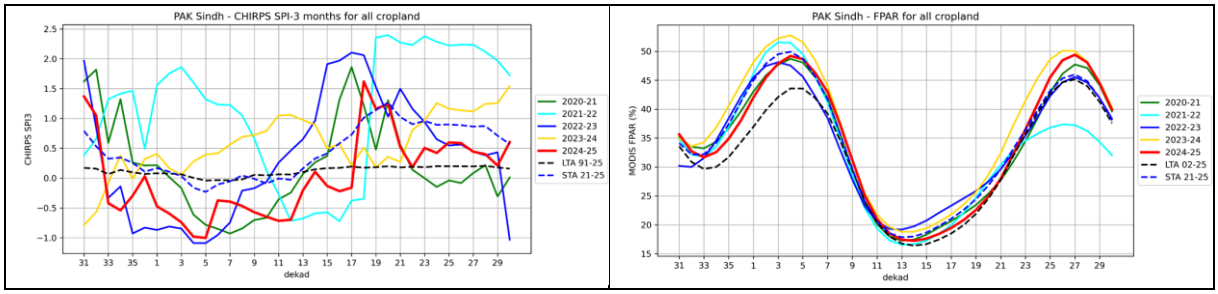

Source: JRC-ASAP

Figure S31. Soil Moisture Index Anomaly, late March 2026.

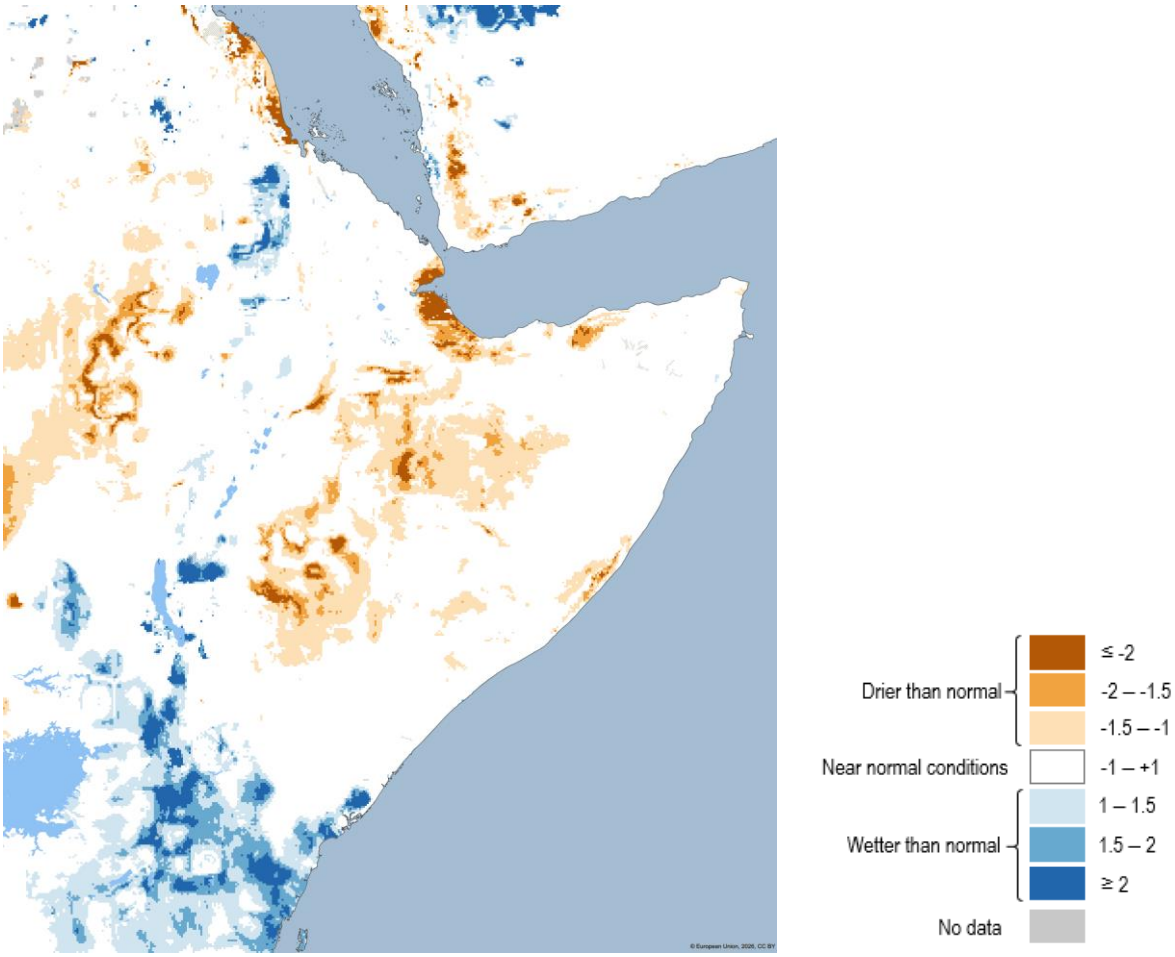

Source: JRC based on OS LISFLOOD hydrological model.

Figure S32. Soil Moisture Index Anomaly, late March 2026.

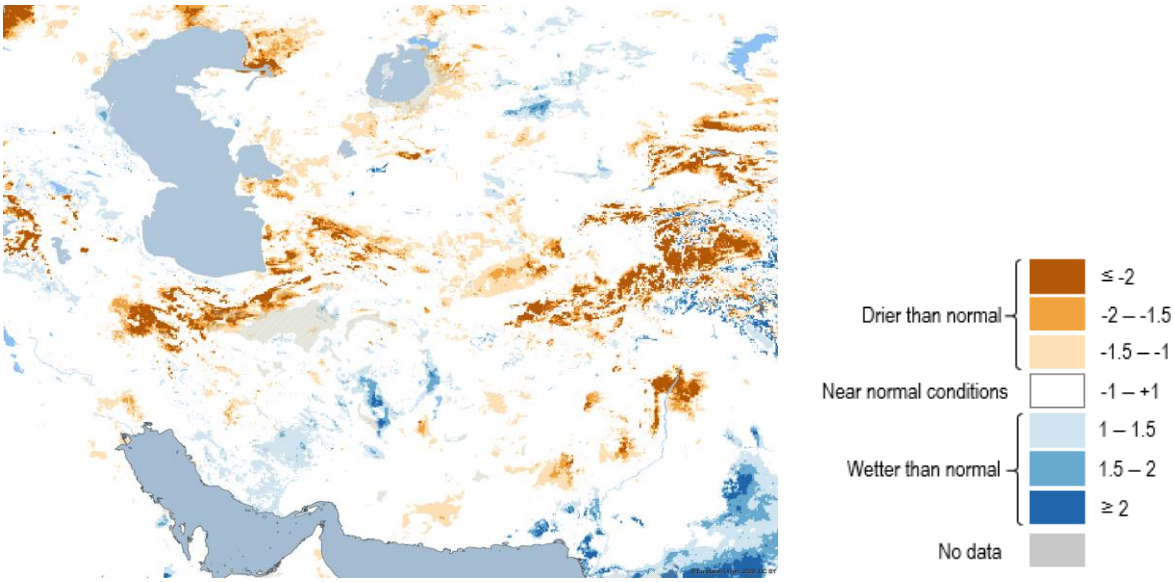

Source: JRC based on OS LISFLOOD hydrological model.

Technical Note for Figure 46

- The regions displayed in Figure 46 are a subset of 204 major basins within the GloFAS (Global Flood Awareness System) domain, the basin delineation was done semi-automatically, and the basin borders align with the 0.05 degree OS LISFLOOD river network in GloFAS. This allows large-scale variability in weather to be captured, and forecast information to be summarized. The map in Figure 46 shows the forecast river flow anomaly per region for the April 2026 step within the 7 months simulation run from April 2026 to October 2026. Different colours indicate the level of anomalies, while the colour intensity shows the confidence level in the anomalies, with the lighter colours highlighting lower confidence.
- The analysis results shown in Figure 46 are based on the OS LISFLOOD hydrological model outputs driven by 51 ensemble members of the ECMWF SEAS5 seasonal forecast. More information on OS LISFLOOD: De Roo et al., 2000. “Physically based river basin modelling within a GIS: the LISFLOOD model”. Hydrological Processes, 14, 1981–1992. Additional and updated information: Open Source Lisflood (https://ec-jrc.github.io/lisflood/)

Getting in touch with the EU

In person

All over the European Union there are hundreds of Europe Direct centres. You can find the address of the centre nearest you online (european-union.europa.eu/contact-eu/meet-us_en).

On the phone or in writing

Europe Direct is a service that answers your questions about the European Union. You can contact this service:

— by freephone: 00 800 6 7 8 9 10 11 (certain operators may charge for these calls),
— at the following standard number: +32 22999696,
— via the following form: european-union.europa.eu/contact-eu/write-us_en.

Finding information about the EU

Online

Information about the European Union in all the official languages of the EU is available on the Europa website (europa.eu).

EU publications

You can view or order EU publications at op.europa.eu/en/publications. Multiple copies of free publications can be obtained by contacting Europe Direct or your local documentation centre (european-union.europa.eu/contact-eu/write-us_en).

EU law and related documents

For access to legal information from the EU, including all EU law since 1951 in all the official language versions, go to EUR-Lex (eur-lex.europa.eu).

Open data from the EU

The portal data.europa.eu provides access to open datasets from the EU institutions, bodies and agencies. These can be downloaded and reused for free, for both commercial and non-commercial purposes. The portal also provides access to a wealth of datasets from European countries.

Science for policy

The Joint Research Centre (JRC) provides independent, evidence-based knowledge and science, supporting EU policies to positively impact society

Scan the QR code to visit:

The Joint Research Centre: EU Science Hub

https://joint-research-centre.ec.europa.eu

Publications Office
of the European Union